# A GPS-IPW Based Methodology for Forecasting Heavy Rain Events

**Srikanth Gorugantula**

Thesis submitted to the Faculty of the
Virginia Polytechnic Institute and State University
in partial fulfillment of the requirements for the degree of

Master of Science
in
Civil Engineering

G.V.Loganathan, Chair
Vinod Lohani
Tamim Younous

December 6, 2002
Blacksburg, Virginia

Keywords: GPS, Integrated Precipitable Water Vapor (IPW), Radar-VIL, Atmospheric Modeling, Atmospheric Delays

**A GPS-IPW Based Methodology for Forecasting Heavy Rain Events**

**By**

**Srikanth Gorugantula**

**(Abstract)**

The mountainous western Virginia is the source of the headwater streams for the New, the Roanoke, and the James rivers. The region is prone to flash flooding, typically the result of localized precipitation. Fortunately, within the region, there is an efficient system of instruments for real-time data gathering with IFLOWS (Integrated Flood Observing and Warning System) gages, WSR-88D Doppler radar, and high precision GPS (Global Positioning System) receiver. The focus of this research is to combine the measurements from these various sensors in an algorithmic framework to determine the flash flood magnitude. It has been found that the trend in the GPS signals serves as a precursor for rain events with a lead-time of 30 minutes to 2 hours. The methodology proposed herein takes advantage of this lead-time as the trigger to initiate alert related calculations. It is shown here that the sum of the rates of change of total cloud water, water vapor contents and logarithmic profiles of partial pressure of dry air and temperature in an atmospheric column is equal to the rain rate. The total water content is measurable as the profiles of integrated precipitable water (IPW) from the GPS, the vertically integrated liquid (VIL) from the radar (representing different phases of the atmospheric water) and the pressure and temperature profiles are available. An example problem is presented illustrating the involving the calculations.

**Acknowledgements**

I would like to sincerely thank the following people and organizations that have it made it possible to complete the work on this thesis.

- Dr. G. V. Loganathan has provided countless hours of support and assistance on this work. He has been very helpful in teaching me how to perform academic research. I would like to express my gratitude to him for the amount of time and effort that he has put in to help me succeed in my academic career as well as in my personal life. Without his support, guidance, and motivation I would not have been able to complete this thesis.
- Dr. Vinod Lohani for his willing ness to serve as one of my committee members.
- Dr. Tamim Younos for his acceptance to serve as my committee member.
- I would like to thank Mr. Stephen J. Keighton and Mr. Michael Gillen, people from NWS involved in the current study. Without their support and time in providing various valuable suggestions and data it would not have been possible for me to complete my thesis. I really appreciate their help.
- I would like to thank the departments of Civil Engineering and Mathematics for their financial support
- The faculty and students of the Hydrosystems division have encouraged and supported me throughout my time at Virginia Tech. I would like to thank them for their assistance.
- I would like to thank all my friends in Virginia Tech for their support in every which way.

.

## TABLE OF CONTENTS

## LIST OF TABLES

## LIST OF FIGURES

# Chapter 1. Introduction

## 1.1 Background

The National Weather Service (NWS) currently relies on the radar for short-term forecasting. The WSR-88D Doppler radar estimates rainfall (R) using the lowest two beam angles (0.5° and 1.5°) to detect reflectivity (Z) and applies the Z-R relationship to convert to an estimated rainfall rate. Forecasters have access to a new radar volume scan and updated precipitation estimates (of one hour or more totals) every five or six minutes. In addition, realtime rain gage data is obtained at select locations every minute, and available in 15 minute or greater intervals. Rainfall readings from rain gages and radar estimates can provide forecasters with a short lead time (usually around 30 minutes) before flash flooding occurs from convective storms. However, when other data sets (such as water vapor data) are incorporated that reveal information about the environment, the lead-time can often be increased if certain trends are observed.

One of the environmental parameters that plays a key role in the development of flash-flood producing storms, is the total available moisture, measured by the vertically integrated precipitable water vapor (IPW) in an atmospheric column. IPW value represents the total amount of water vapor in an atmospheric column at a particular time. Recently, the NOAA Forecast Systems Laboratory (FSL), as well as other federal government agencies, have begun employing global positioning system (GPS) technology to measure IPW from sensors at select locations around the U.S. The temporal resolution of these data is 30 minutes, and new implementation of near real-time processing techniques has made the data available within 75 minutes of real-time. One of these sensors was installed at NWS RNK in 1999 at Blacksburg, VA (BLKV) and is co-located with the upper air observation site. While the horizontal spacing of sensors cannot yet provide a mesoscale analysis over southwestern Virginia, the temporal resolution is more than enough to reveal potentially important short-term fluctuations in IPW that serve as precursors to convective activity. The GPS systems do not suffer from the calibration problems associated with the radiometers; they also overcome the cloud

cover problem associated with the infrared sensors used on satellites (microwave sensor estimates are currently possible only over the oceans). The GPS technology provides unattended, frequent, and accurate measurements at low cost. Being a new technology, how to effectively exploit the GPS measurements in operational forecasting remains a research problem.

### 1.2 Objectives

The overall goal of this study is to apply the GPS technology to forecast heavy rainfall, typically flash flood causing events, with the following specific objectives:

1. Develop a predictive scheme using the short trends in GPS-IPW.
2. Derive a predictive scheme that combines GPS, Radar and Radiosonde instrument based data to yield rainfall.
3. Apply the predictive schemes to assess their performance.

### 1.3 Organization of the thesis

Chapter 1 outlines the background, nature of the problem and the objectives of the report. Chapter 2 summarizes the general working principle of GPS. Chapter 3 presents the algorithms that utilize the GPS technology to calculate the integrated precipitable water (IPW). In Chapter 4 the criteria for predicting an event are derived. Specific case studies are also presented. Chapter 5 deals with the development of a mathematical model to estimate the rainfall amount due to an impending event. An example illustrating the various steps of the methodology is also presented. Chapter 6 summarizes the key contributions of the thesis. The bibliography contains all the cited references and other related studies. Appendices A, B, and C contain the needed procedures for obtaining the rainfall, integrated precipitable water, and radiosonde data respectively.

## Chapter 2 - GPS Methodology

### 2.1 Introduction

Global Positioning System (GPS) is a space-based radio positioning system that provides 24-hour three-dimensional position, and time information to suitably equipped users anywhere on or near the surface of the Earth. The GPS has three segments, space segment, which consists of 24 satellites orbiting the earth every twelve hours at an altitude of about 12,600 nautical miles (20,200 km) above the earth, user segment, which consists of receivers, and the control segment, which consists of five stations around the world to make sure that the satellites work properly. Four satellite vehicles orbit in each of six different planes inclined at $55^{o}$ to the equator. At that altitude there is very little atmospheric drag and the orbit is very stable. The United States Department of Defense (DoD) for its use in military purpose has developed the GPS. The DoD has four ground based monitor stations, three upload stations and a master control station. The master control station calculates the satellite paths and clock correction coefficients and forwards them to an upload station. The upload station transmits data to each satellite at least once in every day.

### 2.2 Working principle of GPS

GPS works on triangulation technique (see Figure 1). GPS determines the position coordinates on the earth using the information from four satellites. If the first satellite gives the altitude as 1000 miles then the point on the earth will be in a sphere whose radius is 1000 miles and the center as the satellite itself. If another satellite gives the elevation as 1100 miles then the position of the point on the earth reduces to the intersection of these two spheres, which is a circle. If a third satellite gives the elevation as 1200 miles then the position of the point on the earth reduces to the intersection of these three spheres, which are two points. Normally one point can be rejected by geometry and only the other point will be a feasible and that will be the position of the exact point on the earth. Else one has to take the elevation measurement from the fourth satellite also to determine the exact location on the earth. Distances measured from the

satellite are affected by certain delays and hence they are referred as pseudo range observations as they are not the exact measurements.

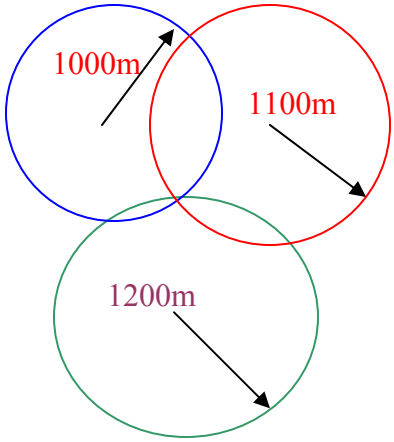


**Figure 2.1. Obtaining the position using Triangulation technique**

Hence four pseudo range observations are needed to resolve a position, but in practice there are even more than four satellites observing the same point. This is due to the clock biases contained both in the satellite and the ground-based receiver, which increases the complexity in obtaining the position coordinates on the ground. A pseudo range observation is equal to the true range from the satellite to the user plus delays due to satellite and receiver clock biases and other effects.

$$R = S + c.\Delta t + d \qquad (1)$$

where

R = observed pseudo range

S = true distance from the satellite (unknown)

c = velocity of propagation (usually velocity of light)

$\Delta t$ = clock biases

d = propagation delays due to atmospheric conditions

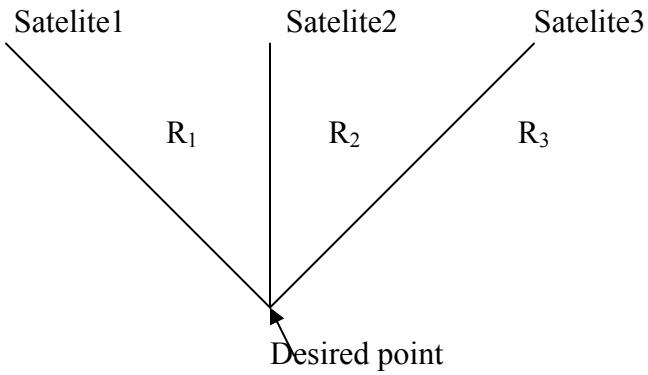

Desired point is the intersection of four spheres. If $t_1$ is the time taken by the signal to reach the ground then

$R_1 = t_1.c$

Where c is the velocity of light.

The following relation can be used to obtain the distance from the satellite to the user.

$$S = \left[(X^s - X^u)^2 + (Y^s - Y^u)^2 + (Z^s - Z^u)^2\right]^{1/2} \quad (2)$$

where

$X^s$, $Y^s$, $Z^s$ are known coordinates of satellite and $X^u$, $Y^u$, $Z^u$ are unknown coordinates of the observer or the user of GPS.

Once the pseudo ranges ($R_1$, $R_2$, $R_3$, $R_4$) are observed then the above equation for S can be used for different satellites. From equation (1) and (2) we get,

$$\left(R_1 - c.\Delta t - d_1\right)^2 = \left(X_1^s - X^u\right)^2 + \left(Y_1^s - Y^u\right)^2 + \left(Z_1^s - Z^u\right)^2$$

$$\left(R_2 - c.\Delta t - d_2\right)^2 = \left(X_2^s - X^u\right)^2 + \left(Y_2^s - Y^u\right)^2 + \left(Z_2^s - Z^u\right)^2$$

$$\left(R_3 - c.\Delta t - d_3\right)^2 = \left(X_3^s - X^u\right)^2 + \left(Y_3^s - Y^u\right)^2 + \left(Z_3^s - Z^u\right)^2$$

$$\left(R_4 - c.\Delta t - d_4\right)^2 = \left(X_4^s - X^u\right)^2 + \left(Y_4^s - Y^u\right)^2 + \left(Z_4^s - Z^u\right)^2$$

In the above equations unknowns are $X^u, Y^u$, $Z^u$ and $\Delta t$. The above solution is dependent on the accuracy of the position of the satellite, accuracy with which the delay can be modeled and the accuracy of the actual time measurement. If the true time for a signal in reaching the receiver is t and the observed time is t' then from the following relation one ca obtain the true time of travel.

$$t = t' + \Delta t \quad (3)$$

In general the time delays are free from satellite clock errors. This is due to the fact that satellite clocks are highly accurate and two station common view transfer technique can be used to remove the biases. The principle is as follows. Two GPS receivers are kept at stations A and B. Both the stations receive the signals of the same satellite at the same time, and synchronize their clocks to the satellite clock. At both the stations, the local clock of the GPS receiver is compared with that of an atomic time standard, by measuring the time delay. If these time interval measurements at stations A and B are respectively,

T A and T B, then (T A -T B) will be the offset. Hence in this approach satellite clock errors contribute nothing where as other errors due to ephemeris, atmosphere contribute to the delay.

### 2.2.1 Pseudo-Ranging

When GPS user performs a navigation solution, only an approximate range or pseudo-range to selected satellites is measured. With pseudo ranging receiver measures only an approximate distance between the satellite and the receiver. The distance the signal has traveled is equal to the velocity of the transmission of the satellite (which is the velocity of the light) multiplied by the elapsed time of transmission, with satellite signal velocity changes due to ionospheric and tropospheric conditions being considered.

## 2.3 Distance Measurement from Satellite

GPS sends radio signals and they travel at the speed of velocity of light in vacuum. If we can find the time traveled by the radio signal to reach the receiver then we can get the total distance between the receiver and the satellite by multiplying the velocity with the time elapsed. One way to get the time is by using the long digital pattern called the pseudo random code, which is transmitted by the satellite. Pseudo Random Code is a fundamental part of GPS. Physically it's just a very complicated digital code, or in other words, a complicated sequence of "on" and “off” pulses. The signal is very complicated and looks like a random electrical pulse. When GPS sends a signal it carries the pseudo random code. Receiver also generates the exact same digital pattern at the exact time when the satellite sends the signal. When the satellite's signal reaches the receiver, there will be a phase lag between the pulses generated by the receiver and the GPS (see Figure 2). The length of the delay is equal to the time of the signal's travel. From this phase lag one can estimate the time lag and hence the distance of the satellite from the receiver (from known velocity of light in vacuum). Receiver multiplies this time by the speed of light to determine how far the signal traveled. If the signal traveled in a straight line, this distance would be the distance to the satellite. These patterns are so complex that it's

highly unlikely that a stray signal will have exactly the same shape. Since each satellite has its own unique Pseudo-Random Code this complexity also guarantees that the receiver won't accidentally pick up another satellite's signal. So all the satellites can use the same frequency without jamming each other.

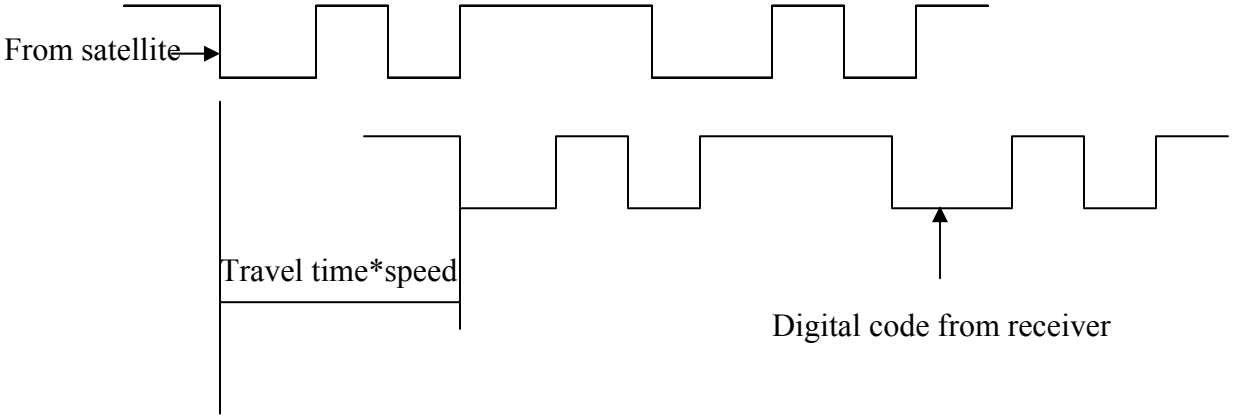


**Figure 2.2. Diagram showing the phase shift in the Pseudo-Random Code**

This technique is highly dependent on the accuracy of clocks in the satellite as well as in the receiver. Satellites use atomic clocks, which are highly accurate. Using the same clocks in the GPS receiver will increase the cost of the instruments enormously. Hence the receivers use quartz clocks and the data from the fourth satellite to correct the clock errors.

## 2.4 Signal Transmission to the Receiver

GPS satellite transmits a unique navigational signal centered on two L-band frequencies of the electromagnetic spectrum. They are L1 at 1575.42MHz and L2 at 1227.60MHz. These signals are easily blocked, reflected by solid objects and water surface. However, clouds are easily penetrated, but these signals can be blocked by dense or wet foliage. A satellite signal from satellite to the receiver basically consists of L band carrier waves, ranging codes and Navigational Message.

### 2.4.1 Carrier waves

Carrier waves provide means by which ranging codes and navigational messages are transmitted to the receiver. Each satellite is equipped with atomic clocks. These clocks

generate sinusoidal waves with frequency 10.23MHz. This is referred to as fundamental frequency. Multiplying this fundamental frequency with integer values gives us microwave L-band carrier waves L1 and L2 respectively. L1 is obtained by multiplying with an integer value of 154 and L2 is obtained by multiplying with 120. Hence these two have frequencies of 1575.42 MHz and 1227.6 MHz respectively. These carrier waves are just electromagnetic waves. They do not carry any information. To retrieve information from these waves they must be modulated. In GPS system normally two codes are used to modulate these L-band carriers. One is ranging code and the other one is the navigational message.

### 2.4.2 Ranging Codes

The main purpose of ranging code is to determine the signal transit time, which is from the satellite to the receiver. This time when multiplied with the velocity of electromagnetic radiation (normally the velocity of light in vacuum) gives the range of the satellite from the receiver. The two ranging codes used are Coarse Acquisition (C/A) code for civilian purposes and the P-code or Precise-Code for military purposes. Both these codes are binary codes but they have the characteristics of random noise. Hence these are called pseudo random noise (or PRN) codes. These codes measure the one-way distance to the satellite from the user or receiver. L1 carrier is designed to be modulated with two codes, one for civilian purposes and the other for military purposes, where as L2 is designed to be modulated for military purposes only. Both these carriers contain the navigational message.

- Coarse Acquisition (C/A) code

This modulates the L1 carrier phase. This is a 1MHz repeating Pseudo Random Noise (PRN) Code. The C/A code repeats every 1023 bits (one millisecond). Each satellite has its own C/A code PRN. Their unique PRN number for each pseudo random noise code often identifies GPS satellites. This is the basis for SPS (Standard Positioning System). The frequency of C/A code is 1MHz, which means this entire sequence repeats itself once in every millisecond. The wavelength of this C/A code is 300 m.

- Standard Positioning System (SPS)

SPS is timing and positioning service, which is provided on the L1 frequency. This contains coarse acquisition (C/A) and navigation data message. The SPS is therefore has the capability to provide a user with one basic C/A code receiver. The P-code and L2 frequency are unavailable for the users.

- P (precise)-code

This modulates both L1 and L2 carrier frequencies. The P-code is 10MHz PRN code and the wavelength is 30 m hence it has 10 times better resolution compared to C/A code. This is the basis for the PPS (Precise Positioning System).

- Precise Positioning System (PPS)

PPS gives a more precise measurement of the position and timing compared to SPS. This uses SPS signal plus P code on L1 and L2 and the carrier phase measurements on L2.

### 2.4.3 Navigation Message

Navigational Message contains the satellite ephemeris, satellite clock parameters, and other pertinent information such as general system status messages and an ionospheric delay model, necessary for real-time navigation to be performed. This modulates the L1-C/A code signal. It is a 50 Hz signal consisting of data bits that describe the GPS satellite orbits, clock corrections, and other system parameters. Navigational Message can only be transferred with the knowledge of ranging codes. Each receiver is capable of replicating the same code sequence. A given C/A (or P) code will correlate with an exact replica of itself only when the two codes are aligned.

As mentioned earlier when GPS performs navigation only an approximate or pseudo range is measured. One reason being receiver clocks are not as precise as the atomic clocks, which are there in the satellite. Hence each range contains receiver clock errors. This is the reason for having the fourth satellite in all practical situations, as there are four variables involved, three for position coordinates and one for the receiver clock offset. Ranging can be done using either P-code or C/A code. As P-code can operate on both L1 and L2 frequencies (or a linear combination of these frequencies) ionospheric delay can be eliminated using P-code. As C/A code resolution is more coarser compared to P-code,

ranges derived from this code will have more error compared to the ranges derived from P-code.

### 2.4.4 Recovering ranging codes

Satellite sends a signal and say L1 carrier and it is modulated on C/A code. At the same time receiver generates a replica of the same code but this is generated on a different time scale that of incoming C/A code. When the incoming code and the code produced by the receiver are aligned (by sliding the received code sequence against that internally generated sequence), carrier signal is modulated only by the Navigational Message. As mentioned earlier C/A code has a wavelength of 300 m and P-code has 30 m. It is generally assumed that incoming and receiver generated codes can be aligned with an accuracy of 1-2% of their wavelengths. Hence precision of C/A code is 3 to 5 meters where as for P-code it is 0.3 to 0.5 meters.

## 2.5 Differential Positioning

Differential GPS (DGPS) is a method of eliminating errors in a GPS receiver to make the output more accurate. Differential GPS (DGPS) corrections have reduced positioning errors from about 100 meters to roughly 1 meter. There are two ways in which differential positioning is done.

### 2.5.1 Pseudo-Range Tracking

It involves using a receiver at a known location, the base station and collecting GPS positions at unknown locations with other receivers, rovers or remotes. In pseudo ranging technique time delay is measured by comparing the pseudo random code generated by the receiver and the satellite. Common errors are caused by factors such as clock deviation, selective availability and changing radio propagation conditions in the ionosphere. Differential GPS requires a minimum of two receivers set up at two stations to collect satellite data. One is stationary and the other one roves around making position measurements. It works in the following way. Stationary reference receiver is placed at a site for which the coordinates are exactly known. This reference site receives the exact signal as the roving receiver but the reference site calculates the equations backwards as

the coordinates of the reference are known. It calculates the time of travel for the microwave from the satellite to the receiver and compares it to the actual time taken from the measurement. The difference is an error correction factor. Since the distance between the receiver and the satellites is very large even if the distance between the two receivers (base receiver and the roving receiver) is few hundred kilometers the signal traveling the base as well as the roving receiver travels through the same atmosphere and hence virtually the same atmospheric errors can be assumed in both the receivers. Since the reference receiver does not know the exact satellites, which the roving receiver might be using to calculate the distance it runs the error calculation for all the available satellites and transmits this information to the roving receiver.

### 2.5.2 Carrier Phase Tracking

Differential positioning using carrier phase tracking uses the same formulation of equations as that of pseudo range technique but it is a bit more complex because the carrier signals are tracked such that range changes are measured by phase resolution. Because of its high wavelength no matter how accurately we match both the codes, they will be a bit out of phase.

### 2.5.3 Comparison between the tracking systems

Pseudo-Range technique has a bit rate of 1MHz where as the carrier frequency has a cycle rate of 1.57GHz. A rule of thumb is to have an accuracy of 1 to 2 percent of the wavelength hence pseudo range tracking has an accuracy of few centimeters. Assuming the same rule of thumb, as the accuracy is 1 to 2 percent of the wavelengths, precision of carrier phase tracking is few millimeters compared to few meters or few centimeters that of ranging codes and hence carrier waves can act as a much more accurate references than pseudo random codes. The problem with carrier phase is that it is hard to count carrier frequency, as it is very uniform where as pseudo random code is intentionally made complex so that one can know the cycle they are looking at, also with carrier phase measurement one cannot differentiate between L1 and L2 frequencies. The phase measurement in carrier phase tracking is always between 0 to 360 degrees but because of its precision it is the basis for GPS surveying.

### 2.5.4 Differential Correction

Once the error is established in the position, correction is applied using this technique. There are two ways to do differential correction, real time and post processed correction.

### 2.5.5 Real-Time differential correction

In real time differential GPS, the base station calculates and broadcasts the error (through radio signals) as it receives the data for each satellite. Rover receives the correction and applies to the position for which it is calculating. The result is that the position is differentially corrected position. This is useful when the person is in the field.

### 2.5.6 Post-Processed Differential Correction

In this the base station records the error for each satellite directly into a computer file. The rover also records its own position on a computer file. These two files are run through a process in the software and the output is a differentially corrected rover file. This is more accurate compared to real time correction.

## 2.6 Summary

This chapter gives a description of the working principle of GPS. Measurement of position, about the carrier waves and the methodology in retrieving the information from the carrier waves are discussed. Finally errors that are incurred in the calculation and the methods to correct these errors are also discussed. In the next chapter calculation of the total available water vapor in an atmospheric column using the delays in the electromagnetic waves when they travel through atmosphere is discussed. This information is used to predict the heavy rain causing events with a better lead-time.

# Chapter 3 - Precipitable Water Estimation by GPS

## 3.1 Introduction

Forecasters at the National Weather Service (NWS) at Blacksburg, VA currently issue a routine quantitative precipitation forecast (QPF) product once per day. This product includes expected precipitation amounts during a 24-hour period (beginning 1200 UTC that morning to 1200 UTC the following morning) for the entire Hydrologic Service Area (HSA), and is divided into four 6-hour periods. The product is created by drawing isohyets of basin average precipitation. The graphical forecasts for each period are then automatically converted to a digital format and sent to the four River Forecast Centers (RFC) that cover main stem river forecasts for the Blacksburg HSA. The RFCs use these QPFs as input to their hydrologic models for river stage (and potential flood) forecasts.

## 3.2 Forecast Methodology

A number of tools are used by forecasters to determine the QPF values they generate for the RFCs in the product described above. For the first 6-hour period the forecast may rely more heavily on observations, including rain gage readings from upstream, radar precipitation estimates, and occasionally precipitation estimates from weather satellites, but may also include QPF output from several numerical forecast models run by the National Center for Environmental Prediction (NCEP) in Washington, DC. The forecasts beyond the first 6 hours tend to rely more heavily on the guidance from the numerical models. In addition, NCEP contains a branch of forecasters who issue manual QPF guidance products when significant precipitation is expected. Local forecasters use their knowledge of individual model strengths and weaknesses, their knowledge of the local terrain influences, and their experience with similar weather regimes to make their final QPF for that 24 hour period. Overall, the methods are quite subjective (especially in the shorter term period). Beyond 6 hours, if a model is thought to be handling the overall forecast well, the QPF values from that model may be followed rather closely, and then the forecast becomes more objective.

### 3.2.1 Very Short Term QPFs

Currently, the NWS has no official QPF product for the very short term period (i.e. 1 to 3 hours). Flooding that may occur on this time frame is considered "flash flooding" and these forecasts generally do not rely on hydrologic stream models from the RFCs. However models of soil moisture provide guidance for rainfall thresholds that might produce flash flooding. However, there is no objective-based methodology used by the NWS in Blacksburg for QPFs in the very short term. Forecasters rely most heavily on real-time rain gage readings in combination with radar estimates, subjectively adjusting the radar estimates based on the "ground truth", and then factor in storm motions observed by the radar. Knowledge of the environment in terms of support for high precipitation amounts, as well as the anticipated strength, organization, longevity, and speed of storms are also used to make short term (1-3 hour) predictions of rainfall amounts. The WSR-88D radar contains algorithms that forecast predicted storm tracks once individual storm cells are identified, but this is a linear extrapolation and does not account for cell mergers, splits, or cell development and demise (which can often occur on the order of 10-20 minutes for the thunderstorm scale).

The potential for heavy rains is determined in terms of moisture, lift, and stability parameters. Obviously, precise QPFs for the very short term would improve warnings, and especially the lead time, as it would for flash flood forecasts. In order to achieve this, a more objective based-methodology or automated series of algorithms need to be developed. In the rainfall mode the WSR-88D radar has a scan range of 230 km radius. Typically, one might use a range of 75 to 150 kms to avoid excessive beam heights at greater ranges in estimating rainfall amounts. For a storm moving at a speed of 40 km/hr from the edge of the radar range to the effective range of consideration, it yields about one to two hour lead time. Also, the parameters of consideration are available for the entire range at about 6 minute increments.

### 3.3 GPS meteorology

Recently, the NOAA Forecast Systems Laboratory (FSL), as well as other federal government agencies, have begun employing global positioning system (GPS) technology to measure IPW from sensors at select locations around the U.S. The temporal resolution of these data is 30 minutes, and new implementation of processing techniques can make the data available within 10 to 20 minutes of real-time with a possibility of retrieval in real time if multiple close-by receivers are available (Seth Gutman, personal communication, 2002). One of these sensors was installed at NWS RNK in 1999 (BLKV, and is co-located with the upper air observation site. The GPS systems do not suffer from the calibration problems associated with the radiometers; they also overcome the cloud cover problem associated with the infrared sensors used on satellites (microwave sensor estimates are currently possible only over the oceans). The GPS technology provides unattended, frequent, and accurate measurements at low cost. Being a new technology, how to effectively exploit the GPS measurements in operational forecasting remains a research problem.

#### 3.3.1 Space based GPS meteorology

The branch of GPS meteorology, using a GPS receiver spaced on board of a Low Earth Orbiting (LEO) satellite is referred to as space based GPS meteorology. This provides profiles of Integrated Refractive Index. As there is a unique relationship between the total refractive bending angle and the measured refractive index, the refractivity for each layer can be determined from the measured angle. Atmospheric refractivity (N) can be approximated (Smith and Weintraub, 1953; Thayer, 1974) by

$$N = 77.6\frac{P_d}{T} + 3.73 * 10^5 \frac{P_w}{T^2}$$

Where $P_d$ is the partial pressure of the dry air (in hPa), T is the temperature of the atmosphere (in K) and $P_w$ is the partial pressure of the water vapor (in hPa) in a layer. Using this refractivity total delay caused by the atmosphere can be obtained.

### 3.3.2 Ground-based GPS meteorology

GPS-IPW is a ground-based technique that measures integrated precipitable water vapor directly above a fixed site. In this methodology satellites send electromagnetic signals to the ground based receivers, which are fixed in location on the earth. Signal delay is measured from these fixed points on ground. Total delay in the signals is measured and the precipitable water vapor is obtained by the delay caused by the water vapor in the troposphere. Water vapor and dry gases of the neutral atmosphere delay the radio signals, received by a ground-based GPS receiver. For this reason the total tropospheric delay (TD) can be partitioned into the wet delay (WD), which is a function of the water vapor distribution and the hydrostatic delay (HD), which depends on the dry gases in the troposphere. Figure 3.1 shows the GPS meteorology.

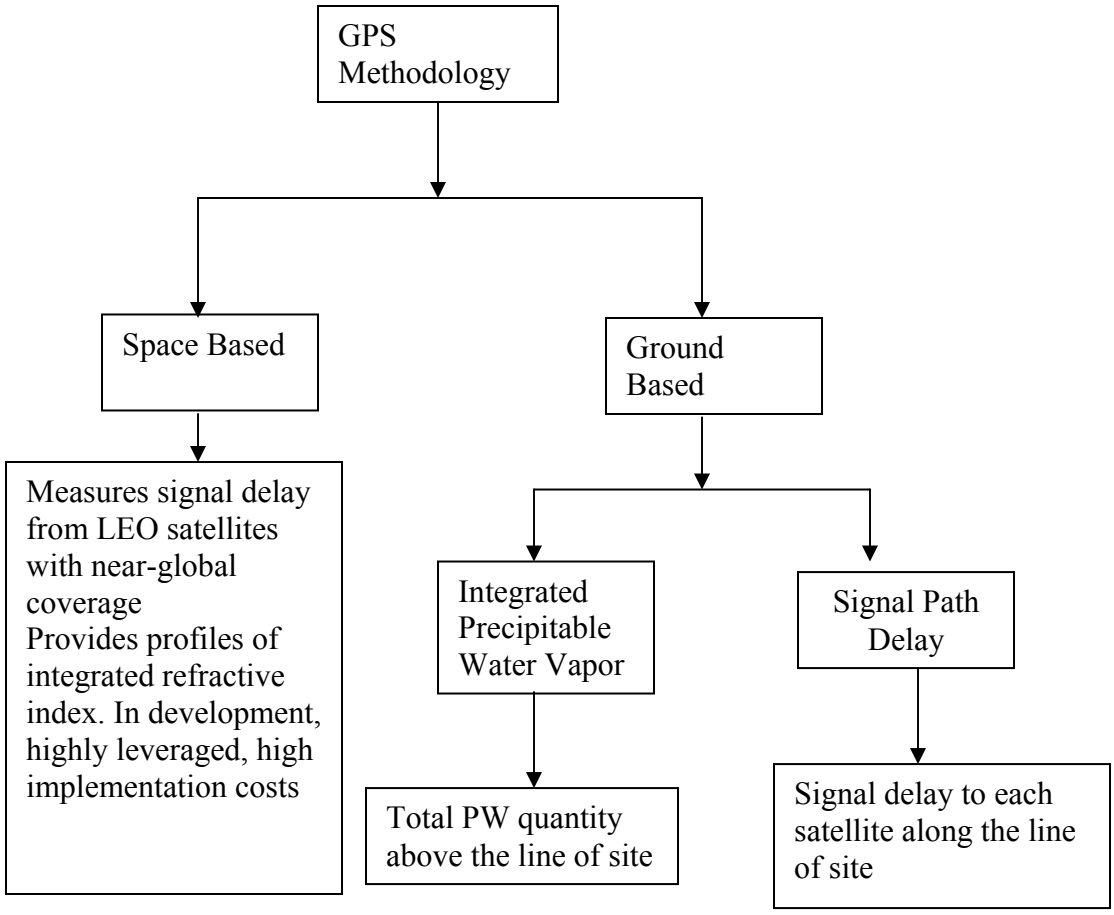


**Figure 3.1. GPS Methodology**

### 3.4 Error Sources in the Ground-based GPS methodology

Propagation delays in the atmosphere are caused by dry air, water vapor, hydrometeors and other particulates (sand, dust and volcanic ash). The delay is defined as the excess path from the satellite to the receiver compared to travel through a vacuum. These delays must be properly characterized to achieve the highest accuracy in surveying and other measurements using Global Positioning System (GPS) signals. Water vapor is typically the largest source of variable atmospheric delay. Signals transmitted by Global Positioning System (GPS) satellites are increasingly used for high accuracy scientific applications including studies of weather, climate etc. Atmosphere-induced propagation path delays are major contributors to GPS measurement error. Changes in the distribution of water vapor are associated with clouds, convection, and storms. Total delay caused by these error sources is estimated to be around 40 to 65 nanoseconds in many cases.

#### 3.4.1 Ephemeris Errors

Ephemeral errors arise due to the error in the prediction of the position of satellite. These errors are dependent on the satellite position and are tough to model, as the forces on the predicted orbit of a satellite are difficult to measure directly. The Department of Defense constantly monitors the orbit of the satellites looking for deviations from predicted values. Any deviations (that is ephemeris errors) determined to exist for a satellite, the errors are sent back up to that satellite, which in turn broadcasts the errors as part of the standard message, supplying this information to the GPS receivers. With this information position of GPS can be very accurately determined.

#### 3.4.2 Clock Errors

If the clock of the receiver were perfect, then all our satellite ranges would intersect at a single point (which is our position). But with imperfect clocks, a fourth measurement, done as a crosscheck, will not intersect with the first three. Since any offset from universal time will affect all of our measurements, the receiver looks for a single

correction factor that it can subtract from all its timing measurements, which would cause them all to intersect at a single point. Once it has that correction, it applies to all the rest of its measurements and precise positioning is achieved. One consequence of this principle is that any decent GPS receiver will need to have at least four channels so that it can make the four measurements simultaneously. Another source of inaccuracy is the speed of the electromagnetic waves, which are sent by the satellite. Velocity of these waves is same as the velocity of light in vacuum but as they travel from satellite before they reach the receiver they travel through ionosphere and troposphere. Hence the velocity also has to be modeled according to the atmospheric conditions. GPS receiver calculates the actual speed of the signal using complex mathematical models of a wide range of atmospheric conditions. Satellites also transmit additional information to the receivers.

### 3.4.3 Atmospheric Delays

GPS signals are delayed and refracted by the gases comprising the atmosphere as they propagate from GPS satellites to the Earth-based receivers. In particular, a significant and unique delay is introduced by water vapor. The distribution of water vapor is closely coupled with the distribution of clouds and rainfall. Because of the large latent heat release of water vapor during a phase change, the distribution of water vapor plays a crucial role in the vertical stability of the atmosphere and evolution of storm systems. The water molecule has a unique structure that results in a permanent dipole moment. This dipole moment results from an asymmetric distribution of charge in the water molecule. Dipole: A molecule that has two opposite electrical poles or regions separated by a distance. The first moment of charge distribution is given my dipole moment.
If the water molecule has an asymmetric distribution of charge then it acts as a dipole. Under normal circumstances water is a neutral molecule. But the orientation of hydrogen and oxygen molecules makes it a polar molecule that is it will have small amount of positive and negative charges at the ends. When the water molecule gains lot of energy mainly from sun, polarization increases, as the atoms in it will be in an excited sate. This causes it to have dipole moment.

This retards the propagation of electromagnetic radiation through the atmosphere. Thus, knowledge of the distribution of water vapor is essential to understand weather and global climate. The delay in GPS signals reaching Earth-based receivers due to the presence of water vapor is nearly proportional to the quantity of water vapor integrated along the signal path. Figure 3.2 shows how the atmospheric delay is modeled.

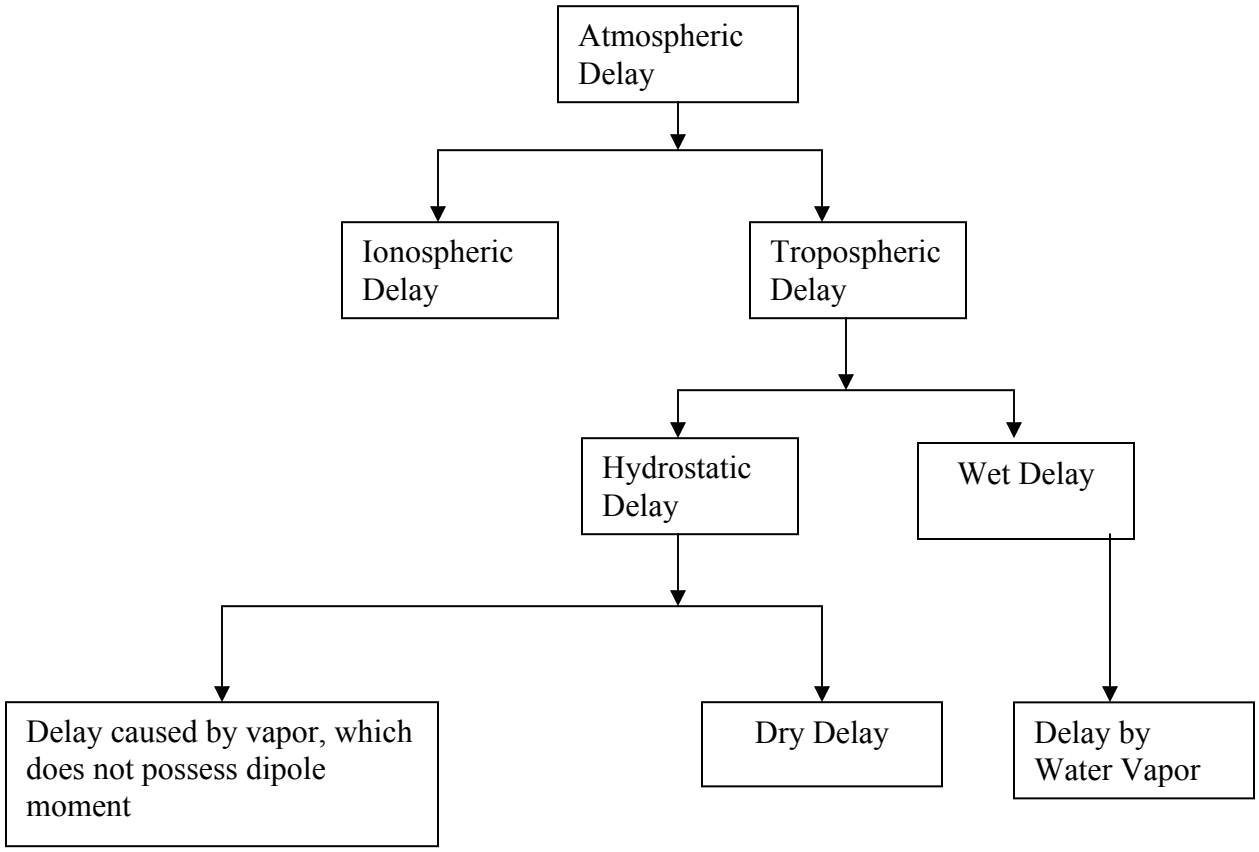


**Figure 3.2. Modeling Atmospheric Delay**

- **Ionospheric delay**

Ionosphere contains electrically charged particles from129 km to 193 km above the earth. Sun's ultra violet rays ionize a gas molecule, which then loses electrons. These free electrons in the ionosphere influence the propagation of microwave signals as they pass through the layer. Ionospheric delay on GPS signals is frequency-dependent and hence impacts on L1 and L2 signals by different amounts. A linear combination of pseudo range or carrier phase observations on L1 and L2 can be made to eliminate ionospheric delay. This is useful for dual frequency receivers. For single frequency receivers a model is contained within the navigational message but this is not as effective as the dual frequency one. Magnitude of the Ionospheric delay is a function of the latitude of the receiver, season, time of the day and solar activity. Ionospheric delay increases inversely with the "sine" of the elevation angle and hence as the elevation angle of the receiver reduces, delay in the zenith increases. Differential positioning mostly eliminates this delay. Dual-frequency GPS receivers intended for surveying applications can make L2 measurements which are essential to eliminate ionospheric delay. If $\phi(L1)$ is the phase observation made on L1 frequency and $\phi(L2)$ is the phase observation made on L2 frequency then combining them in a linear relation results in an ionosphere-free, observable, which is given as

$$\phi(L3) = 2.546\phi(L1) - 1.984\phi(L2) \quad (1)$$

Maximum effect of ionospheric delay is on the speed of the signal, and hence ionosphere primarily affects the measured range. Ionospheric delays can be corrected with millimeter accuracy by sending GPS signals at two different frequencies. Troposphere or neutral atmosphere is nondispersive at GPS frequencies and hence it cannot be corrected in the way the ionospheric delay is corrected.

- **Tropospheric or Neutral atmospheric delay**

Most of the water vapor in the atmosphere resides in the troposphere, which ranges in depth from 9 km at poles to more than 16 km at the equator. Neutral atmosphere is made up of dry gases and water vapor. Water vapor in this possesses a dipole moment to its refractivity. Tropospheric delay can be separated into hydrostatic and wet components. Hydrostatic delay is often erroneously referred to as dry delay. Hydrostatic delay consists

of delay caused by water vapor that does not possess dipole moment as well as the delay caused by the dry gases. Delay caused by dry gases is called the dry delay. Hydrostatic component in the zenith direction is called ZHD (zenith hydrostatic delay). It can be precisely determined by surface pressure measurements. If the atmosphere is in hydrostatic equilibrium and the barometer is well calibrated, then the zenith hydrostatic delay can be determined with an accuracy of few millimeters.

Wet delay is far more variable compared to hydrostatic delay even though its magnitude is very less compared to hydrostatic delay. The ZWD (Zenith Wet Delay), however, cannot be sufficiently modeled by surface measurements due to the irregular distribution of water vapor in the atmosphere. Geodesists have found an alternate approach to estimate the time varying zenith-wet delay from GPS measurements. Since it is highly difficult to predict the wet delay from surface meteorological measurements, geodesists predict the hydrostatic delay from surface measurements and attempt to measure the wet delay by knowing the total delay. Zenith wet delay can be as small as a few centimeters or less in arid regions and as high as 35cm in humid regions. These delays are smallest for paths oriented along the zenith direction and increase inversely with the sin of the elevation angle.

- **Calculation of Zenith Wet Delay**

Get the total delay from the GPS network.

Total Delay = Ionospheric Delay + Neutral Delay

Determine the ionospheric delay from comparison of two different GPS (L1 and L2) signals recorded with dual band GPS receiver and calculate the neutral delay from known total delay.

Neutral Delay = Total Delay – Ionospheric Delay

Zenith Neutral Delay (ZND) is the sum of Zenith Hydrostatic Delay (ZHD) and Zenith Wet Delay (ZWD). ZHD is calculated from surface pressure, temperature and humidity measurements.

ZWD = ZND – ZHD

From ZWD precipitable water vapor (PWD) is done from computer or statistical / analytical temperature model. In estimating the zenith-wet delay it is assumed that there

is an azimuthal symmetry around the GPS receiver. But azimuthal variations of 20% are quite commonly observed in humid areas.

- **Obtaining the total delay**

The atmosphere affects microwave transmission in two ways. First, waves travel slower in atmosphere than they would in vacuum. Second, they travel in a curved path than a straight line. Both these effects arise due to the variability of refractivity in the atmosphere along a ray path (Bevis, 1992).

The excess path length or path delay is $\Delta L = \int_L n(s)ds - G$

Where n(s) is the refractive index as a function of s along the curved path L and G is a straight ling geometrical path length through the atmosphere, which is the path of the ray if a vacuum replaces the atmosphere. Equivalently,

$$\Delta L = \int_L [n(s) - 1]ds + (S - G) \qquad (1)$$

Where S is the path length along L. First term on the right hand side is due to the slowing effect and the second one is due to bending. For paths above 15° the term (S – G) is very small and of the order of 1 cm or less. For the ray path along the zenith the term entirely vanishes in the absence of horizontal gradients in refractivity index (n). The above equation is formulated in terms of atmospheric refractivity N.

$$N = 10^6(n-1)$$

Hence the equation (1) becomes

$$\Delta L = c_0(t - t_0) = \int_H^\infty (n-1)dz = 10^{-6}\int_H^\infty Ndz$$

Where the integration is performed along the ray path, n is the refractive index, N is the refractivity of the atmosphere and H is the height of the receiving station; $c_o$ is the velocity of light in vacuum, t is the propagation time through the atmosphere and $t_o$ is the propagation time for the same distance in vacuum. For directions other than zenith, the delay is usually observed from the zenith delay by using map functions, which depend upon the meteorological parameters and the zenith angle.

Expression used to calculate N (Thayer, 1974) is

$$N = (k_1 p_d / T) / Z_d + (k_2 e / T) / Z_w + (k_3 e / T^2) / Z_w$$

Where $p_d$ and e are the dry air (in millibars) and water vapor partial pressures in millibars and T is the temperature in degrees Kelvin. $Z_d$ and $Z_w$ are compressibility factors for dry air and water vapor respectively. The constants $k_i$, i=1,2,3 are evaluated by actual measurement of refractive index.

These values from the measurements are (Thayer, 1974)

$k_1 = (77.6 \pm 0.014)$ K mbar$^{-1}$

$k_2 = (64.79 \pm 0.08)$ mbar$^{-1}$

$k_3 = (3.776 \pm 0.004) \times 10^5$ K$^2$ mbar$^{-1}$

First two terms in the above equation represent the effect due to air and water vapor molecules which do not possess dipole moment and the third term represents the effect of the permanent dipole moment of the water vapor molecule.

The compressibility factors in the above equation represent the nonideal behavior of their respective atmospheric constituents. The ideal gas law describes this behavior.

$p_i = Z_i \rho_i R_i T$ where $p_i$ is the partial pressure, $Z_i$ is the compressibility, $\rho_i$ is the mass density, $R_i$ is the specific gas constant for that constituent and T is the absolute temperature. For an ideal gas Z = 1 it differs from unity by few parts per thousand for the atmosphere. Expressions for inverse compressibility factors ($Z^{-1}$) are obtained by fitting least squares to thermodynamic data. Expressions are

$$Z_d^{-1} = 1 + p_d \left[ 57.97 \times 10^{-8} \left( 1 + \frac{0.52}{T} \right) - \frac{9.4611 \times 10^{-4} t}{T^2} \right] \text{ and}$$

$$Z_w^{-1} = 1 + 1650 \left( \frac{p_w}{T^3} \right) \left( 1 - 0.01317t + 1.75 \times 10^{-4} t^2 + 1.44 \times 10^{-6} t^3 \right)$$

where t is the temperature in degrees Celsius, $p_d$ and $p_w$ are partial pressures of dry and water vapor in millibars and T is in Kelvin.

As mentioned above the total delay can be written as the sum of two terms. The first term is called the zenith hydrostatic $(\Delta L_h)$ term. Its value is given as

$$\Delta L_h = (2.2779 \pm 0.0024) \frac{P_o}{f(\phi, H)}$$

where $P_o$ is the total pressure at the ground in millibars and

$f(\phi, H) = (1 - 0.00266\cos(2\phi) - 0.00028H)$ is used to model the variation of the acceleration due to gravity with the latitude and height above the station in kilometers. The second term of the total delay, the zenith-wet delay $\Delta L_w$, is defined as

$\Delta L_w = 10^{-6}\left[(17 \pm 10)\int_0^\infty \frac{e}{T}ds + (3.776 \pm 0.03)\times 10^5 \int_0^\infty \frac{e}{T^2}\right]$ expressed as the same units as the path s, T is the temperature in Kelvin, and e is the partial pressure of water vapor in millibars.

Most of the wet delay occurs in the lower troposphere. Although there are approximate models in predicting the zenith-wet delay from surface pressure measurements they are not as accurate compared to the models predicting the dry delay. In practice wet delay must be obtained using radiosonde launches or WVR's (Water Vapor Radiometer) or using GPS technology.

- **Estimation of wet delay using GPS**

The description given here is based on Borbas, 1997; Duan et al., 1996; Rocken et al., 1995; and Bevis et al., 1992. GPS satellites transmit microwave signals at 1.2 and 1.6 GHz through the Earth's atmosphere. The ionosphere and neutral atmosphere (interchangeably called troposphere for this discussion is made up of a mixture of dry gases and water vapor) slow down the speed of these signals. Because the ionospheric delay is approximately proportional to the inverse square of the signal frequency, by utilizing dual frequencies (L1 and L2 dual band receiver) it is possible to measure it. The neutral delay is obtained by subtracting the ionospheric delay from the total delay obtained from the GPS (See http://www.paroscitific.com/gpsmet).

neutral atmospheric delay, ZND = total delay from the GPS – ionospheric delay (1)

The neutral delay, ZND, is the sum of the hydrostatic, ZHD, and wet components, ZWD and

$$ZND = ZHD + ZWD \quad (2)$$

The hydrostatic component in the zenith direction, ZHD is primarily made up of the dry gases in the atmosphere plus the nondipole contribution of the water vapor. It can be determined by surface pressure measurements given by

$$ZHD = \frac{(2.2779 \pm 0.0024)P_S}{1 - 0.00266\cos 2\lambda - 0.00028H} \quad (3)$$

in which: Ps is the total pressure in (hPa) at the earth's surface, the denominator is the variation of the gravitation acceleration with latitude, λ and the height, H above the ellipsoid for the station in Km. Typical value of ZHD is 2.3 m at the sea level in the zenith direction and it varies from 90-100 percent of the total tropospheric delay in the same proportion as the dry to wet substances of the atmosphere. The variability in the total delay is dominated by the wet delay (Wolfe and Gutman, 2000; http://pecny.asu.cas.cz/meteo/Info.html).

The ZWD (zenith wet delay) is hard to model by surface measurements due to the irregular distribution of water vapor in the atmosphere. The wet component, ZWD, is due to water vapor's dipole moment contribution to its refractivity. For most of the troposphere the dipole component of the refractivity is about 20 times larger than the nondipole component (Bevis et al., 1992). Obtain the wet delay, ZWD by

$$ZWD = ZND - ZHD \quad (4)$$

The value of zenith-wet delay (ZWD) can be less than 1 cm in arid regions and its maximum can reach about 40 cm in humid areas.

- **Estimation of zenith precipitable water from wet delay**

GPS calculated wet delay could be converted to PW by the following expressions.

$PW = k\ ZWD$

with (Bevis et al., 1994)

$$k = \frac{10^6}{\left(\rho_W R_V \left(\frac{K_3}{T_m} + K_2'\right)\right)}$$

where: $\rho_w$ is the density of water, Rv = 461.495 Jkg-1K-1 is the specific gas constant of water vapor, $K'_2 = 22.1 \pm 2.2$ (K/hPa) and $K3 = (3.739 \pm 0.012)105$ (K/hPa). The weighted mean temperature of the atmosphere, Tm is defined as

$$T_m = \frac{\int \left(\frac{P_V}{T}\right) dz}{\int \left(\frac{P_V}{T^2}\right) dz}$$

in which: Pv is the partial pressure of water vapor and T is the absolute temperature. $T_m$ can be estimated by $T_m = 70.2 + 0.72\,T_S$ (K), where $T_S$ is the surface temperature.

For a given location zenith wet delay can be calculated from different satellites looking at the location at the same time and these simultaneous measurements can be averaged and perceptible water vapor can be calculated from that averaged wet delay.

### 3.4.4 Multipath Delay

Multipath delay arises due to the reflectance of GPS signal near large reflective surfaces such as metal buildings and tall structures. GPS signals received as a result of multipath give inaccuracies in the time as well as in the position of the GPS. Averaging of GPS signals over a period of time or using the new equipment of receivers and sound prior mission can minimize the effect of multipath.

### 3.4.5 Selective Availability (SA)

Selective Availability is the intentional alteration of the time and epherimis signal by the Department of Defense (DoD). Positional errors caused by SA can be removed by differential correction. The accuracy degradation is implemented by DoD in two ways. First, predetermined errors are introduced into the navigation data transmitted by the satellites; which is called epsilon. By this, unauthorized users get erroneous position. Secondly, the satellite clock is altered and this is called dithering.

### 3.4.6 Anti Spoofing (AS)

AS is the deliberate encryption of P-code. When P-code is encrypted, it is called Y-code. AS accuracy loss in dual frequencies is partly due to the inability to determine the ionospheric delay in real time.

## 3.5 Estimation of errors using differencing

Several characteristics of the GPS phase measurement effect the wet delay measurement. The observed minus computed phase measurement is not only biased by the wet delay but also by the GPS satellite clocks, the receiver clock, and the integer carrier phase cycle ambiguities. Satellite clock errors are cancelled by single differencing method. In this method difference of simultaneous measurements from same satellite using two different receivers is taken. Single differences are nearly free of satellite clock errors but they are affected by receiver clock errors. Receiver clock errors are removed by double differencing, which is the difference between the single differences.
Doubly differenced phase difference observations are virtually free of clock errors but have career ambiguities. As long as the GPS satellite receiver maintains single clock, cycle ambiguities remain constant and are integer multiples of GPS career wavelengths. GPS software can distinguish between carrier ambiguities and wet delay as carrier frequencies remain constant but the wet delay changes roughly as 1/sin(satellite elevation angle).

### 3.5.1 Absolute tropospheric estimation

Absolute estimation requires the distance between the two locations to be at least 500 km. Wet delay can be computed from the GPS data only. Hydrostatic delay is calculated apriori from pressure measurements and then wet delay is calculated knowing the total delay from the GPS measurements. The following equation is used to get the delay (Rocken, 1994).

$ZD_{GPS} = \left(ZD_{actual} - ZD_{apriori}\right) + \delta ZD_{GPS}$ where $ZD_{GPS}$ is estimated GPS zenith delay, $ZD_{actual}$ is tropospheric zenith delay, $ZD_{apriori}$ is the applied apriori correction and $\delta ZD_{GPS}$ is the error of the GPS estimate. Total has hydrostatic and wet delay components.

$$ZD_{actual} = ZD_{hydrostatic} + ZD_{wet}$$

The apriori estimate of the hydrostatic delay has an error $\delta ZD_{hydrostatic}$ due to barometric calibration errors and errors in relating pressure observations to delays.

$$ZD_{apriori} = ZD_{hydrostatic} + \delta ZD_{hydrostatic}$$

Hence we get

$$ZD_{GPS} = ZD_{wet} - \delta ZD_{hydrostatic} + \delta ZD_{GPS}$$

Absolute estimation is effected by hydrostatic delay errors at one site $\delta ZD_{hydrostatic}$ and by GPS errors. The error of the estimated wet delay is given by

$$\delta ZD = \left(\delta ZD^2_{hydrostatic} + \delta ZD^2_{GPS}\right)^{1/2}$$

The main advantage of this method is that it requires only GPS receivers and barometers and the disadvantage is that it does not work over short distances.

### 3.5.2 Differential tropospheric estimation

In differential estimation, tropospheric delays are estimated relative to a reference site. For the reference site both hydrostatic and wet delays are known apriori from barometer and WVR measurements, respectively. Only hydrostatic corrections are

applied at secondary GPS sites and hence GPS estimated differential tropospheric delay is the wet delay at the secondary sites. $ZD_{GPS}$ can be estimated as

$$ZD_{GPS} = \left(ZD_{actual} - ZD_{apriori}\right)_{ref} - \left(ZD_{actual} - ZD_{apriori}\right)_{\sec ond}$$

Apriori delay at the reference site is estimated as

$$ZD_{apriori_{ref}} = \left(ZD_{hydrostatic} + \delta ZD_{hydrostatic} + ZD_{wet} + \delta ZD_{wet}\right)_{ref}$$

and at apriori delay at the secondary site is given as

$$ZD_{apriori_{\sec ondary}} = \left(ZD_{hydrostatic} + \delta ZD_{hydrostatic}\right)_{\sec ondary}$$

Tropospheric GPS estimate can be written by knowing the total delay at the reference site and the hydrostatic delay at the secondary site apriori.

$$ZD_{GPS} = \left(\delta ZD_{hydrostatic} + \delta ZD_{wet}\right)_{ref} + \left(ZD_{wet} + \delta ZD_{hydrostatic}\right)_{\sec ondary} + \delta ZD_{GPS}$$

where $\delta ZD_{wet}$ is the error of the apriori estimation of the wet delay at the reference site. If the apriori-wet delay is estimated with a WVR, $\delta ZD_{wet}$ is due to radiometer errors. The error of the zenith-wet delay can be obtained from

$$\delta ZD = \left[\left(\delta ZD^2_{hydrostatic} + \delta ZD^2_{GPS}\right)_{\sec ondary} + \left(\delta ZD^2_{hydrostatic} + \delta ZD^2_{wet}\right)_{ref}\right]^{1/2}$$

The main advantage of this technique is that it works for all distances and is the most accurate method to estimate zenith-wet delay with GPS. Disadvantage with this method is that it requires at least one independent measurement of zenith-wet delay. If there are any errors in the calculation of wet delay due to WVR or any other method in the reference site, then those errors are carried through out the calculations as the wet delay data of the reference is used for calculating the zenith-wet delay for secondary site and so on.

### 3.6 Drawbacks and Conclusions

GPS Meteorology shows a lot of improvement in environmental sensing technology. More accurate prediction of storm systems will not only benefit agriculture and farming but also improve the travel (space, ground) safety. Measurement of precipitable water vapor depends on the accuracy of the measurement of the wet delay

and if the errors in that measurement are reduced, it can be used as a very comprehensive tool for meteorological purposes.

### 3.7 Summary

This chapter discusses the delays that are incurred in the electromagnetic waves when they traverse from the satellite to the receiver. Using one of the delays methods to obtain the precipitable water vapor quantity in an atmospheric column is discussed. In the next chapter predicting the actual event causing heavy rain using water vapor quantity in the atmosphere is discussed.

# Chapter 4. Use of GPS Integrated Water Vapor Estimates in Short-term Rainfall Prediction

## 4.1 Introduction

The mountainous southwest Virginia is prone to flash flooding, typically the result of localized precipitation. Fortunately, within the region, there is an efficient system of instruments for real-time data gathering with IFLOWS (Integrated Flood Observing and Warning System) gages, the National Weather Service's WSR-88D Doppler radar and high precision GPS (Global Positioning System) receiver. This chapter focuses on utilizing the trends in GPS integrated water vapor content in forecasting heavy rainfall. The analysis concentrates on improving forecast lead-time for flash flood producing rainfall by combining WSR88-D Doppler radar, radiosonde, IFLOWS and GPS (Global Positioning System) integrated water vapor data.

## 4.2 GPS-IPW Analysis

The region influenced by the GPS-IPW estimates while accounting for the radar beam blockage has been delineated as the 40-nautical mile radius circle centered at the weather office (about the GPS receiver). Also, the radar products namely, the base reflectivity and the vertically integrated liquid (VIL) and the IFLOWS realtime raingage data have been selected for comparison with the GPS Integrated Precipitable Water (IPW) estimates**.** The IPW and the IFLOWS data are available in digital format. To test the power of the IPW in identifying significant rainfall events the following approach is taken. At first significant rain events were identified solely based on the IPW values. Using the integrated daily IPW peak values (as shown in Figure 4.1 for June 2000) the following events were observed for the year 2000:

May: 13, 19-21, 25, 27-29; June: 5-6, 10-11, 13-17, 18-21, 24-25; July: 5-6, 9-12, 18-19, 21-25, 28-31; August: 1-4, 6-10, 18-19, 24-31; and Sept: 1-5, 9-14.

Then the NWS provided the list of the flash flood events that they identified based on the actual rainfall. These details are given in Table 4.1. The IPW analysis identified such events with success. The IPW values are also correlated with the observed rainfall as shown in Figure 4.2. In Figure 4.2, the lower set of curves denotes the observed rainfall at various gages. At around the Julian day 155, no meaningful IPW value was recorded. Figure 4.2 shows the correlation between recorded rainfall and the IPW values.
Having shown the ability to identify an event on a broad scale, the real time progression of rainfall to IPW is the primary focus for enhancing the spatial and temporal identification of events. This task involves the real time correlation of IPW to the base reflectivity and the VIL. The subtle waveform variations in the IPW are to be related to the VIL and the base reflectivity at half hour intervals. Figure 4.3 shows a plot of IPW and Maximum VIL (Maximum value of VIL at a particular time in the 40 nautical mile region) within the forty nautical mile region. In this figure, we observe the troughs in the IPW and the crests in the VIL to have a correlation. Figure 4.4 shows the relationship between IPW and maximum base reflectivity. Figures 4.5 and 4.6 show similar trends for the July 29-30 event. Figures 4.7 and 4.8 show a comparison between the GOES satellite estimate of PW against the GPS-PW estimate and the radiosonde data. The estimates are quite close. The GPS data has the following advantages. The GPS has a temporal resolution of half an hour and the electromagnetic rays from GPS satellite are not obstructed by cloud coverage. The GOES satellite data are available at hourly intervals and radiosonde data are obtained once in twelve hours.

### 4.3 Application

Figure 4.9 shows the monthly climatology of PW for Blacksburg based on six years of radiosonde measurements. From Figure 4.9(also see Table 4.2), the 75th percentile and (mean + 2SD) [98th percentile] cutoff values are selected as the threshold for forecasting impending significant rainfall events based on the GPS-PW observations. There are about 108 raingages within the 40 nm radius centered on the GPS receiver. Subjective observations suggest that often when the IPW trend rises above the 75th percentile or especially the 98th percentile threshold, significant rainfall occurs within a few hours.

Secondary rises, once already above the 75th percentile threshold, appear to offer even a higher correlation. Tables 4.3 and 4.4 show listings of identified events solely based on the GPS-PW values. Column 4 contains Yes or No flags based on whether the 75th percentile threshold was exceeded for that day. An exceedance is indicated by a Yes. In column 3, the areal average rain is given. All events that had at least 0.1 inch of rain were identified.

### 4.4 Plotting IPW and Rain data

IPW data is available at half an hour intervals. This data is measured in centimeters and is available at UTC (Coordinated Universal Time) time. Rain data obtained from RAIN program is available at local time (eastern Pacific Time). From the first Sunday in April to the last Sunday in October difference between the UTC time and the local time is 4 hours and from October to April it is 5 hours. Hence while matching the times at different months different time lags have to be adopted. As the UTC time is ahead of the local time one has to subtract the corresponding number of hours in that particular month in the UTC time to convert it to the local time. IPW values are available at 00:15, 00:45,…,23:45 for each day. When we obtain the rain data at half an hour intervals it gives the amount of rainfall between 00:00 and 00:30, 00:30 and 1:00,…,23:30-24:00 for each day. IPW value at 00:15 is matched with the rain value between 00:00 and 00:30

Example: In the month of June to match UTC and local time we have to subtract four hours from UTC to match the local time. If we have a good rainfall between say 6:15 to 14:15 local time then corresponding UTC time is going to be 10:15 and 18:15.

### 4.5 Spatial resolution of GPS-IPW

While IPW is just a single time series controlled by the receiver and satellite coverage, the convective events can occur at several points within that spatial domain. For example, Figure 4.10 shows the IPW trends with the observed rainfall collected at different locations. While the rain events are discrete, the IPW is not. The IPW in Figure 4.10 is

plotted above the 75th percentile and IPW values less than that limit have been masked. The IPW covering a large area indicates the formation of several convective events at different points within the domain. It is also possible for a second rain event to occur at the same spatial point, but within the duration considered, only different gages reported rain values. The crucial point is that as seen in Figure 4.10, a lead time of 30 minutes to 2 hours exists for heavy rain events capable of producing a flash flood. It should also be noted that Figure 4.10 shows the standardized IPW values (standardized IPW = (IPW-monthly average IPW)/monthly standard deviation). The reason for standardization is as follows. Figure 4.11 shows plots of IPW for the receivers at Blacksburg (southwest VA) and Driver (southeast VA). The values of the IPW are understandably distinct due to the horizontal separation of approximately 250 km and the elevation separation of approximately 800 m. Figure 4.12 shows the same IPW values after standardization and translation (shift). This superimposed-coincident trend seems to be typical for the wintertime except that a constant shift even within the same month is not possible. We attribute this behavior for the lack of moisture in the atmosphere. In opposition, the summertime plots of standardized IPW values are shown in Figure 4.13. For the month of June, Figure 4.13 does not display wintertime uniformity attributed to the availability of significant moisture between locations.

## 4.6 Event Prediction Methodology

### 4.6.1 Criteria for predicting the events

Occurrence of significant rainfall within the selected region during a period of time is considered an event. The significant occurrence is identified as criterion (a) with a rain amount of 0.25 inches per half an hour and 0.5 inches per half an hour is considered as heavy rain. Even though the preliminary analysis using the 75th percentile earlier covered all the event days, it also showed some false alarms. A false alarm is one in which an event is predicted from the criterion but the event never occurs. To decrease the false alarm rate a second criterion is established by further analyzing the data. The second criterion (b) is that the IPW should remain above the 75th percentile value for more than

four hours. This is attributed to the fact that the buildup of water vapor will take certain time before it converts to liquid water and the ensuing precipitation. These two criteria fit a large number of events; but for events during the summer due to the availability of significant amount of vapor IPW there may be thunder storms even before the threshold for four hours. For such days monitoring the trend of IPW for the neighboring stations help in predicting the events with better accuracy. In summary the following three criteria (a), (b), and (c) are established to identify the potential rain events:
Criterion (a) = exceedance of IPW value above the $75^{th}$ percentile (Table 4.2).
Criterion (b) = exceedance duration of four hours above the $75^{th}$ percentile.
Criterion (c) = High values of IPW for neighboring stations and IPW.

IPW and half an hour Rain values are plotted by taking into consideration of the UTC and the local time differences. Figure 4.14 shows the plot between IPW and Rain for June 4 to 6 in the year 2001. The vertical axis scale is adopted such that the chosen minimum identifies only gauges with significant rain.

Moving Average values are calculated for the IPW values above the $75^{th}$ percentile after four hours till IPW falls below the $75^{th}$ percentile value. Moving Averages are adopted because they will smooth out fluctuations in magnitude over time of the IPW data. It is observed from the IPW data that calculating the values for durations less than the first four hours will increase the false alarm rate. Moving averages are calculated starting from the $8^{th}$ one half hour IPW value (as IPW is available at half an hour intervals) and are plotted at the end of the time. Average of the first eight values are calculated and is placed at the eighth value as moving average one, average of the second eight values is calculated and is placed at the ninth value as moving average two and so on. Calculation of moving averages is performed till IPW falls below the $75^{th}$ percentile value. If the duration of IPW is less than four hours exceeding the $75^{th}$ percentile, the IPW values are not considered.

- Alert Time: This is the time elapsed between the first rain peak in an event and the nearest $75^{th}$ percentile crossing of IPW observed value.

- Lead Time: This is the time between first rain peak in an event and the first moving average.

Figure 4.15 shows a lead-time of one to two hours. Using the above criteria, an analysis is performed for the summer months of June and July 2001. Tables 4.5 and Table 4.6 contain the respective results. Only rainfall values (by gage) of more than 0.25 inches in half an hour (that is 0.65 cm in half an hour) are identified as event days. Yes or No under IPW criteria indicates whether a particular criterion is satisfied or not.

- Missed event: If none of the criteria are satisfied then it is a missed event.
- Long duration exceedance: If IPW crosses 75th percentile value of that month and stays for more than four hours above that value then there is a significant chance for an event to occur as long as the IPW stays above 75th percentile value. When IPW lingers for long duration exceeding the threshold value wide spread and/or multiple events can occur within the domain. In Figure 4.15 the IPW exceeds the 75th percentile value from June 14th till the end of June 15th and shows multiple rain events.
- Simultaneous peaking of Rain and IPW: For events with simultaneous occurrence of the 75th percentile crossing and significant rain, there are no lead or alert times. For such events the exceedance of the 75th percentile and high IPW values at the neighboring stations (criteria a and c) should be satisfied.

During the month of June only two gauges that received significant rain were missed under all three criteria on two days. All other event days are identified by the stated criteria. Satisfying criteria a ($75^{th}$ percentile exceedance) and b (an exceedance duration of at least 4 hours) indicates a strong evidence for an event on that day. On some rare occasions an event may occur even before criterion (b) is satisfied. Hence in prediction one should always examine the IPW trends at the neighboring stations (criterion (c)). If the third criteria (a) and (c) are satisfied, an alert alarm should be considered.

- False alarms: False alarm is defined as the number of days which did not register any rain, though IPW exceeded 75$^{th}$ percentile value and stayed for more than four hours above the 75$^{th}$ percentile value.

For the month of June-2001 number of false alarms is zero and for the month of July-2001 it is one. On July 10$^{th}$, 2001 the IPW exceeded the threshold for more than four hours but there is no significant rain registered within the 40 nautical mile region. Of course, we are studying only rain collected at point rain gage locations. It is possible that there was rain but none of the gages received any catch.

### 4.7 Case Studies

#### 4.7.1 Event on April 28-2002

The IPW plot as observed at time 2:45 PM on April 27$^{th}$, 2002 is shown in Figure 4.17. The IPW trend exceeds 75$^{th}$ percentile value of 1.9 cm at 13:45 or 1:45 pm (local time) on 27$^{th}$ April. Based on criterion (a), a forecaster should watch the IPW trend carefully. Continued monitoring shows (see Figure 4.18) that at 18:45 local time on 27$^{th}$ April-2002, the IPW exceeds even the 95$^{th}$ percentile cut off value of 2.67 cm. By criterion (b), a four-hour duration exceeding the 75$^{th}$ percentile is a strong signal for an impending heavy rain event. However, in this case even the 95$^{th}$ percentile is exceeded within a 5 ½ hour duration indicating potential occurrence of heavy rain. It should be noted that these analyses are performed solely based on the IPW behavior without considering the rainfall data.

Figures 4.19, 4.20, and 4.21 contain the IPW trends until 10:15 pm on April 28. The IPW continued to exceed the 75$^{th}$ percentile indicating possible occurrences of heavy rain at several locations. Figure 4.22 shows the IPW plot when the series started receding below the 75$^{th}$ percentile possibly representing the end of rain events. Forecaster watching the IPW trend only will be issuing warning when IPW stayed for more than four hours above 75$^{th}$ percentile value. In this case IPW crossed 75$^{th}$ percentile at 1:45 pm

and stayed above it till 5:45 pm on April 27th and at that time forecaster will issue a warning. On April 29, 2002, the rain data were obtained from the NWS and plotted along with the IPW values as shown in Figure 4.22. From this plot it is seen that rain occurred on April 28th, which gives more than one day of lead time.

### 4.7.2 Event on May 02-2002

Figure 4.23 shows the observed IPW plot from April 29th to May 1st, 2002. At 7:45 pm on May 1st IPW exceeds 75th percentile cut off value of 2.54 cm for the month of May. Based on criterion (a), an alert should be in place. Continuous monitoring of IPW pattern shows that it stayed for more than four hours above the 75th percentile cutoff value (See Figure 4.24). At 11:15 pm on May 1st it is still above 75th percentile value satifying the 4-hr exceedance criterion. At this stage forecaster issues a warning and observes the IPW pattern further. Figure 4.25 shows the IPW pattern at 6:15 pm on May 2nd. The IPW crossed 95th percentile value of 3.43 cm on May 1st at 11:45 pm and it remained about the 95th percentile value after that time.

Figure 4.26 shows IPW pattern till 12:45 pm on May 3rd, 2002. IPW started decreasing and fell below 75th percentile value at 2:45 am on May 3rd and it continued decreasing. Hence there may not be any event after that time. Figure 4.27 shows the IPW as well as rain patterns from May 1st to May 3rd. From the figure we observe that heavy rain was registered on May 2nd starting from 1:15 pm. There was heavy precipitation within the region as long as the IPW stayed above 75th percentile value and the rain stopped after 2:45 am on May 3rd when IPW fell below 75th percentile value. Figure 4.28 shows the alert and lead times of the event. We see that there is more than a day of lead time for this event. For frontal events in April and May we may see such large lead times.

### 4.7.3 Event on June 14th, 2001

Figure 4.29 shows the IPW pattern on June 14th, 2001. At 12:15 pm on that day IPW crossed the 75$^{th}$ percentile value of 3.3 cm for the month of June. In Figure 4.30 it is seen that IPW stayed above 75th percentile value after 12:15 pm for four hours. Hence from criterion (b) we can predict an event into the future at 3:45 pm. For the event on June-14$^{th}$ lead-time is two hours unlike the events of April and May which had a lead time of more than a day. As long as the IPW exceeds the 75$^{th}$ percentile value, the same event may continue or multiple events can occur within the domain. Figure 4.31 shows the IPW and Rain pattern from June 14th to June 15th, 2001. This is observed from the pattern on June-15$^{th}$, for which the IPW stays above the 75$^{th}$ percentile for more than a day.

### 4.8 Comparison of Radar products and GPS-IPW

From Figure 4.16 we see that IPW exceeds the 75$^{th}$ percentile value of 1.9 cm at 13:45 or 1:45 pm (local time) on 27$^{th}$ April. At 18:45 local time on 27$^{th}$ April-2002, the IPW exceeds the 95$^{th}$ percentile with a value of 2.67 cm; also it continued to exceed the 75$^{th}$ percentile value for four hours. During that time the radar did not register any rain. From this we may state that the GPS is able to predict the event in advance of the radar. We know that GPS measures the total available moisture in the atmospheric column and the radar measures the droplet water content. Theoretically there should be a time lapse in the phase transfer between vapor and liquid water and this is supported by our data from IPW and VIL. Hence measurement of the total available moisture in the atmosphere should serve as an indicator in predicting an event. In this case from the GPS-IPW data we obtain a lead-time of more than a day and from the Radar-VIL a lead-time of around four hours is observed. Table 4.7 shows the VIL data for the event on April-28$^{th}$, 2002.

### 4.9 Summary

The downstream rain events are correlated with the IPW trend. The wintertime IPW almost replicates the same pattern at different receiver locations as synoptic scale storm systems dominate the signals as they propagate across portions of the network, as evidenced in Figures 4.11 and 4.12. In contrast, smaller scale fluctuations in the

summertime IPW trend (as shown in Figure 4.13) show little correlation between the two sites, suggesting these subtle variations are likely due to mesoscale or even storm scale phenomena, but which are nonetheless important to the behavior of convection. The frequently available GPS-PW data identifies impending events correctly. There is a lead time of about 2 hours for heavy rain events providing sufficient warning.

**Table 4.1. List of events selected by the NWS (Year 2000)**

| Date | Time Window | Comments |
|---|---|---|
| 14-Jun | 2200 UTC - 0300 UTC | Many severe weather reports |
| 15-Jun | 1800 UTC - 0300 UTC | Many severe weather reports; flash flooding well east of Blue Ridge (outside 40 nm) |
| 17-Jun | 2000 UTC - 2300 UTC | Flash flooding in Carroll Co. |
| 27-Jun | 1600 UTC - 2359 UTC | Forget |
| 5-Jul | 1600 UTC - 2200 UTC | Several waves of moderate to heavy rain with isolated deep convection. Some flash flooding in WV |
| 19-Jul | 2100 UTC - 2330 UTC | GPS showed good correlation with weaker showers, dropping, then peaking over 5cm with developing severe storms that passed over Blacksburg (then GPS quit). Very high rain rates (but no flash flooding due to fast movement of storm). |
| 28-Jul | 1800 UTC - 2000 UTC | Severe warning for Montgomery and Floyd Co. |
| 29-Jul | 1900 UTC - 0500 UTC | Flash flooding in Christiansburg and Roanoke |
| 1-Aug | 1700 UTC - 2200 UTC | Flash flooding in Roanoke, Botetourt, and Franklin Co. |
| 9-Aug | 1800 UTC - 0500 UTC | Two severe lines, the first may not have reached very far into the 40km range as it skirted to the north, but the second came roaring through (Severe) later in the evening. |
| 27-Aug | 2200 UTC - 0300 UTC | Severe thunderstorm and heavy rain in Blacksburg (canceled football game). |
| 1-Sep | 1800 UTC - 0100 UTC | Several waves of moderate to heavy showers and thunderstorms. Flash flooding was generally outside of 40 nm range. |
| 2-Sep | 1600 UTC - 2100 UTC | Flash flooding (Pulaski, Franklin, Mercer). |
| 3-Sep | 1800 UTC - 2300 UTC | Flash flooding (Pulaski, Franklin). Other storms in Craig, Botetourt. |
| 4-Sep | 1700 UTC - 0200 UTC | Up to two inches in part of Montgomery Co. (not sure what time within this window though). |

**Table 4.2. 1995-2000 RNK Surface-500 MB Precipitable Water(cm)**

| | | Percentile | | | | |
|---|---|---|---|---|---|---|
| Month | MAX | 75th | 50th | 25th | Min | 2SD |
| January | 3.429 | 1.270 | 0.889 | 0.508 | 0.127 | 2.032 |
| February | 2.794 | 1.397 | 0.889 | 0.635 | 0.127 | 2.032 |
| March | 3.302 | 1.397 | 0.889 | 0.635 | 0.127 | 2.159 |
| April | 3.302 | 1.905 | 1.270 | 0.762 | 0.254 | 2.667 |
| May | 4.064 | 2.540 | 1.905 | 1.397 | 0.508 | 3.429 |
| June | 4.699 | 3.302 | 2.667 | 2.032 | 0.762 | 4.064 |
| July | 4.699 | 3.429 | 2.921 | 2.286 | 0.762 | 4.191 |
| August | 4.699 | 3.302 | 2.667 | 2.159 | 0.635 | 4.191 |
| September | 4.572 | 3.175 | 2.286 | 1.524 | 0.381 | 4.191 |
| October | 3.937 | 2.032 | 1.397 | 0.889 | 0.127 | 2.921 |
| November | 3.556 | 1.524 | 0.889 | 0.635 | 0.254 | 2.286 |
| December | 3.048 | 1.143 | 0.762 | 0.508 | 0.127 | 2.032 |

**Table 4.3. Event Prediction for August 2000**

| Julian day | Gregorian day | Average Rain (inches) | 75th Percentile cutoff Exceedance |
|---|---|---|---|
| 214 | 1 | 0.4662 | yes |
| 215 | 2 | 0.2421 | yes |
| 216 | 3 | 0.1441 | yes |
| 217 | 4 | 0.1000 | yes |
| 218 | 5 | 0.0145 | no |
| 219 | 6 | 0.0254 | yes |
| 220 | 7 | 0.2238 | yes |
| 221 | 8 | 0.1605 | yes |
| 222 | 9 | 0.2668 | yes |
| 223 | 10 | 0.2742 | yes |
| 224 | 11 | 0.0125 | no |
| 225 | 12 | 0.0136 | no |
| 226 | 13 | 0.0845 | no |
| 227 | 14 | 0.0109 | no |
| 228 | 15 | 0.0100 | no |
| 229 | 16 | 0.0160 | no |
| 230 | 17 | 0.0111 | no |
| 231 | 18 | 0.2371 | yes |
| 232 | 19 | 0.0202 | no |
| 233 | 20 | 0.0170 | no |
| 234 | 21 | 0.0157 | no |
| 235 | 22 | 0.0111 | no |
| 236 | 23 | 0.0227 | yes |
| 237 | 24 | 0.0878 | yes |
| 238 | 25 | 0.1554 | yes |
| 239 | 26 | 0.0311 | yes |
| 240 | 27 | 0.7932 | yes |
| 241 | 28 | 0.2990 | yes |
| 242 | 29 | 0.0186 | no |
| 243 | 30 | 0.1411 | yes |
| 244 | 31 | 0.3586 | yes |

**Table 4.4. Event Prediction for June 2001**

| Jun-01 | | | |
|---|---|---|---|
| Julian Day | Gregorian Date | Average Rain (inches) | 75th percentile cutoff Exceedance |
| 152 | 1 | 0.19850 | Yes |
| 153 | 2 | 0.06692 | No |
| 154 | 3 | 0.01421 | No |
| 155 | 4 | 0.06617 | Yes |
| 156 | 5 | 0.15729 | Yes |
| 157 | 6 | 0.22112 | Yes |
| 158 | 7 | 0.23327 | Yes |
| 159 | 8 | 0.02206 | No |
| 160 | 9 | 0.00598 | No |
| 161 | 10 | 0.00112 | No |
| 162 | 11 | 0.01701 | No |
| 163 | 12 | 0.01037 | no |
| 164 | 13 | 0.06832 | yes |
| 165 | 14 | 0.04383 | yes |
| 166 | 15 | 0.09542 | yes |
| 167 | 16 | 0.07168 | yes |
| 168 | 17 | 0.00075 | no |
| 169 | 18 | 0.00037 | no |
| 170 | 19 | 0.01037 | no |
| 171 | 20 | 0.02953 | no |
| 172 | 21 | 0.19056 | yes |
| 173 | 22 | 0.82935 | yes |
| 174 | 23 | 0.05907 | yes |
| 175 | 24 | 0.07701 | no |
| 176 | 25 | 0.02206 | no |
| 177 | 26 | 0.34402 | yes |
| 178 | 27 | 0.06449 | yes |
| 179 | 28 | 0.03168 | yes |
| 180 | 29 | 0.02533 | yes |
| 181 | 30 | 0.02009 | yes |

**Table 4.5. Analysis of Events in June-2001**

| Jun-01 | | | | | | | |
|---|---|---|---|---|---|---|---|
| Julian Day | Date | Rain greater than 0.65 cm/half hour | IPW Criteria* | | | Alert Time (hrs) | Lead Time (hrs) |
| | | | a | b | c | | |
| 152 | 1 | 0.81 | Yes | no | yes | 0.50 | 0 |
| 153 | 2 | 0.71 | Yes | no | yes | More than a day | |
| 156 | 5 | 2.97 | Yes | yes | yes | 5.75 | 2 |
| 157 | 6 | 2.10 | Yes | yes | yes | 4.75 | 1 |
| 158 | 7 | 1.12 | Yes | yes | yes | IPW more than a day | |
| 162 | 11 | 1.60 | Missed Event | | | | |
| 164 | 13 | 1.09 | Yes | yes | yes | 3.75 | 0 |
| 165 | 14 | 1.49 | Yes | yes | yes | 5.75 | 2 |
| 166 | 15 | 2.10 | Yes | yes | yes | IPW more than a day | |
| 167 | 16 | 1.70 | Yes | yes | yes | IPW more than a day | |
| 172 | 21 | 4.39 | Yes | no | yes | 1.50 | 0 |
| 173 | 22 | 3.88 | Yes | yes | yes | 4.75 | 1 |
| 175 | 24 | 1.60 | Missed Event | | | | |
| 177 | 26 | 2.09 | Yes | no | yes | Simultaneous peaking of IPW and Rain | |
| 178 | 27 | 1.80 | Yes | no | yes | | |
| 179 | 28 | 1.60 | Yes | yes | yes | 7.75 | 4.00 |
| 180 | 29 | 1.09 | Yes | yes | yes | IPW more than a day | |
| 181 | 30 | 1.29 | Yes | yes | yes | IPW more than a day | |

Criterion (a) = exceedance of IPW value above the 75$^{th}$ percentile (Table 4.1).

Criterion (b) = exceedance duration of four hours above the 75$^{th}$ percentile.

Criterion (c) = High values of IPW for neighboring stations and IPW.

**Table 4.6. Analysis of Events in July-2001**

| Jul-01 | | | | | | | |
|---|---|---|---|---|---|---|---|
| Julian Day | Date | Rain greater than 0.65 (cm/half hr) | | IPW Trend Criteria* | | Alert Time (hrs) | Lead Time (hrs) |
| | | | a | b | c | | |
| 184 | 3 | 2.82 | yes | yes | yes | 12.00 | 8.5 |
| 185 | 4 | 4.29 | More than a day | | | | |
| 189 | 8 | 2.38 | yes | yes | yes | 5.50 | 2 |
| 192 | 11 | False Alarm | | | | | |
| 198 | 17 | 1.39 | yes | yes | yes | 15.5 | 12 |
| 199 | 18 | 1.32 | | | | | |
| 200 | 19 | 2.79 | More than a day | | | | |
| 207 | 26 | 1.80 | More than a day | | | | |
| 210 | 29 | 1.90 | yes | yes | yes | 10 | 6.5 |
| 211 | 30 | 1.49 | More than a day | | | | |
| 212 | 31 | 2.38 | Missed Event | | | | |

Criterion (a) = exceedance of IPW value above the 75$^{th}$ percentile (Table 4.1).

Criterion (b) = exceedance duration of four hours above the 75$^{th}$ percentile.

Criterion (c) = High values of IPW for neighboring stations and IPW.

**Table 4.7. VIL (kg/m$^2$) data for April 28$^{th}$-2002**

| | | | County | | | |
|---|---|---|---|---|---|---|
| Time(UTC) | Botetourt | Montgomery | Craig | Alleghany | Franklin | Henry |
| 19:34 | | | 35 | | | |
| 19:39 | | | 45 | | | |
| 19:44 | 35 | | 50 | | | |
| 19:49 | 40 | | 50 | | | |
| 19:54 | 50 | | 50 | | | |
| 19:59 | 45 | | 45 | | | |
| 20:04 | 50 | | 45 | | | |
| 20:09 | 50 | | 50 | | | |
| 20:14 | 40 | | 40 | | | |
| 20:19 | 25 | | | | | |
| 20:24 | 20 | | | | | |
| 20:29 | 40 | | | | | |
| 20:34 | | 25 | | | | |
| 20:39 | | 20 | | | | |
| 20:44 | | 20 | | | | |
| 20:49 | | 20 | | | | |
| 20:54 | | | | | | |
| 20:59 | | | | | | |
| 21:04 | | | | | 20 | |
| 21:09 | | | | | 40 | |
| 21:14 | | | | | 35 | |
| 21:19 | | | | | 40 | |
| 21:24 | | | | | 40 | |
| 21:29 | | | | | 15 | |
| 21:34 | | | | | | 15 |
| 21:39 | | | | | | 15 |
| 21:44 | | | | | | 40 |
| 21:49 | | | | | | 55 |
| 21:54 | | | | | | 50 |
| 21:59 | | | | | | 50 |
| 22:04 | | | | | | 50 |
| 22:09 | | | | | | 50 |
| 22:14 | | | | | | 20 |
| 0:34 | | | | | 15 | |
| 0:39 | | | | | 30 | |
| 0:44 | | | | | 20 | |
| 0:49 | | | | | 20 | |

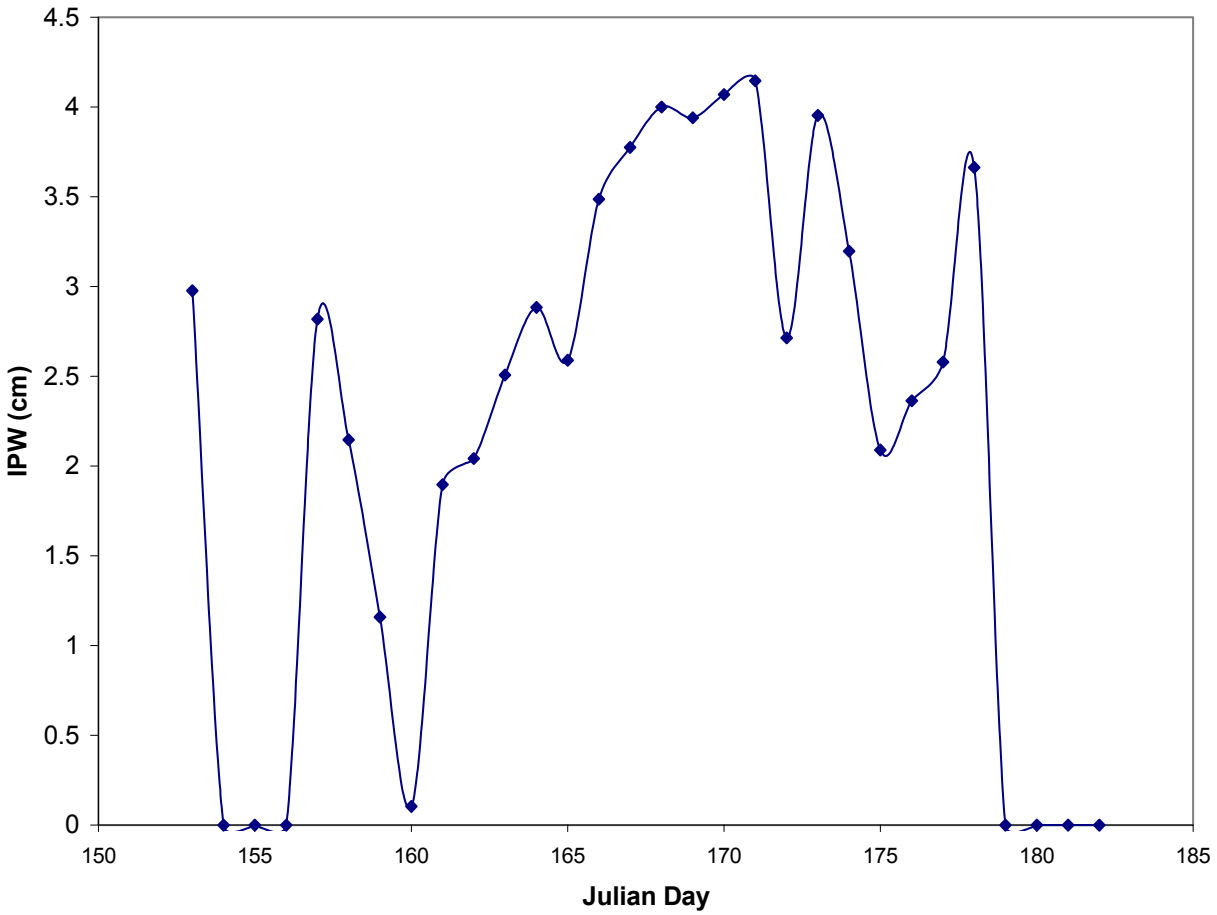


**Figure 4.1. Daily IPW plot for the month of June, 2000**

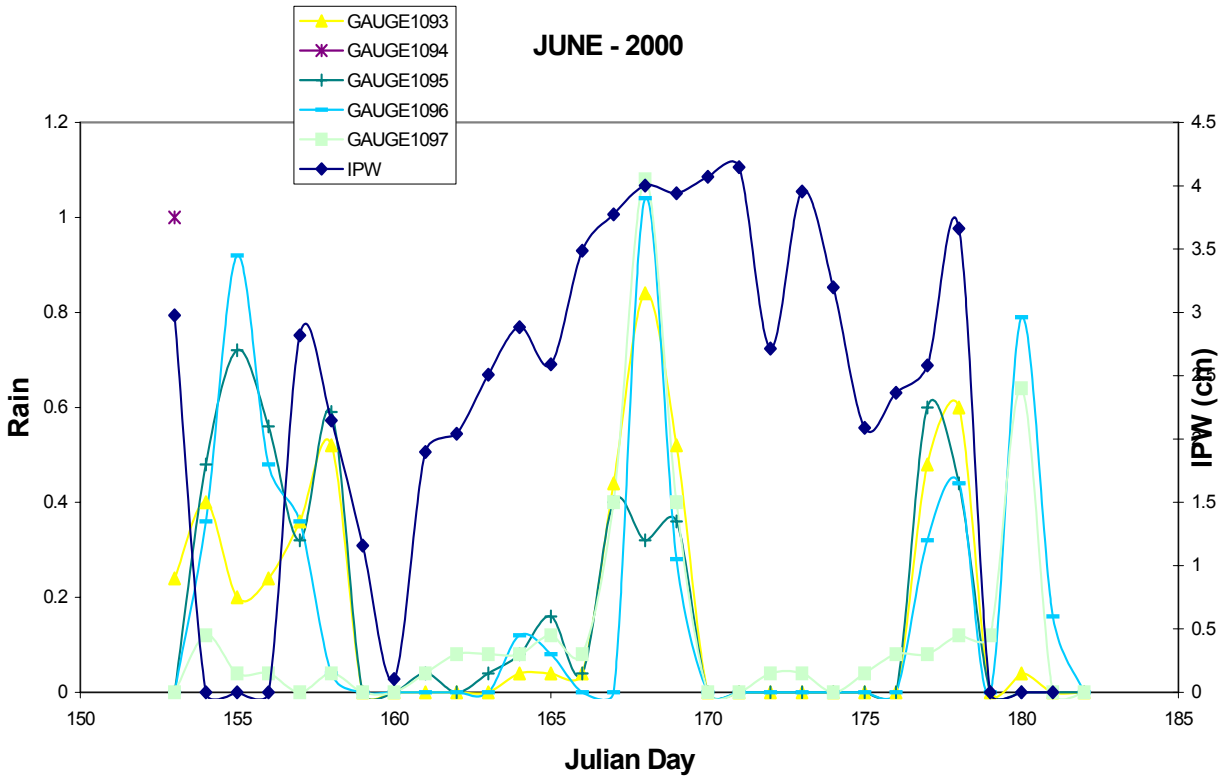


**Figure 4.2. Time series plot for IPW and Rainfall for June 2000**

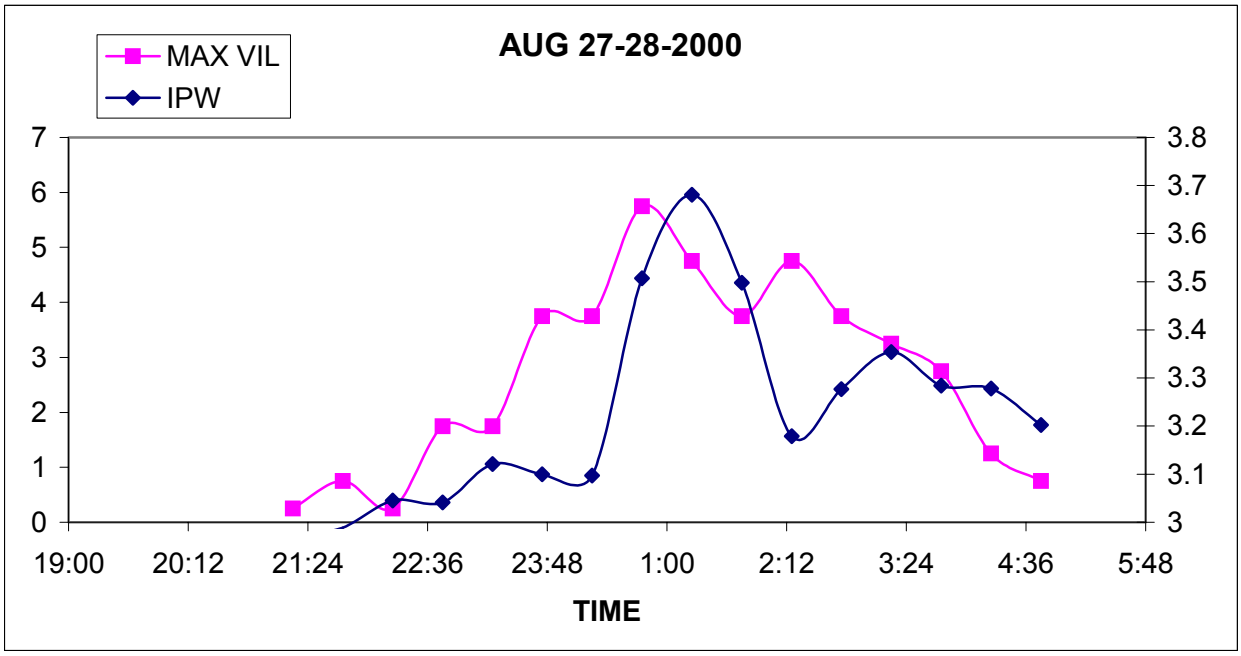


**Figure 4.3. Time series plot for IPW and VIL for August 27-28, 2000 event.**

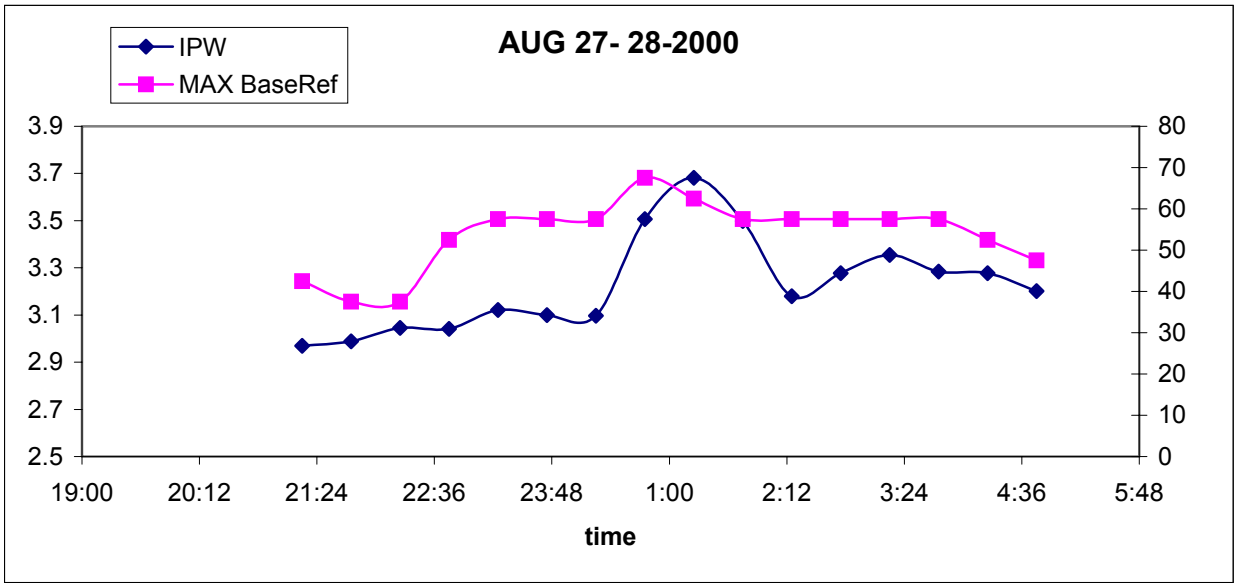


**Figure 4.4. Time series plot for IPW and Maximum Base Reflectivity for August 27-28, 2000 event**

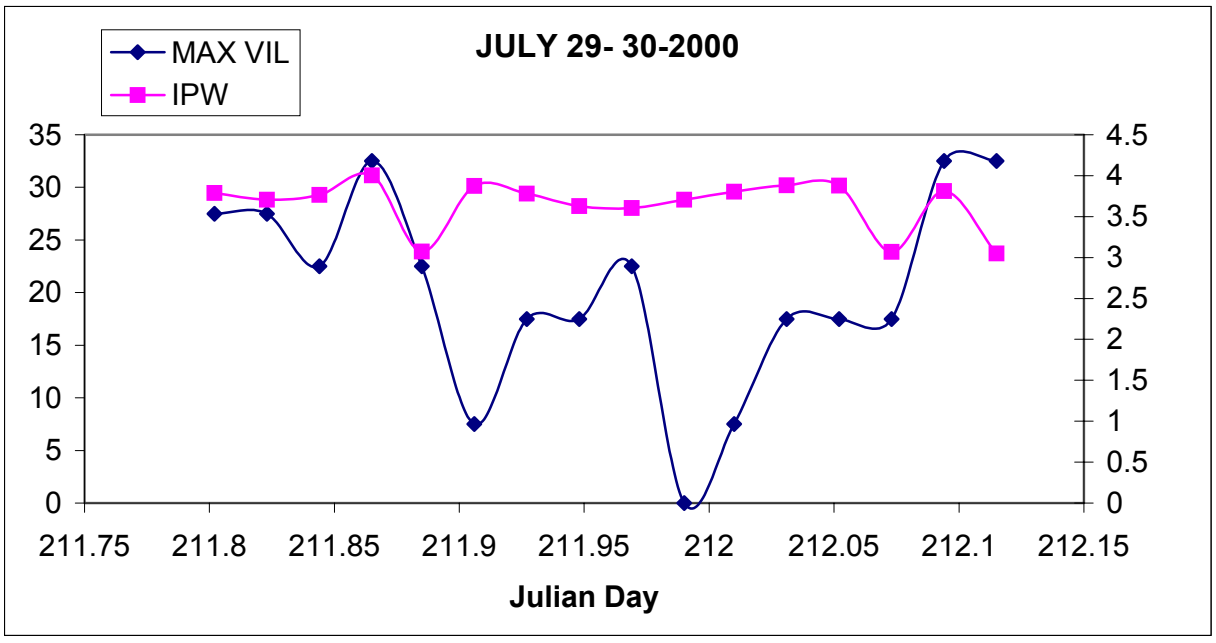


**Figure 4.5. Time series plot for IPW and Maximum VIL on July 29-30, 2000**

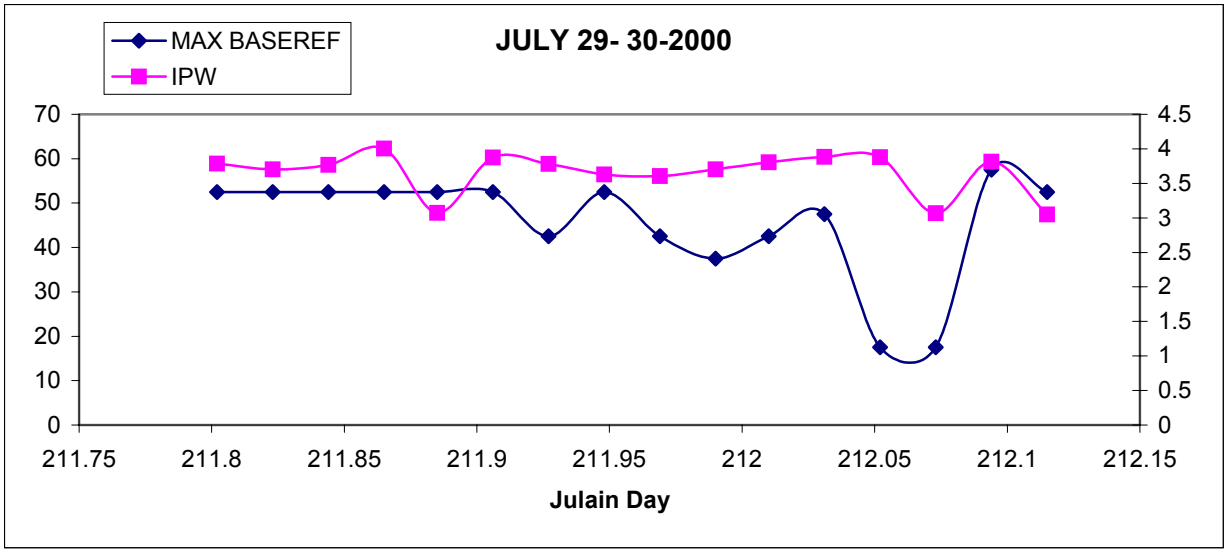


**Figure 4.6. Time series plot for IPW and Maximum Base Reflectivity on July 29-30, 2000**

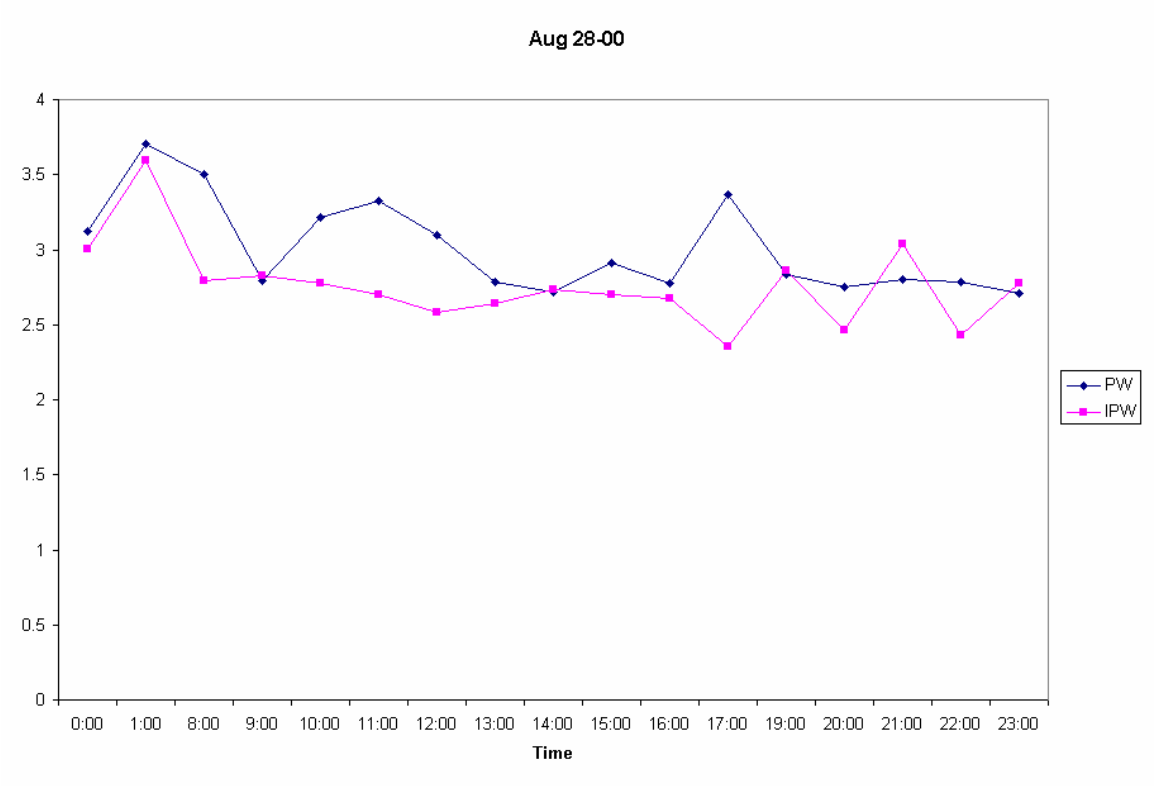


**Figure 4.7. Comparison of GOES-PW and GPS-IPW**

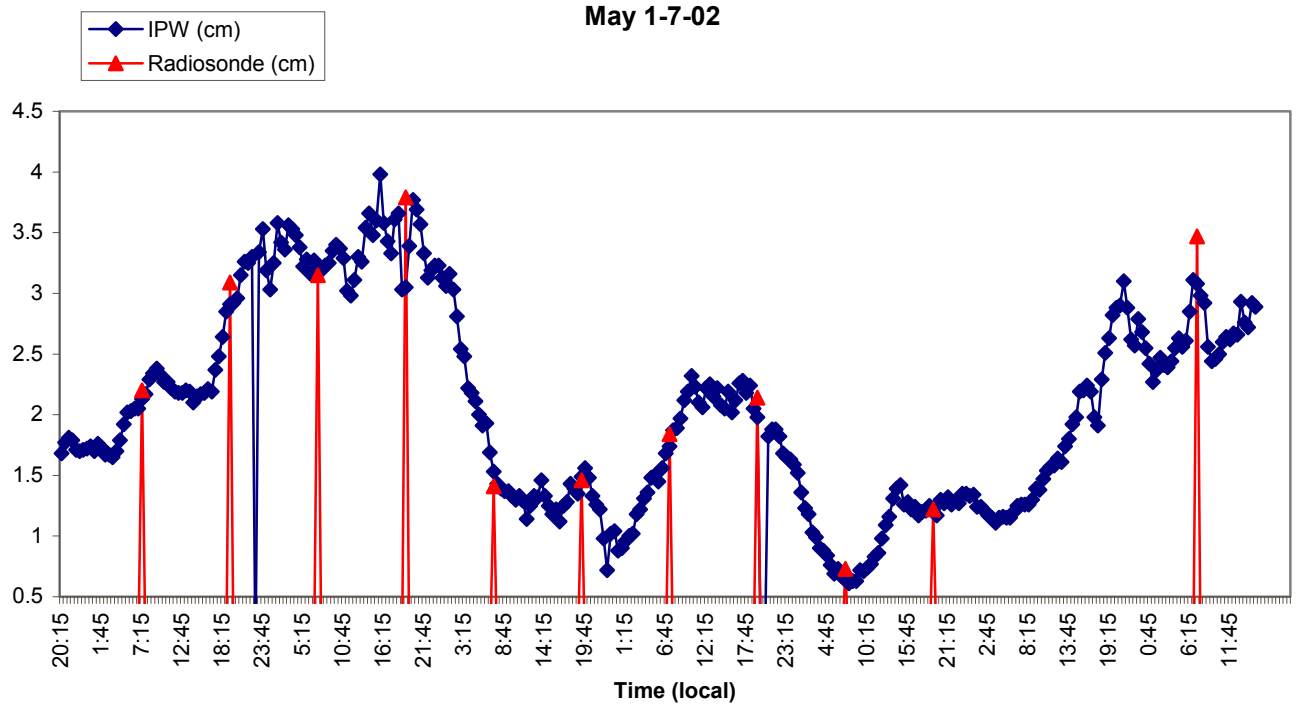


**Figure 4.8. Comparison of GPS-IPW and Radiosonde data**

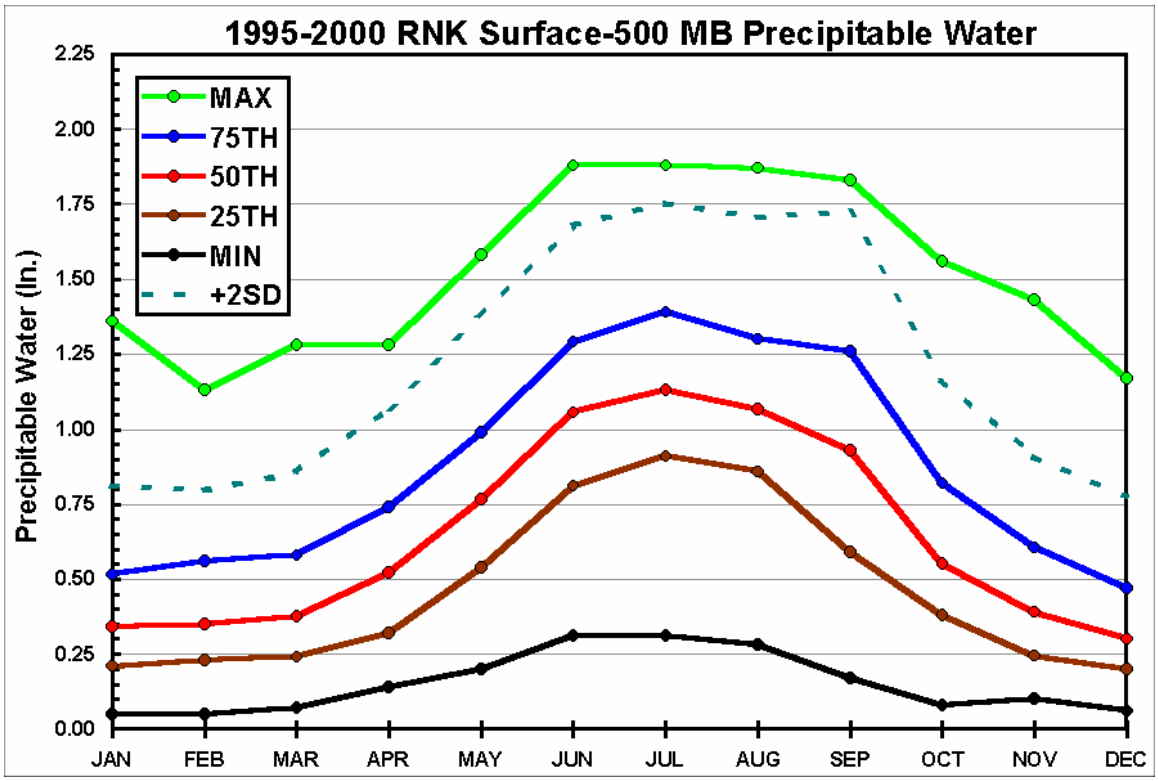


**Figure 4.9. Monthly Climatology of Radiosonde PW for Blacksburg**

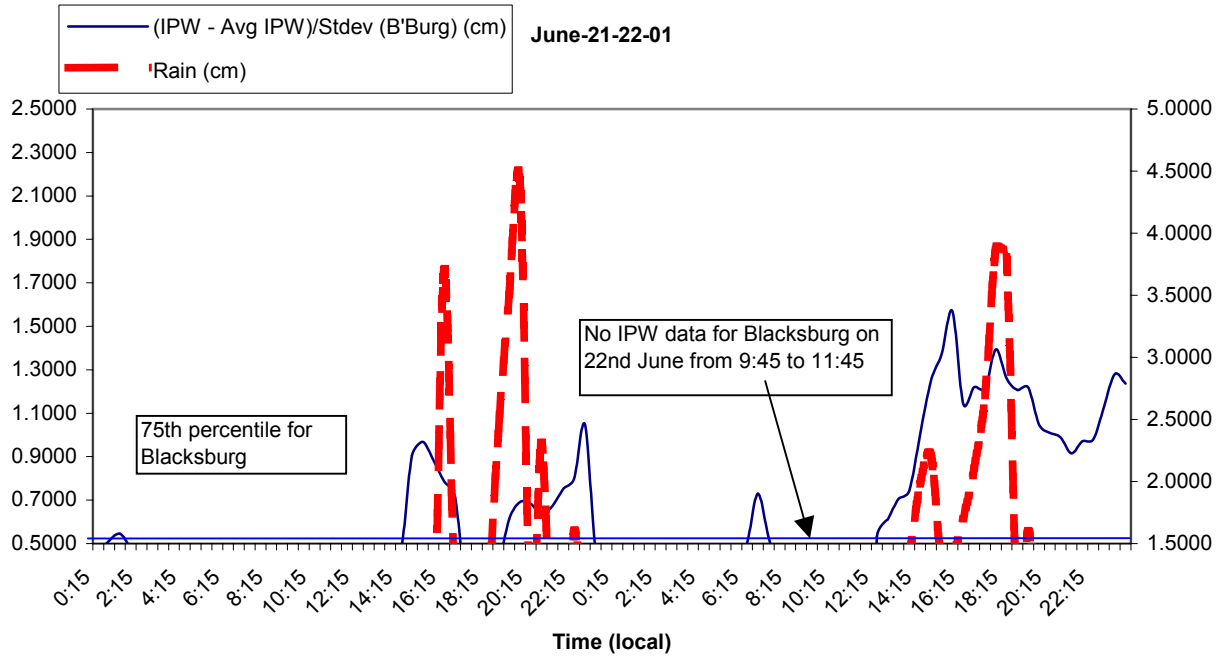


**Figure 4.10. An Example GPS_IPW and Rainfall Relationship**

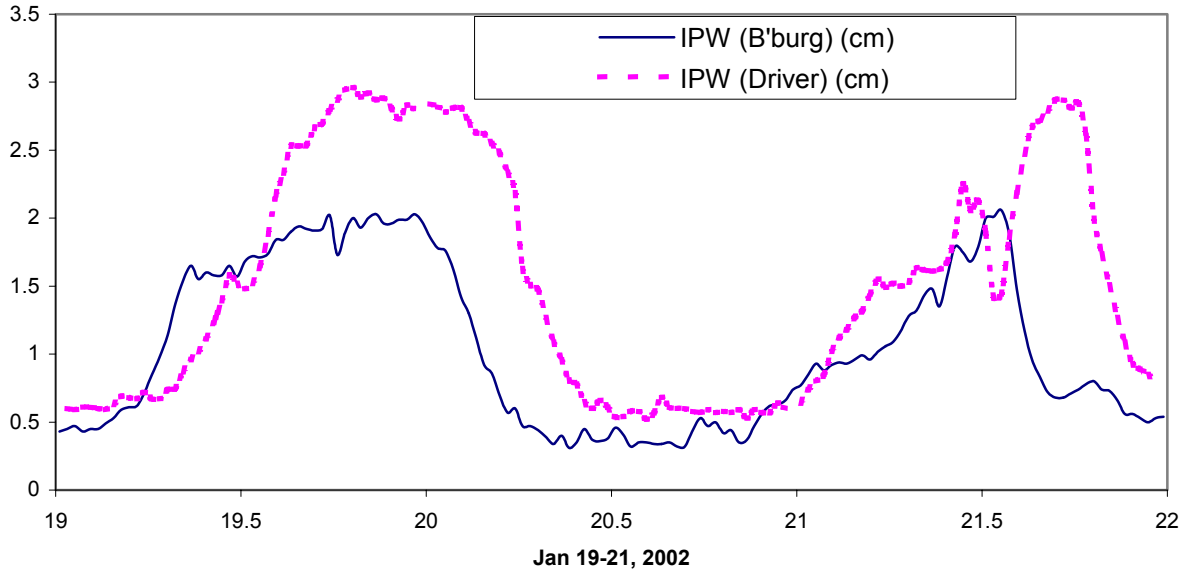


**Figure 4.11 IPW plots for Blacksburg and Driver, January 19-21, 2001.**

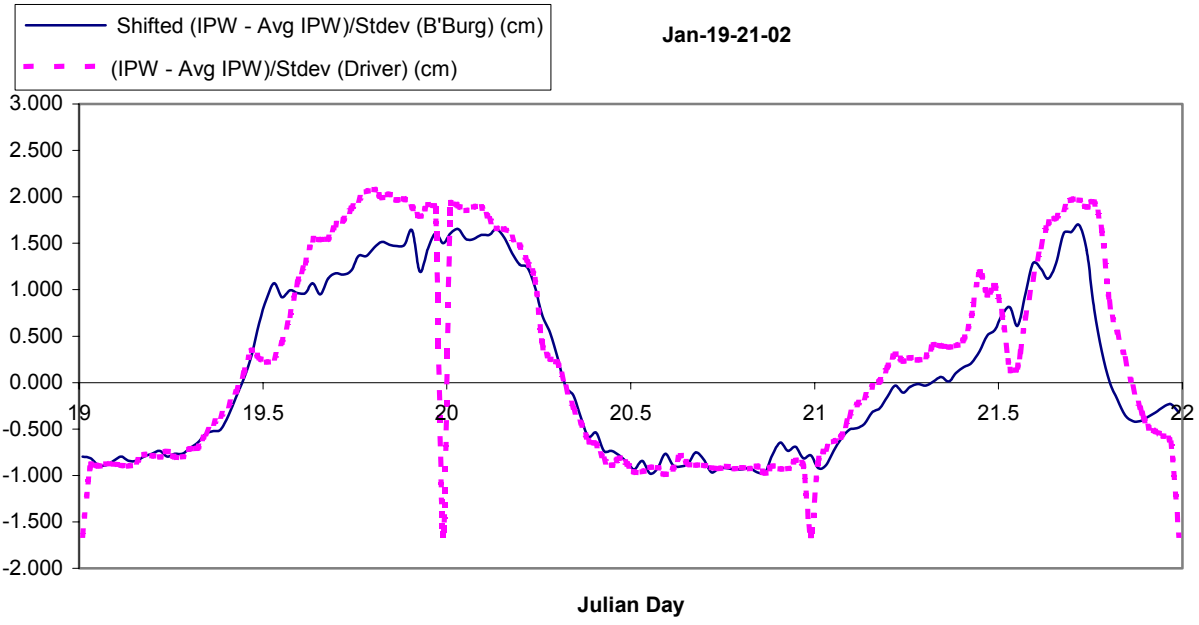


**Figure 4.12. Standardized –Shifted IPW plots for Blacksburg and Driver, January 19-21, 2001.**

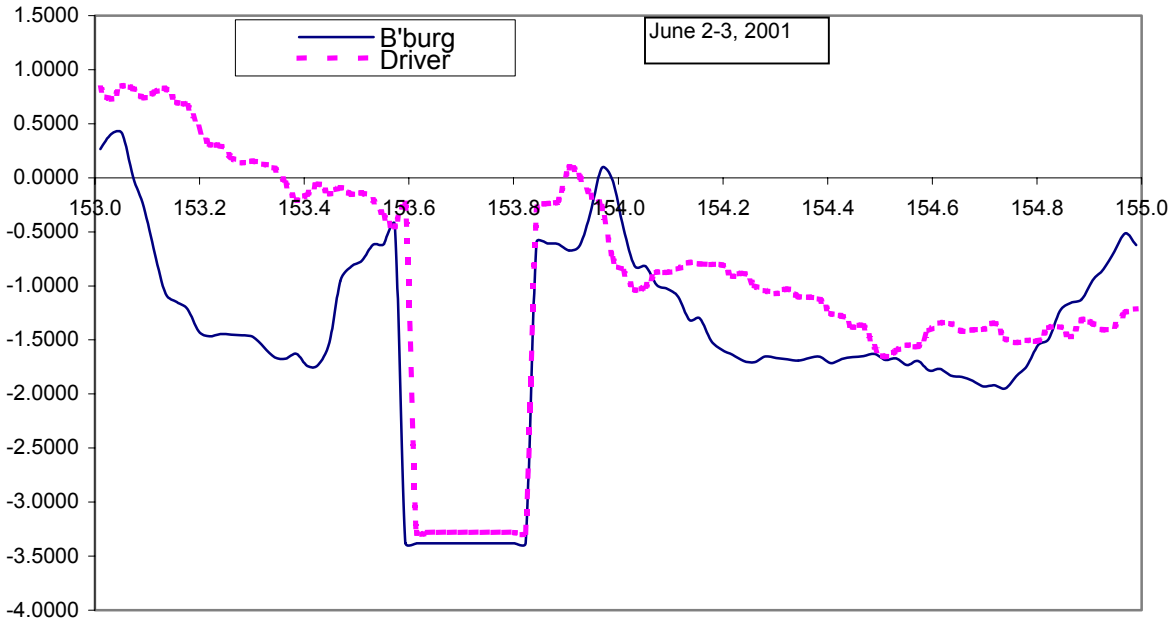


**Figure 4.13 Standardized IPW Plots for Blacksburg and Driver, June 2-3, 2001**

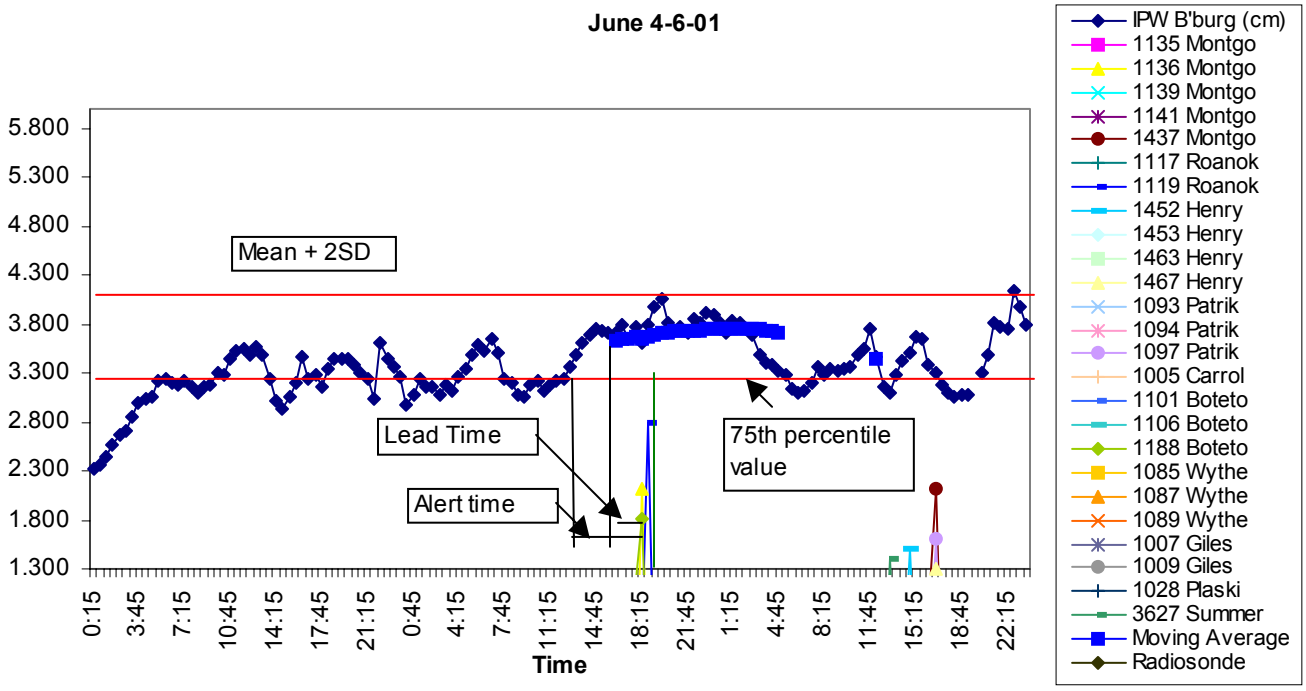


**Figure 4.14. Plot showing IPW and Rain trends for June 4-6, 2001**

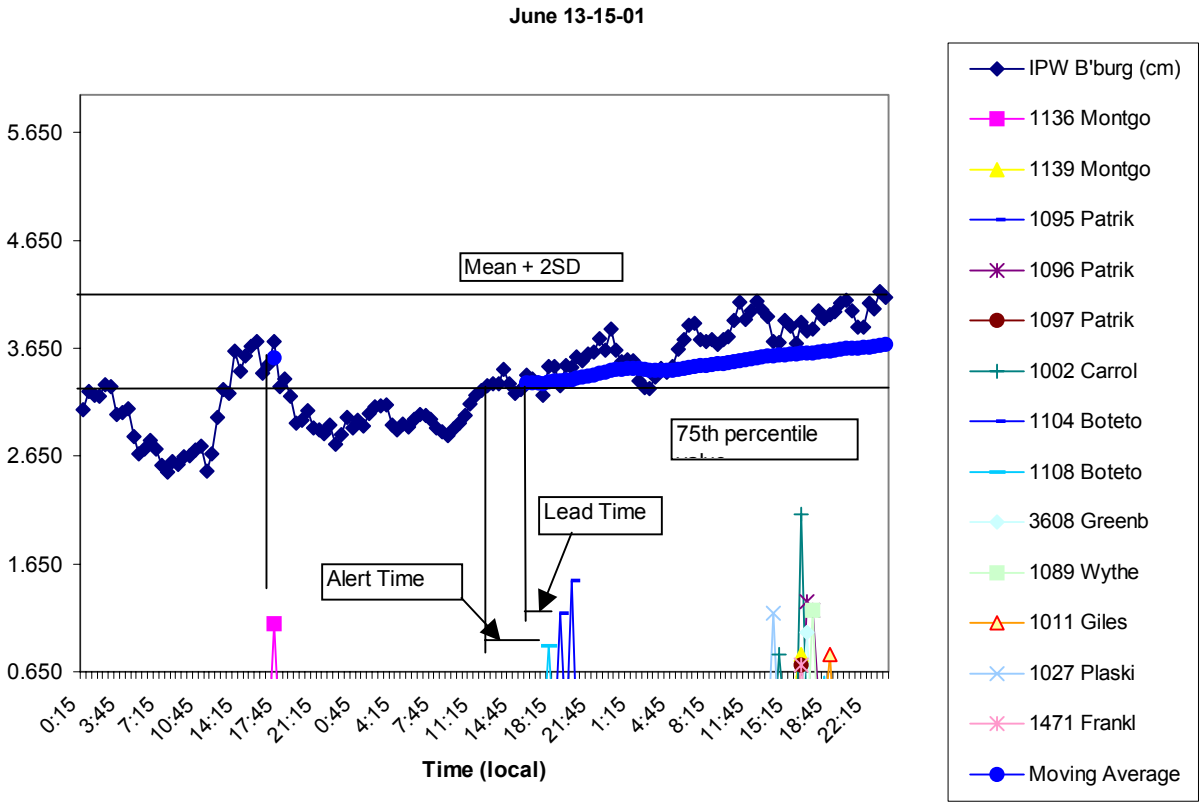


**Figure 4.15. Plot showing IPW and Rain tends for June 13-15-01**

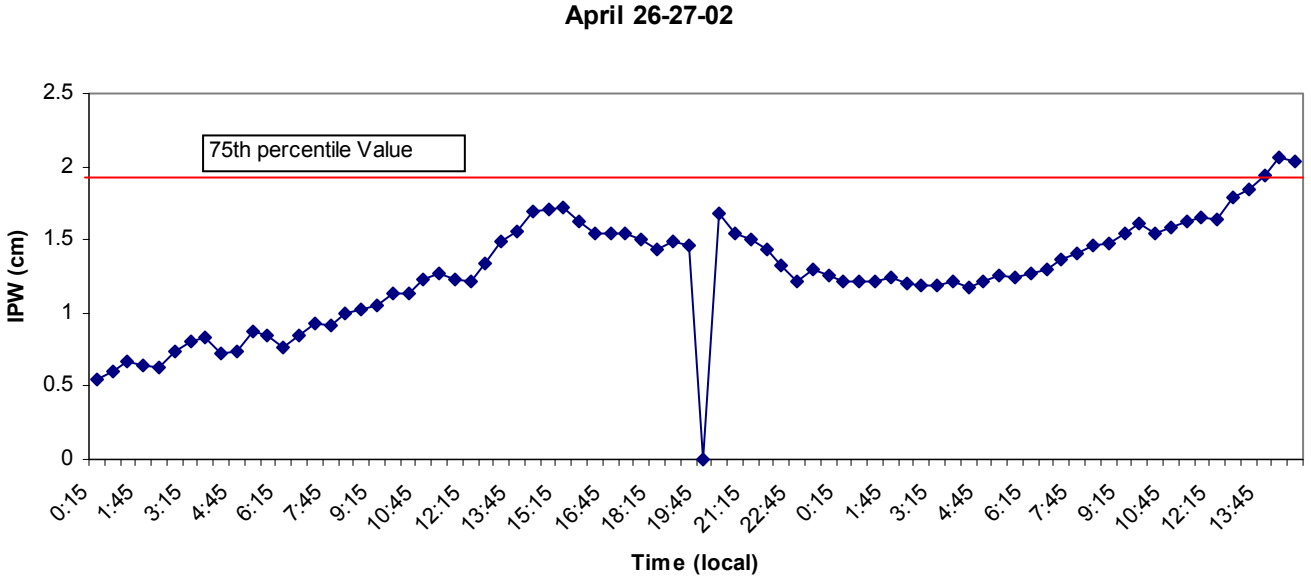


**Figure 4.16. Plot showing the IPW variation on April 26 to 14:45 (local time) on 27th April-2002**

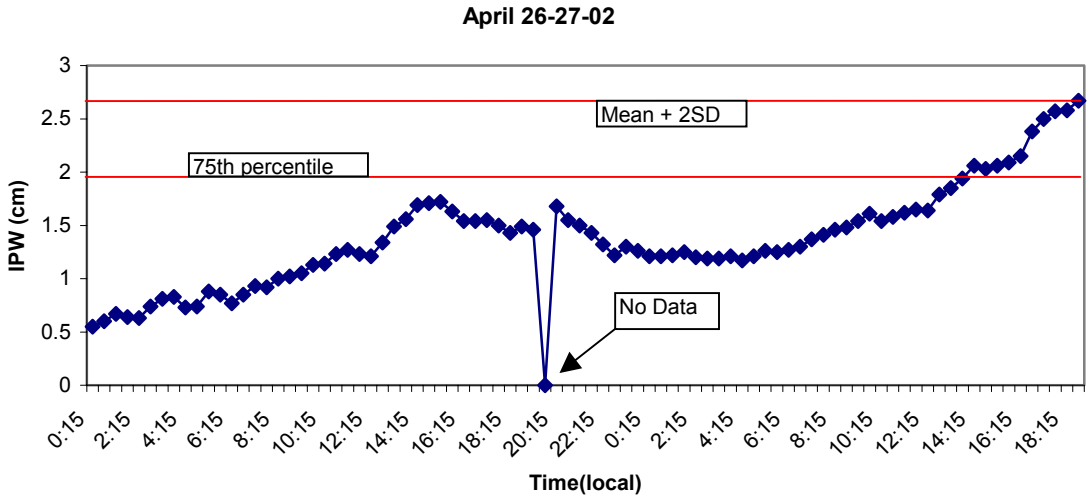


**Figure 4.17. Plot showing the IPW variation on April 26 to 18:45 (local time) on 27th April-2002**

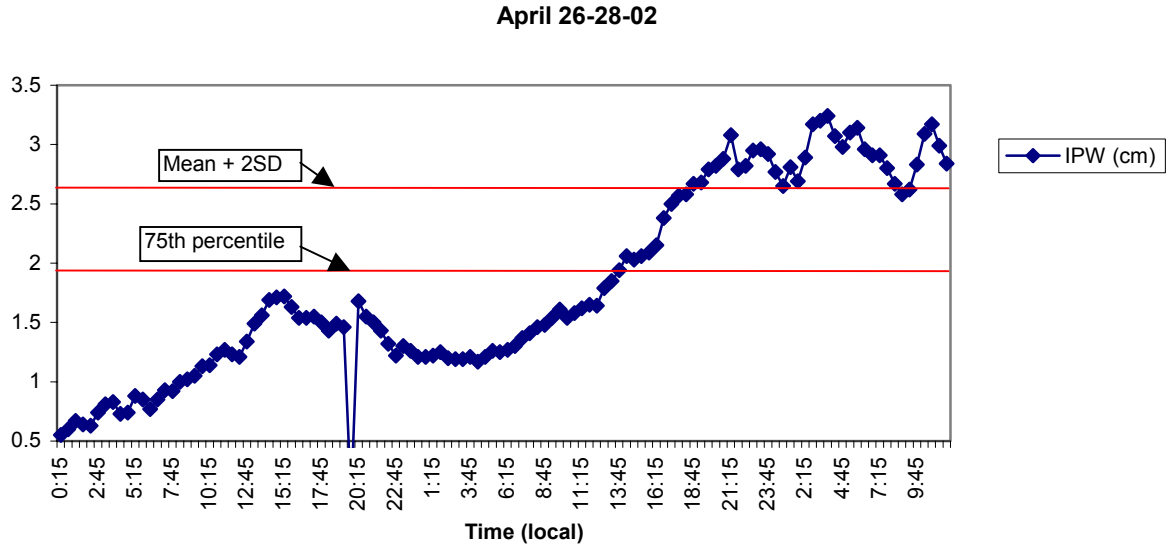


**Figure 4.18. Plot showing the IPW variation on April 26 to 11:45 (local time) on 28th April-2002**

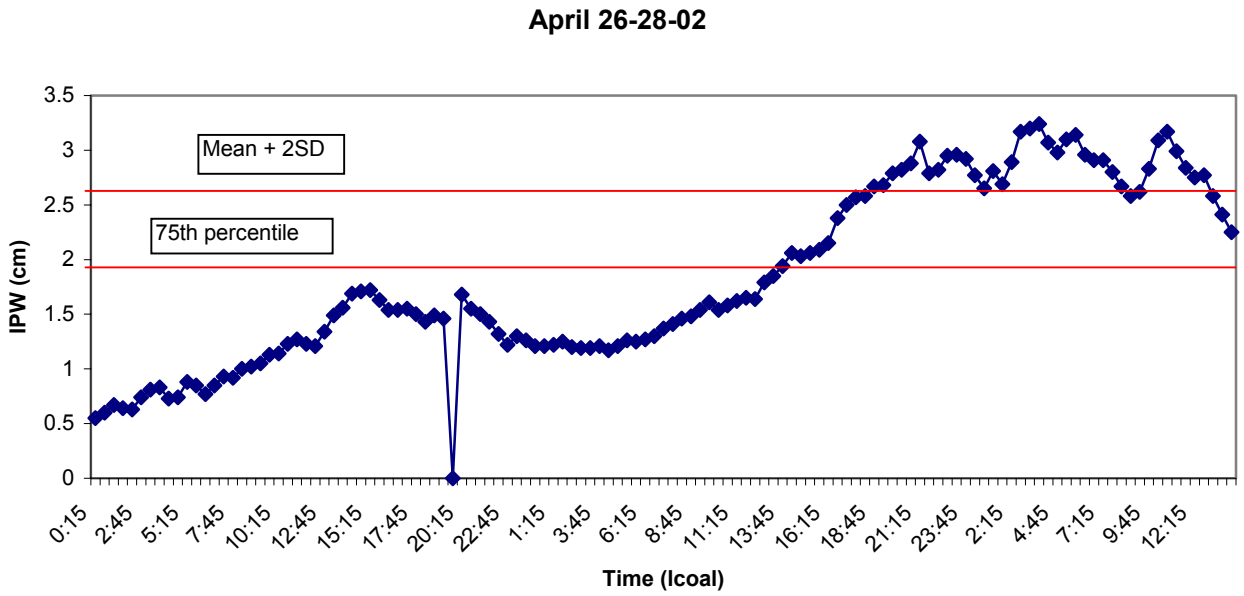


**Figure 4.19. IPW plot from April 26th till 14:15 local time on April 28th 2002**

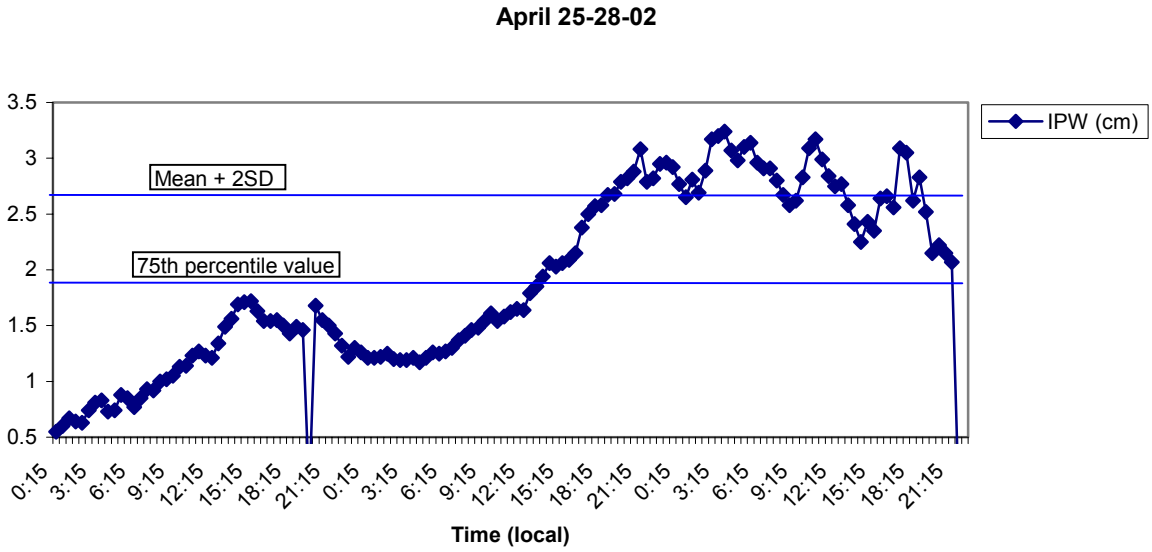


**Figure 4.20. Plot showing IPW and rain from April 26th to April 28th 2002**

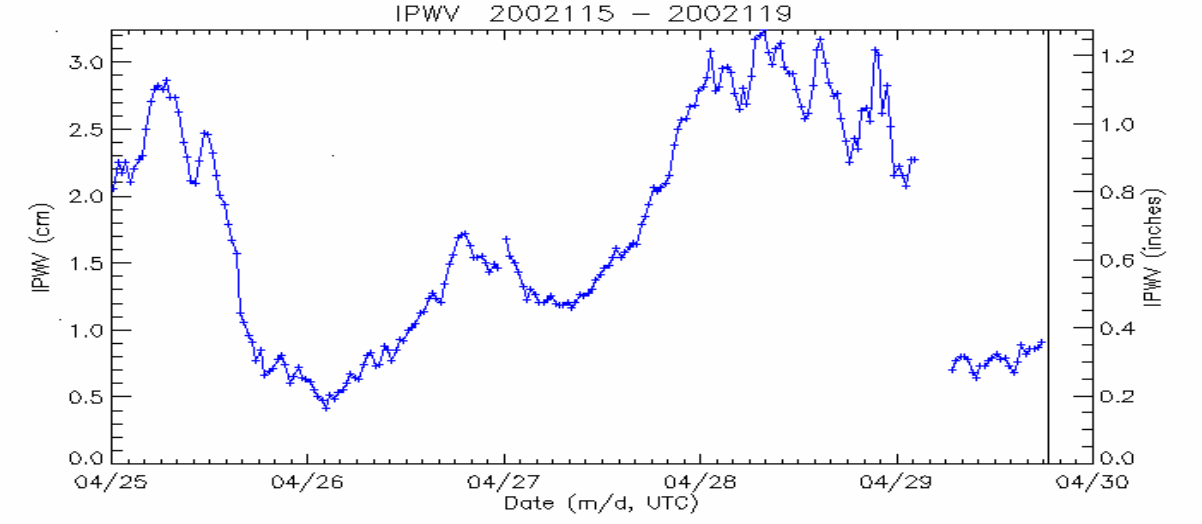


**Figure 4.21. IPW plot from April 25th till 14:33 local time on April 29th 2002**

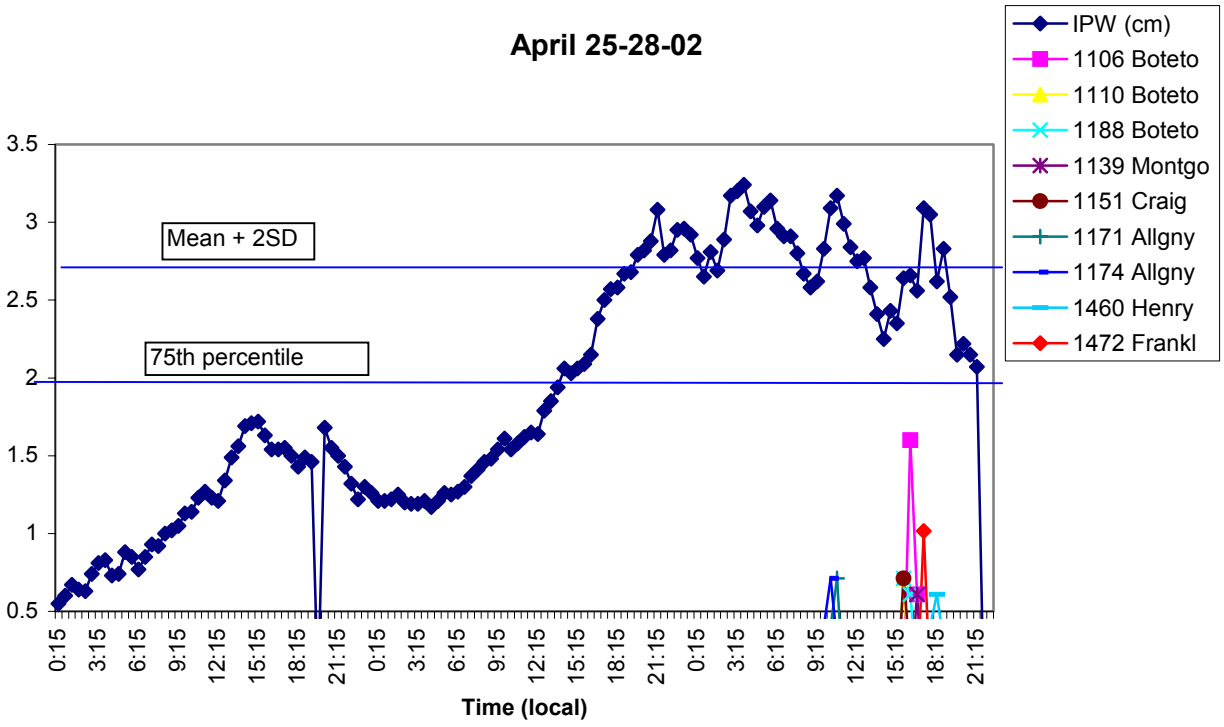


**Figure 4.22. Plot showing IPW and rain on April 28th-2002**

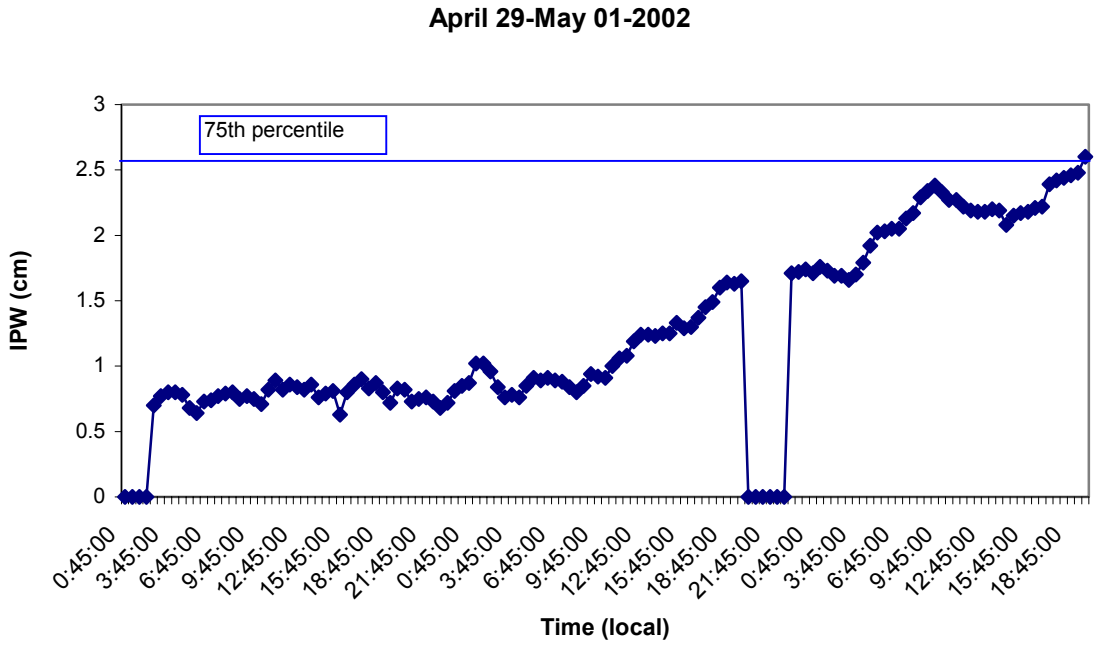


**Figure 4.23. IPW Pattern from April 29th till 7:45 pm on May 1st, 2002**

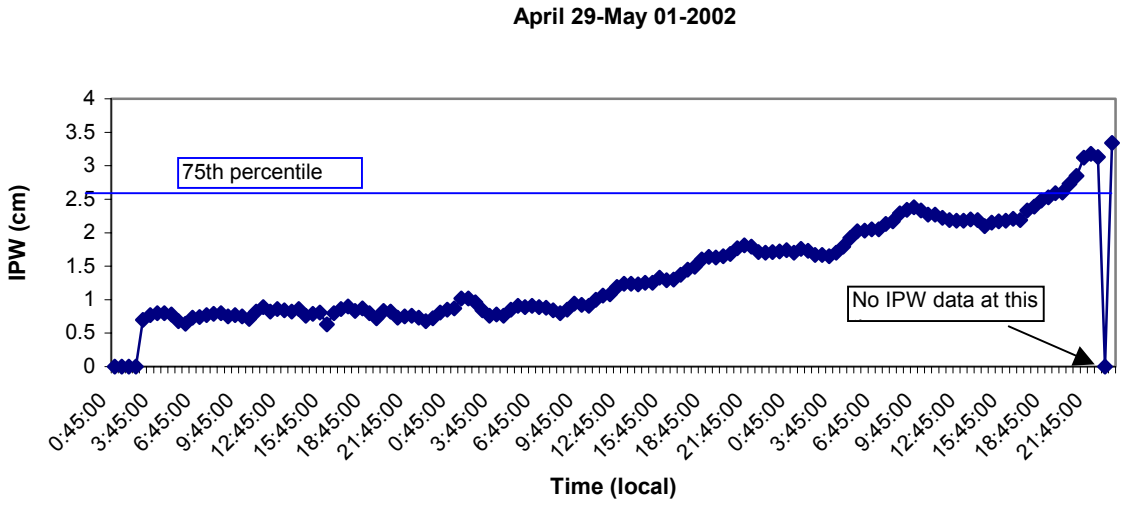


**Figure 4.24. IPW pattern from April 29th till 11:15 pm on May 1st, 2002**

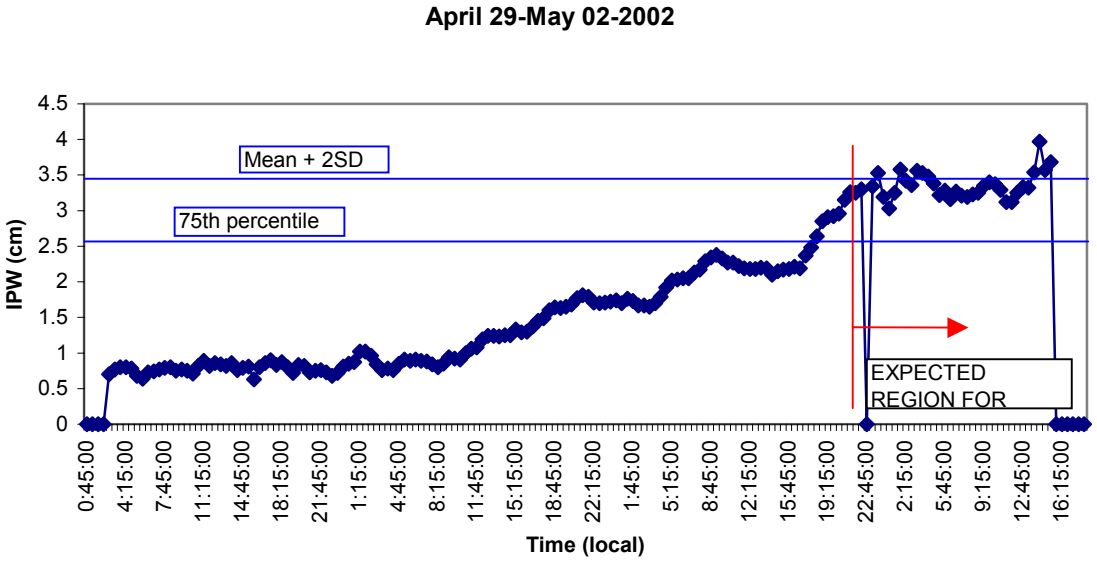


**Figure 4.25. IPW trend from April 29th till 6:15 pm on May 2nd, 2002**

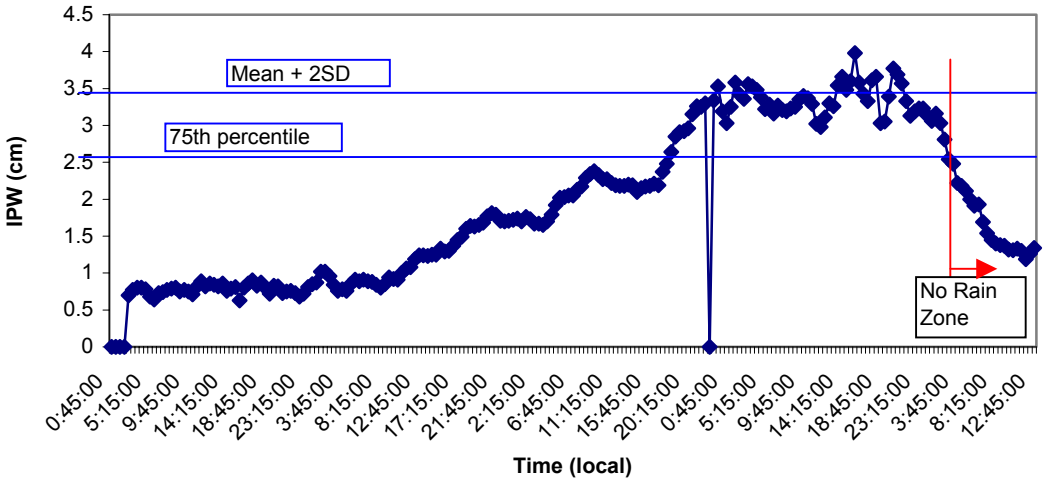


**Figure 4.26. IPW pattern from April 29th till 12:45 pm on May 3rd, 2002**

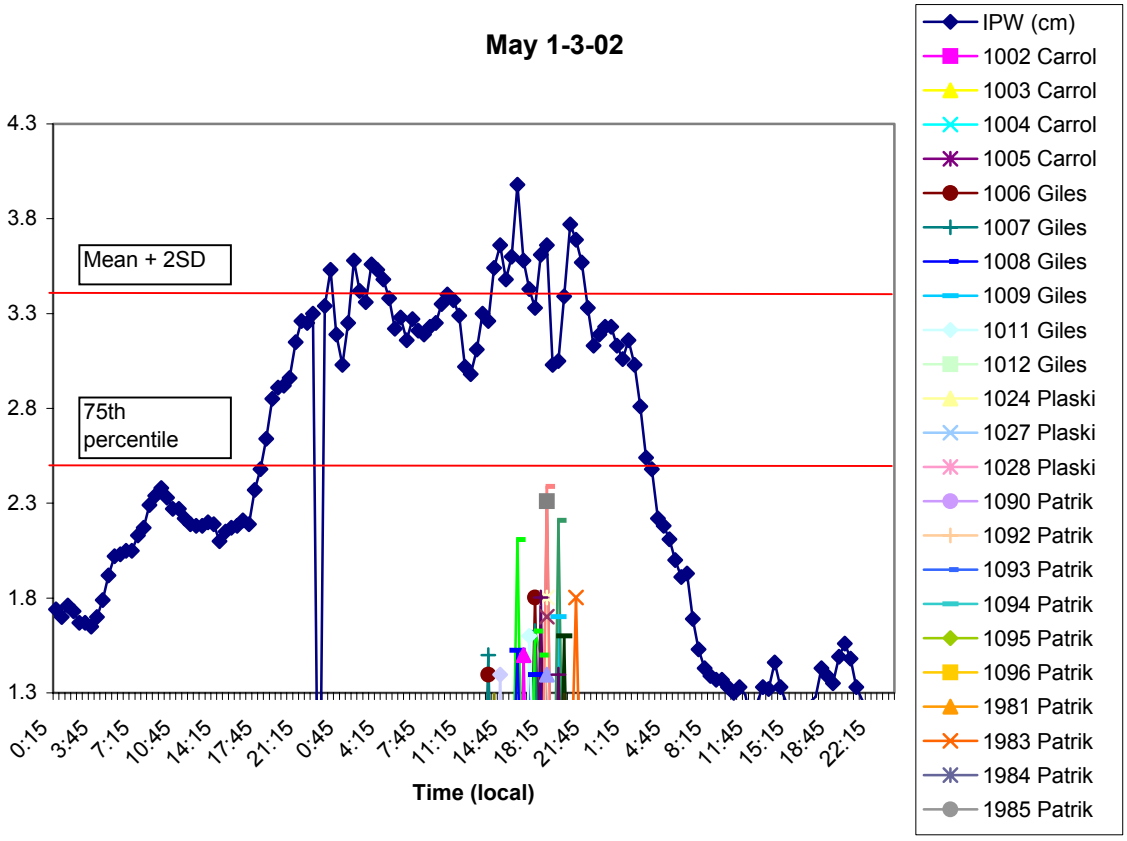


**Figure 4.27. IPW and Rain pattern on May 2nd, 2002**

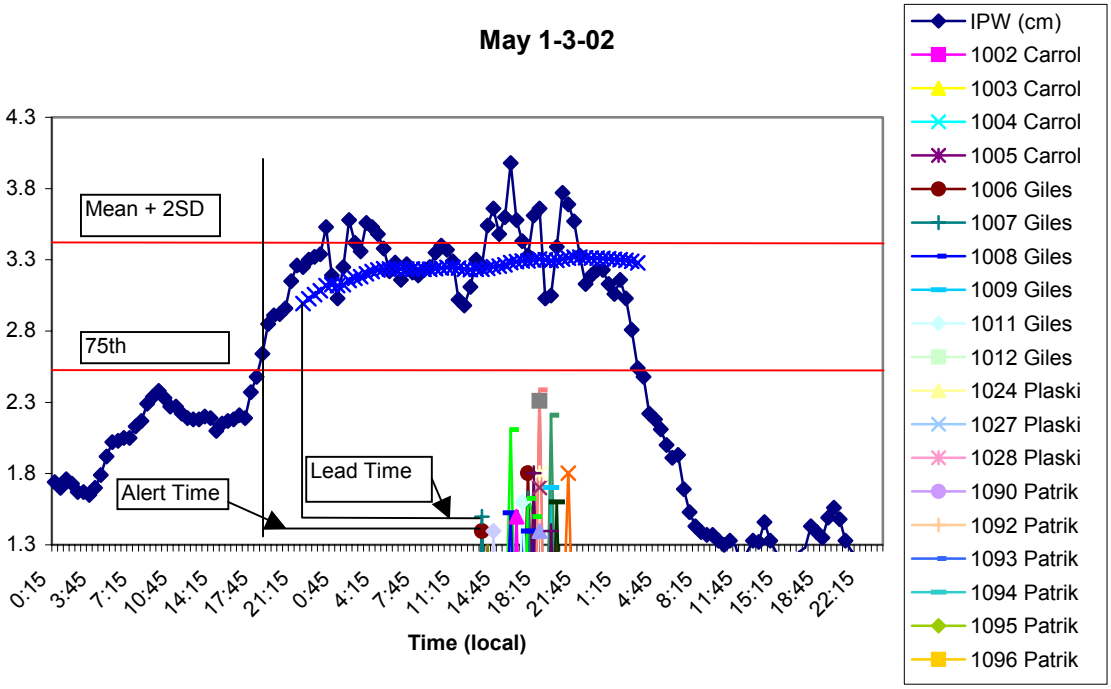


**Figure 4.28. Plot showing Alert and Lead times for the event on May 2nd, 2002**

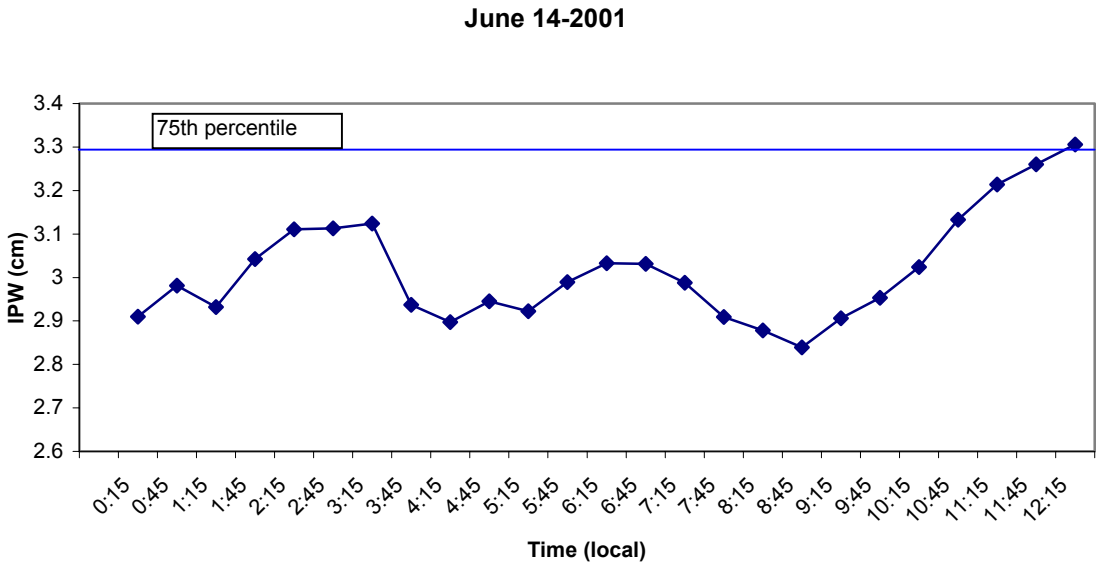


**Figure 4.29. IPW pattern on June 14th, 2001**

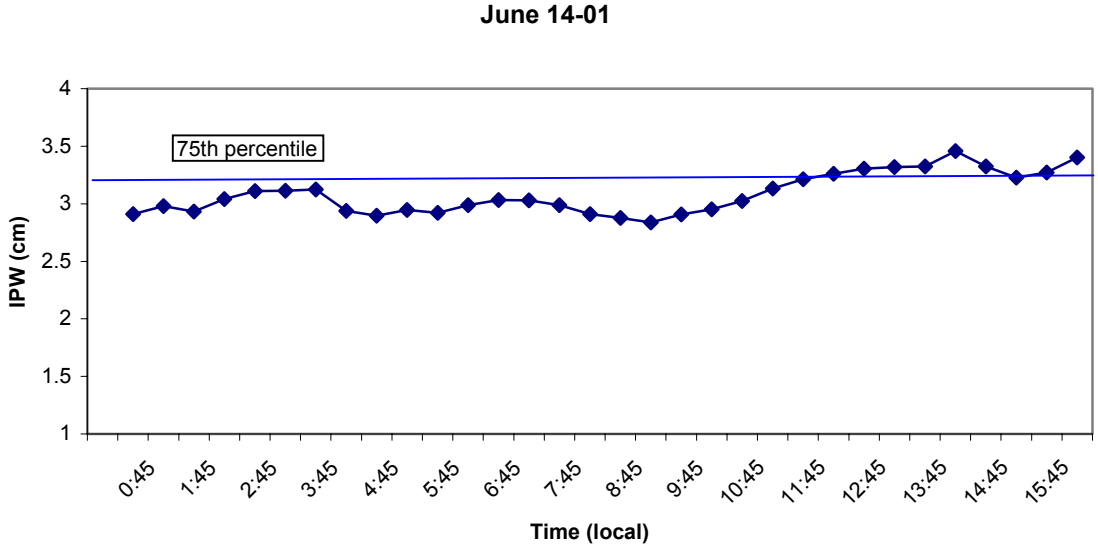


**Figure 4.30. IPW pattern at 3:45 pm on June 14th, 2001**

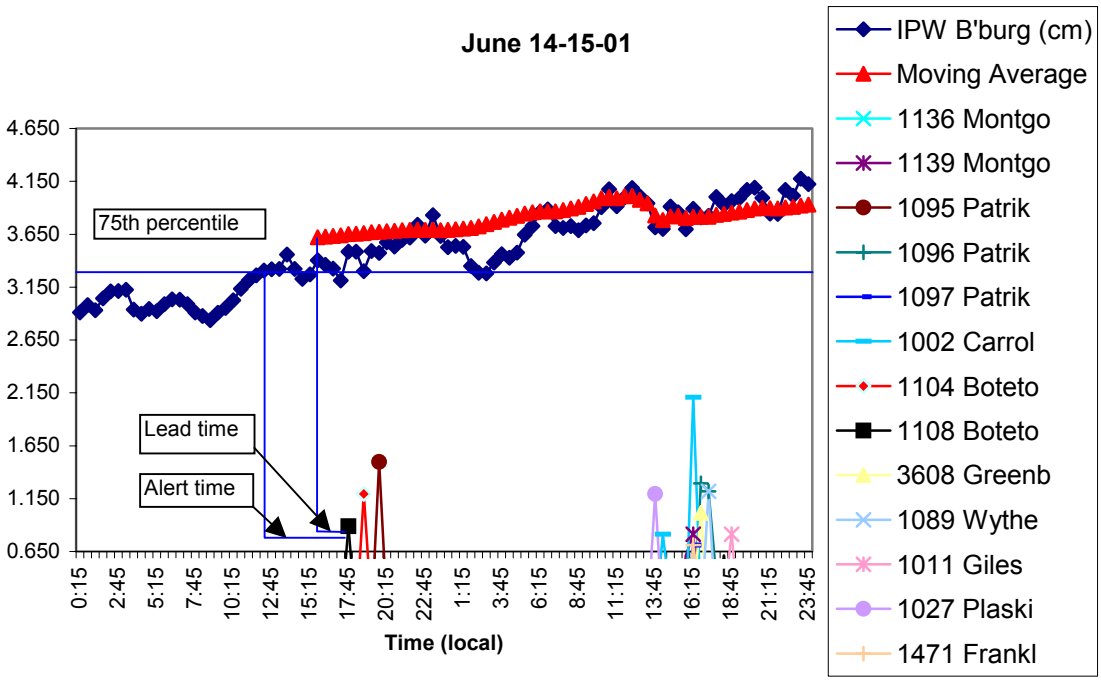


**Figure 4.31. Plot showing IPW and Rain on June14-15-2001**

## Chapter 5 – Rainfall prediction from measuring atmospheric variables

### 5.1 Introduction

This chapter presents a mathematical derivation using the atmospheric variables to predict the amount of rainfall over a region. The final equation incorporates measurable GPS-IPW, radar VIL (Vertically Integrated Liquid), and radiosonde data including atmospheric pressure, vapor pressure and temperature. A worked out example is provided along with the data tables illustrating the calculations involved.

### 5.2 Methodology

We adopt the following notation: $\rho_d$, $\rho_{v,}$ $\rho_{cl,}$ and $\rho_R$ = densities of dry air, water vapor, cloud water, and rain water; u, v, and w = dry air velocity components in the x, y, and z directions; $V_d$ = fall velocity of rain droplets with respect to the air, t = time, $m_{cl}$ = rate of mass of cloud water formation, AC = rate of mass of rain drop expansion by accretion of cloud particles, CC = rate of mass of rain drop formation by cloud water conversion, and EV = evaporation of rain water. The component wise continuity equations for the dry air and different phases of the atmospheric water are written as

**Dry Air**

$$\left[\left(\frac{\partial \rho_d}{\partial t}\right)+u\frac{\partial \rho_d}{\partial x}+v\frac{\partial \rho_d}{\partial y}+\frac{\partial \rho_d}{\partial z}\right]+\rho_d\left(\frac{\partial u}{\partial x}+\frac{\partial v}{\partial y}+\frac{\partial w}{\partial z}\right)=0 \qquad (1)$$

and the divergence

$$\frac{\partial u}{\partial x}+\frac{\partial v}{\partial y}+\frac{\partial w}{\partial z}=-\frac{1}{\rho_d}\frac{d\rho_d}{dt}=-\frac{d(\ln\rho_d)}{dt} \qquad (2)$$

**Water vapor**

$$\frac{\partial \rho_v}{\partial t} + \vec{\nabla} \cdot \rho_v \vec{v} - EV + m_{cl} = 0 \qquad (3)$$

**Cloud water**

$$\frac{\partial \rho_{cl}}{\partial t} + \vec{\nabla} \cdot \rho_{cl} \vec{v} - m_{cl} + CC + AC = 0 \qquad (4)$$

**Rainwater**

$$\frac{\partial \rho_R}{\partial t} + u\frac{\partial \rho_R}{\partial x} + v\frac{\partial \rho_R}{\partial y} + (w + v_d)\frac{\partial \rho_R}{\partial_z} + \rho_R\left[\frac{\partial u}{\partial x} + \frac{\partial v}{\partial y} + \frac{\partial (w + V_d)}{\partial z}\right]$$
$$+ EV - CC - AC = 0 \qquad (5)$$

and $V_d$ = fall velocity with respect to the moving air.

Adding (3), (4), and (5) we obtain

$$\frac{\partial}{\partial t}[\rho_v + \rho_{cl}] + \vec{\nabla} \cdot \vec{v}(\rho_v + \rho_{cl}) + \frac{\partial \rho_R}{\partial t} + u\frac{\partial \rho_R}{\partial x} + v\frac{\partial \rho_R}{\partial y} + (w + v_d)\frac{\partial \rho_R}{\partial z}$$
$$+ \rho_R\left[\frac{\partial u}{\partial x} + \frac{\partial v}{\partial y} + \frac{\partial w}{\partial z}\right] + \rho_R \frac{\partial v_d}{\partial z} = 0 \qquad (6)$$

In terms of the total derivatives, expressing the rates of change of the involved quantities we obtain

$$\frac{d}{dt}(\rho_v + \rho_{cl} + \rho_R) + (\rho_v + \rho_{cl} + \rho_R)\left[\frac{\partial u}{\partial x} + \frac{\partial v}{\partial y} + \frac{\partial w}{\partial z}\right] + \rho_R \frac{\partial v_d}{\partial z} = 0 \qquad (7)$$

Using eq.(2) in in eq.(7) we have

$$\frac{1}{(\rho_v + \rho_{cl} + \rho_R)}\frac{d}{dt}(\rho_v + \rho_{cl} + \rho_R) - \frac{1}{\rho_d}\frac{d\rho_d}{dt} + \frac{\rho_R \frac{\partial v_d}{\partial z}}{(\rho_v + \rho_u + \rho_R)} = 0 \qquad (8)$$

By putting $X = \rho_v + \rho_{cl} + \rho_R$, we have

$$\frac{1}{X}\frac{dX}{dt} - \frac{1}{\rho_d}\frac{d\rho_d}{dt} + \frac{\rho_R}{X}\frac{\partial V_d}{\partial z} = 0 \tag{9}$$

$$\frac{d(\ln X)}{dt} - \frac{d(\ln \rho_d)}{dt} + \frac{\rho_R}{X}\frac{\partial V_d}{\partial z} = 0 \tag{10}$$

$$\frac{d\left(\ln \frac{X}{\rho_d}\right)}{dt} + \frac{\rho_R}{X}\frac{\partial V_d}{\partial z} = 0 \tag{11}$$

It is pointed out that up to the development of eq. (11), no restrictive assumptions have been made. In eq. (9) with the aid of the gas law we have $\frac{d\rho_d}{dt} = \frac{d}{dt}\left[\frac{p_d}{R_d T}\right]$ in which $p_d$ = partial pressure of dry air, $R_d$ = dry air gas constant, T = absolute temperature. We can show that

$$\frac{1}{\rho_d}\frac{d\rho_d}{dt} = \frac{d(\ln p_d)}{dt} - \frac{d(\ln T)}{dt} = -\frac{d}{dt}\left[\ln(\frac{p_d}{T})\right] \tag{12}$$

Substituting eq.(12) in eq.(9) we have

$$\frac{d[\ln(\rho_v + \rho_{cl} + \rho_R)]}{dt} - \frac{d(\ln p_d)}{dt} + \frac{d(\ln T)}{dt} + \frac{\rho_R}{X}\frac{\partial V_d}{\partial z} = 0 \tag{13}$$

Equation (13) may also be written as

$$\frac{1}{(\rho_v + \rho_{cl} + \rho_R)}\{\frac{d}{dt}\rho_v + \frac{d}{dt}\rho_{cl} + \frac{d}{dt}\rho_R\} - \frac{d(\ln p_d)}{dt} + \frac{d(\ln T)}{dt} + \frac{\rho_R \frac{\partial v_d}{\partial z}}{(\rho_v + \rho_u + \rho_R)} = 0 \tag{14}$$

As shown in Fig. 2, we can integrate eq. (14) from the cloud base to its top. This integration becomes

$$\int_{base}^{top} \frac{1}{(\rho_v + \rho_{cl} + \rho_R)} \{\frac{d}{dt} \rho_v) dz + \int_{base}^{top} \frac{1}{(\rho_v + \rho_{cl} + \rho_R)} \{\frac{d}{dt} \rho_{cl}) dz +$$

$$\int_{base}^{top} \frac{1}{(\rho_v + \rho_{cl} + \rho_R)} \{\frac{d}{dt} \rho_R) dz - \int_{base}^{top} \frac{d(\ln p_d)}{dt} dz + \int_{base}^{top} \frac{d(\ln T)}{dt} dz +$$

$$\int_{base}^{top} \frac{\rho_R \frac{\partial v_d}{\partial z}}{(\rho_v + \rho_{cl} + \rho_R)} dz = 0 \qquad (15)$$

By definition, the respective per unit area quantities within the cloud are given by

$$\int_{base}^{top} \rho_V dz = \text{GPS-IPW} \qquad (16)$$

$$\int_{base}^{top} \rho_R dz = \text{Radar-VIL} \qquad (17)$$

$$\int_{base}^{top} \ln p_d dz = \text{integral of log } (p_a\text{-}e) \text{ pressure profile} \qquad (18)$$

in which: $p_a$ = atmospheric pressure, e = water vapor pressure (get saturation vapor pressure $e_s$ can be obtained from Clausius-Clapeyron equation. By knowing the relative humidity data from radiosonde one can obtain vapor pressure)

$$\int_{base}^{top} \ln T dz = \text{integral of log temperature profile} \qquad (19)$$

$$\int_{base}^{top} \rho_R \frac{\partial v_d}{\partial z} dz = \text{rainfall} \qquad (20)$$

Except for the term $\int_{base}^{top} \rho_{cl} dz$ = mass of cloud water, all other terms can be evaluated from the existing instruments including the radiosonde. Following Rogers and Yau (1989) we may write a relationship between the VIL and the cloud water by

$$\text{VIL} = (\text{rain water efficiency, } \eta)(\text{cloud water content}) \qquad (21)$$

Equation (21) may be substituted in place of cloud water content to express it in terms of the VIL. Assuming that the log dry air pressure and temperature profile terms are about equal, we can simplify eq. (7) as

$$\int_{base}^{top} \frac{d}{dt}(\rho_v + \rho_{cl} + \rho_R)dz + \int_{base}^{top} \rho_R \frac{\partial v_d}{\partial z}dz = 0 \quad (22)$$

Using eq. (21), we can rewrite eq. (22) as

$$\int_{base}^{top} \frac{d}{dt}\left(\rho_v + \frac{\rho_R}{\eta} + \rho_R\right)dz + \int_{base}^{top} \rho_R \frac{\partial v_d}{\partial z}dz = 0 \quad (23)$$

which is interpreted as

Rate of change of (GPS-IPW + Radar-VIL) = -rainfall rate (24)

**5.3 Case Study**

We present an analysis based on Equation 6, which is restated below for convenience.

$$\frac{\partial}{\partial t}[\rho_v + \rho_{cl}] + \vec{\nabla}\cdot\vec{v}(\rho_v + \rho_{cl}) + \frac{\partial \rho_R}{\partial t} + u\frac{\partial \rho_R}{\partial x} + v\frac{\partial \rho_R}{\partial y} + (w + v_d)\frac{\partial \rho_R}{\partial z}$$

$$+\rho_R\left[\frac{\partial u}{\partial x} + \frac{\partial v}{\partial y} + \frac{\partial w}{\partial z}\right] + \rho_R \frac{\partial v_d}{\partial z} = 0$$

Assumptions:

1. No cloud water content (initially when there is no cloud)
2. One dimensional analysis (in z direction)
3. Water vapor amount at the cloud top is zero
4. There is no velocity variation (dry air velocity in the upward direction) with respect to height (that is we can replace the dry air velocity (w) with an average velocity).
5. If the air is assumed to be totally saturated at the time of precipitation then vapor pressure (e) can be replaced by saturation vapor pressure ($e_S$).

From assumptions (1) and (2) following relations can be derived.

$$\frac{\partial \rho}{\partial t} = u\frac{\partial \rho}{\partial x} = v\frac{\partial \rho}{\partial y} = 0$$

$$w\frac{\partial \rho}{\partial z} = -\rho\left(\frac{\partial u}{\partial x} + \frac{\partial v}{\partial y} + \frac{\partial w}{\partial z}\right)$$

$$\vec{\nabla}.\vec{V} = -\frac{w}{\rho}\frac{\partial \rho}{\partial z} = -w\frac{\partial(\ln \rho)}{\partial z}$$

From ideal gas law we get

$$\frac{\mathrm{d}\rho_\mathrm{d}}{\mathrm{dt}} = \frac{\mathrm{d}}{\mathrm{dt}}\left[\frac{\mathrm{p_d}}{\mathrm{R_d T}}\right]$$

Hence $\frac{1}{\rho_\mathrm{d}}\frac{\mathrm{d}\rho_\mathrm{d}}{\mathrm{dt}} = \frac{d}{dt}\left[\ln(\frac{p_d}{T})\right]$

Substituting these relations into the equation 6 we get

$$\frac{\partial \rho_v}{\partial t} + w\frac{\partial \rho_v}{\partial z} - \rho_v w\frac{\partial}{\partial z}\left[\ln\left(\frac{p_d}{T}\right)\right] + \frac{\partial \rho_R}{\partial t} + w\frac{\partial \rho_R}{\partial t} - \rho_R w\frac{\partial}{\partial z}\left[\ln\left(\frac{p_d}{T}\right)\right] + v_d\frac{\partial \rho_R}{\partial z} + \rho_R\frac{\partial v_d}{\partial z} = 0$$

(25)

Integrating the Equation 25 (term by term) from cloud base to the cloud top we get

Term 1:

We assume assumption (3) in the following relationship as

$$\int_{z_B}^{z_T}\frac{\partial \rho_v}{\partial t}dz = \frac{d}{dt}\int_{z_B}^{z_T}\rho_v dz + \left(\frac{\partial z_B}{\partial t}\rho_v\right)_{z_B}$$

Term 2:

$$\int_{z_B}^{z_T} w\frac{\partial \rho_v}{\partial z}dz \approx -(w\rho_v)_{z_B} - \int_{z_B}^{z_T}\rho_v\frac{\partial w}{\partial z}dz$$ (applying the product rule in integration)

Term 3:

$$\int_{z_B}^{z_T}\rho_v w\frac{\partial}{\partial z}\left[\ln\left(\frac{p_d}{T}\right)\right]dz = -\left(\rho_v w\ln\left(\frac{p_d}{T}\right)\right)_{z_B} - \int_{z_B}^{z_T}\rho_v\ln\left(\frac{p_d}{T}\right)\frac{\partial w}{\partial z}dz - \int_{z_B}^{z_T} w\ln\left(\frac{p_d}{T}\right)\frac{\partial \rho_v}{\partial z}dz$$

(using product rule in integration)

$$\frac{\partial \rho_v}{\partial z} = \frac{\partial}{\partial z}\left(\frac{0.622e}{R_d T}\right) = \frac{-0.622e}{R_d^2 T}\frac{\partial T}{\partial z} + \frac{0.622}{R_d T}\frac{\partial e}{\partial z} = \frac{0.622e}{R_d T}\left[-\frac{1}{T}\frac{\partial T}{\partial z} + \frac{1}{e}\frac{\partial e}{\partial z}\right] = \rho_v \frac{\partial}{\partial z}\left(\ln\left(\frac{e}{T}\right)\right)$$

(using Clausius-Clapeyron Equation)

$$\int_{z_B}^{z_T} \rho_v w \frac{\partial}{\partial z}\left[\ln\left(\frac{p_d}{T}\right)\right]dz = -\left(\rho_v w \ln\left(\frac{p_d}{T}\right)\right)_{z_B} - \int_{z_B}^{z_T} \rho_v \ln\left(\frac{p_d}{T}\right)\frac{\partial w}{\partial z}dz - \int_{z_B}^{z_T} w\rho_v \ln\left(\frac{p_d}{T}\right)\frac{\partial}{\partial z}\left(\frac{e_s}{T}\right)dz$$

(From assumption (5))

Term 4:

$$\int_{z_B}^{z_T} \frac{\partial \rho_R}{\partial t}dz \approx \frac{d}{dt}\int_{z_B}^{z_T} \rho_R dz + \left(\frac{\partial z_B}{\partial t}\rho_R\right)_{z_B}$$

Term 5:

$$\int_{z_B}^{z_T} w\frac{\partial \rho_R}{\partial z}dz \approx -(w\rho_R)_{z_B} - \int_{z_B}^{z_T} \rho_R \frac{\partial w}{\partial z}dz \text{ (using product rule in integration)}$$

Term 6:

$$\int_{z_B}^{z_T} \rho_R w \frac{\partial}{\partial z}\left[\ln\left(\frac{p_d}{T}\right)\right]dz = -\left(\rho_R w \ln\left(\frac{p_d}{T}\right)\right)_{z_B} - \int_{z_B}^{z_T} \rho_R \ln\left(\frac{p_d}{T}\right)\frac{\partial w}{\partial z}dz - \int_{z_B}^{z_T} w\ln\left(\frac{p_d}{T}\right)\frac{\partial \rho_R}{\partial z}dz$$

(using product rule in integration)

Terms 7 and 8:

Note that $v_d \frac{\partial \rho_R}{\partial z} + \rho_R \frac{\partial v_d}{\partial z} = \frac{\partial}{\partial z}(\rho_R v_d)$

$$\int_{z_B}^{z_T} \frac{\partial}{\partial z}(\rho_R v_d)dz = (\rho_R v_d)_{z_B}^{z_T} = -(\rho_R v_d)_{z_B} \text{ (From Assumption (3))}$$

Substituting all the above values in equation 25 we get

$$\frac{d}{dt}\int_{z_B}^{z_T} \rho_v dz + \left(\frac{\partial z_B}{\partial t}\rho_v\right)_{z_B} - (w\rho_v)_{z_B} - \int_{z_B}^{z_T} \rho_v \frac{\partial w}{\partial z}dz + \left(\rho_v w \ln\left(\frac{p_d}{T}\right)\right)_{z_B} + \int_{z_B}^{z_T} \rho_v \ln\left(\frac{p_d}{T}\right)\frac{\partial w}{\partial z}dz + \int_{z_B}^{z_T} w\rho_v \ln\left(\frac{p_d}{T}\right)\frac{\partial}{\partial z}\left(\frac{e_s}{T}\right)dz$$

$$+\frac{d}{dt}\int_{z_B}^{z_T} \rho_R dz + \left(\frac{\partial z_B}{\partial t}\rho_R\right)_{z_B} - (w\rho_R)_{z_B} - \int_{z_B}^{z_T} \rho_R \frac{\partial w}{\partial z}dz + \left(\rho_R w \ln\left(\frac{p_d}{T}\right)\right)_{z_B} + \int_{z_B}^{z_T} \rho_R \ln\left(\frac{p_d}{T}\right)\frac{\partial w}{\partial z}dz + \int_{z_B}^{z_T} w\ln\left(\frac{p_d}{T}\right)\frac{\partial \rho_R}{\partial z}dz$$

$$-(\rho_R v_d)_{z_B} = 0$$

(26)

From assumption (4) we get

$$\frac{\partial w}{\partial z} = 0.$$

From this assumption equation 25 reduces to the form

$$\frac{d}{dt}\int_{z_B}^{z_T}\rho_v dz + \left(\frac{\partial z_B}{\partial t}\rho_v\right)_{z_B} - (w\rho_v)_{z_B} + \left(\rho_v w \ln\left(\frac{p_d}{T}\right)\right)_{z_B} + \int_{z_B}^{z_T} w\rho_v \ln\left(\frac{p_d}{T}\right)\frac{\partial}{\partial z}\left(\frac{e_s}{T}\right)dz + \frac{d}{dt}\int_{z_B}^{z_T}\rho_R dz + \left(\frac{\partial z_B}{\partial t}\rho_R\right)_{z_B} - (w\rho_R)_{z_B}$$

$$+\left(\rho_R w \ln\left(\frac{p_d}{T}\right)\right)_{z_B} + \int_{z_B}^{z_T} w \ln\left(\frac{p_d}{T}\right)\frac{\partial\rho_R}{\partial z}dz - (\rho_R v_d)_{z_B} = 0 \qquad (27)$$

$$\frac{d}{dt}\int_{z_B}^{z_T}\rho_v dz + \int_{z_B}^{z_T} w\rho_v \ln\left(\frac{p_d}{T}\right)\frac{\partial}{\partial z}\left(\frac{e_s}{T}\right)dz + \frac{d}{dt}\int_{z_B}^{z_T}\rho_R dz + \left((\rho_R+\rho_v)w\ln\left(\frac{p_d}{T}\right)\right)_{z_B} + \int_{z_B}^{z_T} w\ln\left(\frac{p_d}{T}\right)\frac{\partial\rho_R}{\partial z}dz - (\rho_R v_d)_{z_B} = 0 \qquad (28)$$

### 5.3.1 Event on April-28-02

Meteorological data is collected for the event on April-28-02 and the rain amount is calculated from the equation 28.

Equation 28:

$$\frac{d}{dt}\int_{z_B}^{z_T}\rho_v dz + \int_{z_B}^{z_T} w\rho_v \ln\left(\frac{p_d}{T}\right)\frac{\partial}{\partial z}\left(\frac{e_s}{T}\right)dz + \frac{d}{dt}\int_{z_B}^{z_T}\rho_R dz + \left((\rho_R+\rho_v)w\ln\left(\frac{p_d}{T}\right)\right)_{z_B} + \int_{z_B}^{z_T} w\ln\left(\frac{p_d}{T}\right)\frac{\partial\rho_R}{\partial z}dz - (\rho_R v_d)_{z_B} = 0$$

In the above equation the following assumptions are made to fit the meteorological data.

1. $\frac{\partial\rho_R}{\partial z} = 0$

2. Density of rainwater ( $\rho_R$ ) is assumed to be zero in the fourth term of equation (28) that is the rain amount calculated at the cloud base.

Hence equation 28 reduces to

$$\text{Rain rate } ((\rho_R v_d)_{z_B}) = \frac{d}{dt}\int_{z_B}^{z_T}\rho_v dz + \frac{d}{dt}\int_{z_B}^{z_T}\rho_R dz + \int_{z_B}^{z_T} w\rho_v \ln\left(\frac{p_d}{T}\right)\frac{\partial}{\partial z}\left(\frac{e_s}{T}\right)dz + \left(\rho_v w\ln\left(\frac{p_d}{T}\right)\right)_{z_B} \qquad (29)$$

**Example Problem:** Using the equation 29 and given meteorological data estimate the amount of rainfall in Botetourt County on April 28, 2002 between 15:44 and 16:29 eastern pacific time and compare with the actual rain gauge data.

Given meteorological data: Table 5.1 contains the GPS-IPW data for the event. Table 5.2 contains the Radar-VIL data. Table 5.3 contains the meteorological parameters and their values obtained at 12:00Z from the radiosonde database.

**Solution:**

From Equation 29

Rainfall amount at the cloud base ( $(\rho_R v_d)_{z_B}$ ) =

$$\frac{d}{dt}\int_{z_B}^{z_T}\rho_v dz + \frac{d}{dt}\int_{z_B}^{z_T}\rho_R dz + \int_{z_B}^{z_T} w\rho_v \ln\left(\frac{p_d}{T}\right)\frac{\partial}{\partial z}\left(\frac{e_s}{T}\right)dz + \left(\rho_v w \ln\left(\frac{p_d}{T}\right)\right)_{z_B}$$

Evaluation of each term in the above equation:

Term 1:

$$\int_{\text{base}}^{\text{top}} \rho_V dz = \text{GPS-IPW}$$

Using the IPW data on April-28, 2002 (Table 5.1) first term in the equation 29 can be evaluated. A lead time of one hour is taken for IPW values in predicting the rain amount. IPW values at 14:45,15:15 and 15:45 are taken and method of backward differencing is used to obtain the derivative of IPW. Calculations are shown in the Table 5.4.

Term 2:

$$\frac{d}{dt}\int_{\text{base}}^{\text{top}} \rho_R dz = \text{Radar-VIL}$$

Using the data in the Table 5.2, time derivative of VIL is calculated by taking VIL values at 15:44 and 15:59. Difference between VIL values in this time interval (5 minutes) is -5 kg/m$^2$. Hence the derivative of VIL with time is -5/(5*60) = -0.0167. We assume an

efficiency of 20% for the VIL values in the calculation. Hence we obtain thetime derivative of VIL = 0.2*-0.0167 = -0.00334.
Table 5.5 shows the results. We also assume that VIL fluctuates in equal an amount; that is it increases and decreases in the same amount in the time interval between 15:45 to 16:45.

Evaluation of other terms in the equation (29) involves the calculation of cloud base. Cloud base is calculated using the data from the Radiosonde (using the pseudoadiabatic chart). In calculating the cloud base partial pressure of dry air, temperature and saturated vapor pressure profiles are used and these can be calculated from the temperature, pressure and dew point profiles obtained from the radiosonde database (See Appendix B). Table 5.3 shows the data obtained from radiosonde database for the current event. Table 5.6 represents the calculation of various metorological parameters needed to evaluate the cloud base using the data from the radiosonde data base. From table 5.6 it can be seen that at higher levels(after 300 mb) density of water vapor is negligible. This justifies the assumption of neglecting the vapor quantity at the cloud top in deriving the mathematical formulation.
Equations used to calculate above parameters are:

1. Saturation Vapor Pressure ($e_s$) = $611\exp\left(\frac{17.27T}{237.3+T}\right)$

Where T is the temperature in degrees Celsius and $e_s$ in millibars.

2. Vapor Pressure (e) = $611\exp\left(\frac{17.27T}{237.3+T}\right)$

Where T is the dew point temperature in degrees Celsius and e in millibars.

3. Dry air pressure $P_d$ (Pa) = Total pressure (P) – Vapor pressure (e) (observed)

4. Vapor density ($\rho_v$) (kg / $m^3$) = $0.622\frac{e_S}{R_d T}$

where $R_d$ is dry air gas constant, which is equal to 287 J/K/kg.

5. All the terms are calculated when it is raining. At that time it is assumed that the cloud is saturated. Hence the temperature inside the cloud is the dew point temperature.

6. From Table 5.6 it is seen that $\frac{e_S}{T_d}$ values are negligible after 10730 m. Hence in calculating the derivative of the logarithmic for $\frac{e_S}{T_d}$ values after that elevation are neglected.

Table 5.7 shows the calculation of the cloud base for the event. To calculate the cloud base dry adiabatic lapse rate is used. This is a constant in the troposphere.

The notations in Table 5.7 are as follows:
LFC: Lifting Condensation Level
DALR: Dry Adiabatic Lapse Rate is –0.006 $^{o}$C/km. This is valid only in the troposphere, which extends from the ground level to 12 km.
At LCL (Cloud Condensation Level) saturation mixing ration and the mixing ration at the surface should be equal. Form the Table 5.5 we can see that it is between 3395 m and 5780 m. If we linearly interpolate we get LCL to be at 3600 m, which is the cloud base. Using pseudoadiabatic chart we get the cloud base to be 3150 m. These two (from chart and the calculated one) values are very close.
From Table 5.6 we can evaluate the integral (Term 3) and the value of the rain at the cloud base (Term 4) in equation 29 in the following manner.
Term 4:

$$\left(\rho_v w \ln\left(\frac{p_d}{T}\right)\right)_{z_B} = w(0.0307)$$

Term 3:

$\int_{z_B}^{z_T} w\rho_v \ln\left(\frac{p_d}{T}\right)\frac{\partial}{\partial z}\left(\frac{e_s}{T}\right)dz$ : Assuming that only $\frac{\partial}{\partial z}\left(\frac{e_s}{T}\right)$ varies in this term we get

$$\int_{z_B}^{z_T} w\rho_v \ln\left(\frac{p_d}{T}\right)\frac{\partial}{\partial z}\left(\frac{e_s}{T}\right)dz = w\rho_v \ln\left(\frac{p_d}{T}\right)\int_{z_B}^{z_T} \frac{\partial}{\partial z}\left(\frac{e_s}{T}\right)dz$$

$$\int_{z_B}^{z_T} \frac{\partial}{\partial z}\left(\frac{e_s}{T}\right)dz = \left(\left(\frac{e_s}{T}\right)\right)_{Z_T} - \left(\left(\frac{e_s}{T}\right)\right)_{Z_B} = -2.467$$

Hence

$$\int_{z_B}^{z_T} w\rho_v \ln\left(\frac{p_d}{T}\right)\frac{\partial}{\partial z}\left(\frac{e_s}{T}\right)dz = w(0.0307)*(-2.467) = w(-0.0757)$$

Calibration of w:

Observed rain is taken from table 5.8 and rain rate is estimated. In the equation 29 if we neglect the rate of change of VIL we get

Rainfall amount (observed) at the cloud base ($(\rho_R v_d)_{z_B}$) =

$$\frac{d}{dt}\int_{z_B}^{z_T}\rho_v dz + \int_{z_B}^{z_T} w\rho_v \ln\left(\frac{p_d}{T}\right)\frac{\partial}{\partial z}\left(\frac{e_s}{T}\right)dz + \left(\rho_v w \ln\left(\frac{p_d}{T}\right)\right)_{z_B} =$$

$$\frac{d}{dt}(IPW) + w(-0.0757) + w(0.0307) = \frac{d}{dt}(IPW) - w(0.045)$$

Hence

Rainfall amount (observed) at the cloud base ($(\rho_R v_d)_{z_B}$) - $\frac{d}{dt}(IPW)$ = -w(0.045)

Table 5.10 shows the calculation of downdraft velocities at times 15:45,16:15 and 16:45 and the average downdraft velocity.

Using the equation 29 and estimated average w, rainfall in the Botetourt County can be calculated. Results are shown in the Table 5.10.

## 5.4 Summary

The GPS-IPW trend yields a lead-time of 30 minutes to 2 hours in predicting rainfall. A water substance continuity approach yields rainfall estimates in terms of measurable atmospheric parameters through eq. (14) and its simplified form eq. (24). Because the GPS-IPW covers a wider area, it precedes the radar-VIL in predicting a rain event. To refine this process, the estimated rain from the GPS-IPW and current location VIL are combined with the observed upstream radar and rain gage measurements within a mathematical model to yield the final forecast for the location under consideration. All the steps involved in this rainfall prediction framework are subject to measurements by

various instruments and have the potential to provide sufficient prediction time with good accuracy.

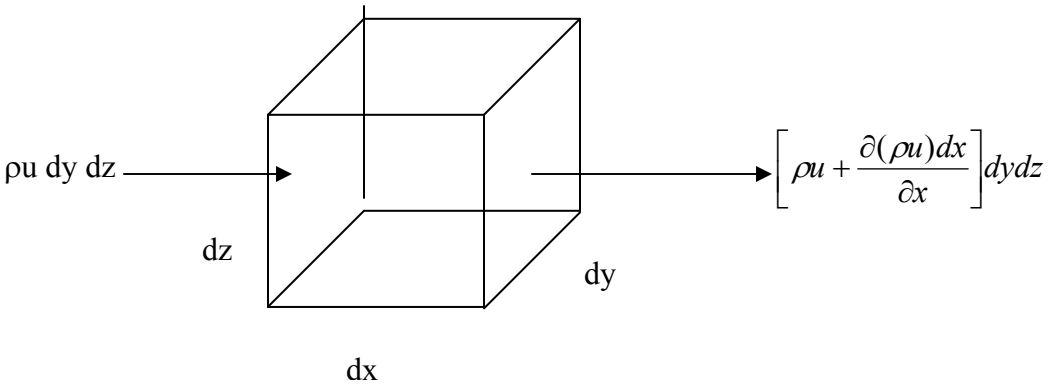


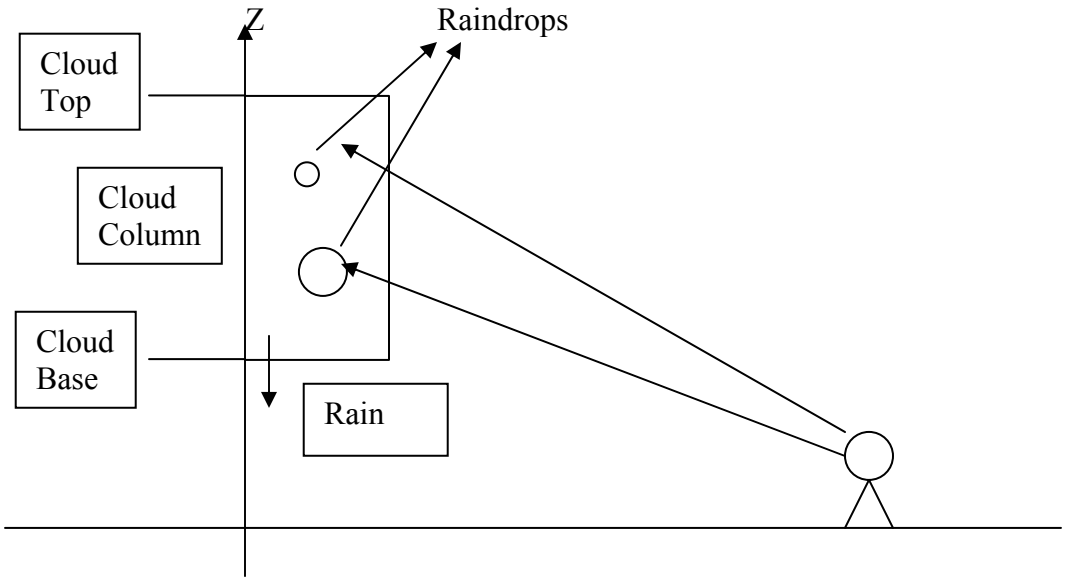


**Figure 5.1. Control volume and cloud column description**

**Table 5.1. GPS-IPW data on April 28, 2002**

| April-28-02 | | |
|---|---|---|
| Time (local) | Time (sec) | IPW (cm) |
| 11:15 | 40500 | 2.99 |
| 11:45 | 42300 | 2.84 |
| 12:15 | 44100 | 2.75 |
| 12:45 | 45900 | 2.77 |
| 13:15 | 47700 | 2.58 |
| 13:45 | 49500 | 2.41 |
| 14:15 | 51300 | 2.25 |
| 14:45 | 53100 | 2.43 |
| 15:15 | 54900 | 2.35 |
| 15:45 | 56700 | 2.64 |
| 16:15 | 58500 | 2.66 |
| 16:45 | 60300 | 2.56 |
| 17:15 | 62100 | 3.09 |
| 17:45 | 63900 | 3.05 |
| 18:15 | 65700 | 2.62 |
| 18:45 | 67500 | 2.83 |

**Table 5.2. Radar-VIL data for Botetourt County**

| April-28-02 | | |
|---|---|---|
| Time (local) | Time (sec) | VIL ($kg/m^2$) |
| | | Botetourt |
| 15:34 | 56040 | |
| 15:39 | 56340 | |
| 15:44 | 56640 | 35 |
| 15:49 | 56940 | 40 |
| 15:54 | 57240 | 50 |
| 15:59 | 57540 | 45 |
| 16:04 | 57840 | 50 |
| 16:09 | 58140 | 50 |
| 16:14 | 58440 | 40 |
| 16:19 | 58740 | 25 |
| 16:24 | 59040 | 20 |
| 16:29 | 59340 | 40 |

**Table 5.3. Data obtained from Radiosonde database**

| Pressure (mb) | Pressure P (Pa) | Elevation (m) | Temp °C | Temp °K | Dewpoint °C |
|---|---|---|---|---|---|
| 947 | 94700 | 648 | 16 | 289 | 3 |
| 925 | 92500 | 837 | 14.2 | 287.2 | 3.2 |
| 850 | 85000 | 1543 | 7.6 | 280.6 | 1.6 |
| 816 | 81600 | 1876 | 4.6 | 277.6 | 1.3 |
| 791 | 79100 | 2128 | 3.4 | 276.4 | 3.4 |
| 773 | 77300 | 2314 | 5 | 278 | 5 |
| 700 | 70000 | 3126 | 2.8 | 275.8 | 2.8 |
| 677 | 67700 | 3395 | 2 | 275 | 2 |
| 500 | 50000 | 5780 | -12.3 | 260.7 | -12.6 |
| 478 | 47800 | 6121 | -15.1 | 257.9 | -15.7 |
| 419 | 41900 | 7105 | -19.7 | 253.3 | -20.9 |
| 400 | 40000 | 7460 | -22.1 | 250.9 | -23.3 |
| 340 | 34000 | 8631 | -30.7 | 242.3 | -32.5 |
| 300 | 30000 | 9510 | -38.1 | 234.9 | -41.5 |
| 250 | 25000 | 10730 | -49.1 | 223.9 | -53.5 |
| 200 | 20000 | 12160 | -61.1 | 211.9 | -64.7 |
| 182 | 18200 | 12737 | -65.9 | 207.1 | -68.9 |
| 162 | 16200 | 13452 | -65.3 | 207.7 | -68.5 |
| 150 | 15000 | 13920 | -59.7 | 213.3 | -63.6 |
| 141 | 14100 | 14306 | -59.7 | 213.3 | -64.1 |
| 113 | 11300 | 15663 | -66.9 | 206.1 | -71.7 |
| 100 | 10000 | 16410 | -64.7 | 208.3 | -69.7 |
| 96.2 | 9620 | 16646 | -64.9 | 208.1 | -69.9 |
| 74.6 | 7460 | 18183 | -67.5 | 205.5 | -72.5 |
| 70 | 7000 | 18570 | -65.5 | 207.5 | -70.5 |
| 63.7 | 6370 | 19145 | -63.1 | 209.9 | -68.1 |
| 50 | 5000 | 20640 | -62.5 | 210.5 | -67.5 |
| 44.6 | 4460 | 21344 | -61.7 | 211.3 | -66.7 |
| 40.7 | 4070 | 21917 | -55.9 | 217.1 | -60.9 |
| 30 | 3000 | 23860 | -55.7 | 217.3 | -60.7 |
| 22.8 | 2280 | 25610 | -53.9 | 219.1 | -58.9 |
| 20 | 2000 | 26470 | -50.3 | 222.7 | -55.3 |
| 14.4 | 1440 | 28627 | -46.3 | 226.7 | -52.3 |
| 10 | 1000 | 31050 | -46.1 | 226.9 | -52.1 |
| 9 | 900 | 31749 | -45.9 | 227.1 | -52.9 |
| 8.5 | 850 | 32131 | -43.1 | 229.9 | -50.1 |
| 8.3 | 830 | 32291 | -44.1 | 228.9 | -51.1 |

**Table 5.4. Derivative of IPW values between 15:44 and 16:29 on April-28-02**

| April-28-02 | | | |
|---|---|---|---|
| Time (local) | Time (sec) | IPW (cm) | d/dt (IPW) (cm/s) |
| 11:15 | 40500 | 2.99 | |
| 11:45 | 42300 | 2.84 | -0.0000833 |
| 12:15 | 44100 | 2.75 | -0.0000500 |
| 12:45 | 45900 | 2.77 | 0.0000111 |
| 13:15 | 47700 | 2.58 | -0.0001056 |
| 13:45 | 49500 | 2.41 | -0.0000944 |
| 14:15 | 51300 | 2.25 | -0.0000889 |
| 14:45 | 53100 | 2.43 | 0.0001000 |
| 15:15 | 54900 | 2.35 | -0.0000444 |
| 15:45 | 56700 | 2.64 | 0.0001611 |
| 16:15 | 58500 | 2.66 | 0.0000111 |
| 16:45 | 60300 | 2.56 | -0.0000556 |
| 17:15 | 62100 | 3.09 | 0.0002944 |
| 17:45 | 63900 | 3.05 | -0.0000222 |
| 18:15 | 65700 | 2.62 | -0.0002389 |
| 18:45 | 67500 | 2.83 | 0.0001167 |

$$\frac{d}{dt}\int_{\text{base}}^{\text{top}} \rho_R \, dz = \text{Radar-VIL}$$

**Table 5.5. Derivative of VIL values between 15:44 and 16:29 on April-28-02**

| April-28-02 | |
|---|---|
| Time (local) | d/dt (VIL) ($kg/m^2/s$) |
| 15:45 | -0.00334 |
| 16:15 | 0.00334 |
| 16:45 | -0.00334 |

**Table 5.6. Parameters calculated using the data from table 5.3**

| $e_s$ (Pa) | Vapor Pressure (e) (Pa) | $P_d$ (Pa) = P - e (observed) | $\ln(P_d)$ | $\ln(T_d)$ | $[\ln(P_d) - \ln(T_d)]$ | $e_s / T_d$ | $\rho_v$ ($kg/m^3$) |
|---|---|---|---|---|---|---|---|
| 1587.999 | 737.017 | 93962.983 | 11.451 | 5.620 | 5.830 | 2.670 | 0.006 |
| 1433.802 | 746.180 | 91753.820 | 11.427 | 5.621 | 5.806 | 2.702 | 0.006 |
| 974.917 | 675.608 | 84324.392 | 11.342 | 5.615 | 5.727 | 2.460 | 0.005 |
| 813.188 | 663.054 | 80936.946 | 11.301 | 5.614 | 5.687 | 2.417 | 0.005 |
| 755.444 | 755.444 | 78344.556 | 11.269 | 5.622 | 5.647 | 2.733 | 0.006 |
| 833.283 | 833.283 | 76466.717 | 11.245 | 5.628 | 5.617 | 2.997 | 0.006 |
| 727.953 | 727.953 | 69272.047 | 11.146 | 5.620 | 5.526 | 2.639 | 0.006 |
| 692.674 | 692.674 | 67007.326 | 11.113 | 5.617 | 5.496 | 2.519 | 0.005 |
| 270.757 | 265.181 | 49734.819 | 10.814 | 5.562 | 5.252 | 1.018 | 0.002 |
| 222.542 | 213.266 | 47586.734 | 10.770 | 5.550 | 5.220 | 0.829 | 0.002 |
| 159.739 | 146.211 | 41753.789 | 10.640 | 5.530 | 5.110 | 0.580 | 0.001 |
| 133.717 | 122.185 | 39877.815 | 10.594 | 5.520 | 5.073 | 0.489 | 0.001 |
| 68.693 | 59.396 | 33940.604 | 10.432 | 5.483 | 4.950 | 0.247 | 0.001 |
| 37.246 | 27.749 | 29972.251 | 10.308 | 5.445 | 4.863 | 0.120 | 0.000 |
| 13.915 | 9.130 | 24990.870 | 10.126 | 5.391 | 4.735 | 0.042 | 0.000 |
| 4.231 | 2.882 | 19997.118 | 9.903 | 5.339 | 4.564 | 0.014 | 0.000 |
| 2.529 | 1.811 | 18198.189 | 9.809 | 5.319 | 4.490 | 0.009 | 0.000 |
| 2.700 | 1.894 | 16198.106 | 9.693 | 5.321 | 4.372 | 0.009 | 0.000 |
| 4.895 | 3.246 | 14996.754 | 9.616 | 5.344 | 4.271 | 0.015 | 0.000 |
| 4.895 | 3.076 | 14096.924 | 9.554 | 5.342 | 4.212 | 0.015 | 0.000 |
| 2.265 | 1.314 | 11298.686 | 9.332 | 5.305 | 4.028 | 0.007 | 0.000 |
| 2.882 | 1.654 | 9998.346 | 9.210 | 5.315 | 3.895 | 0.008 | 0.000 |
| 2.820 | 1.616 | 9618.384 | 9.171 | 5.314 | 3.858 | 0.008 | 0.000 |
| 2.119 | 1.197 | 7458.803 | 8.917 | 5.301 | 3.616 | 0.006 | 0.000 |
| 2.642 | 1.509 | 6998.491 | 8.853 | 5.311 | 3.543 | 0.007 | 0.000 |
| 3.424 | 1.981 | 6368.019 | 8.759 | 5.323 | 3.437 | 0.010 | 0.000 |
| 3.650 | 2.119 | 4997.881 | 8.517 | 5.325 | 3.191 | 0.010 | 0.000 |
| 3.972 | 2.315 | 4457.685 | 8.402 | 5.329 | 3.073 | 0.011 | 0.000 |
| 7.203 | 4.321 | 4065.679 | 8.310 | 5.357 | 2.953 | 0.020 | 0.000 |
| 7.348 | 4.412 | 2995.588 | 8.005 | 5.358 | 2.647 | 0.021 | 0.000 |
| 8.779 | 5.316 | 2274.684 | 7.730 | 5.366 | 2.363 | 0.025 | 0.000 |
| 12.424 | 7.646 | 1992.354 | 7.597 | 5.383 | 2.214 | 0.035 | 0.000 |
| 18.041 | 10.259 | 1429.741 | 7.265 | 5.397 | 1.868 | 0.046 | 0.000 |
| 18.374 | 10.459 | 989.541 | 6.897 | 5.398 | 1.500 | 0.047 | 0.000 |
| 18.713 | 9.679 | 890.321 | 6.792 | 5.394 | 1.397 | 0.044 | 0.000 |
| 24.087 | 12.662 | 837.338 | 6.730 | 5.407 | 1.324 | 0.057 | 0.000 |
| 22.026 | 11.513 | 818.487 | 6.707 | 5.402 | 1.305 | 0.052 | 0.000 |

**Table 5.7. Calculation of Cloud base**

| Elevation (m) | Temp °C | LFC DALR Mixing Ratio | Dewpoint °C | $e_s$ (Pa) | Vapor Pressure (e) (Pa) | $P_d$ (Pa) = P - e (observed) | Saturated mixing ratio at various heights (g/kg) | Mixing ratio at the surface (g/kg) |
|---|---|---|---|---|---|---|---|---|
| 648 | 16 | 16 | 3 | 1587.999 | 737.017 | 93962.983 | 10.608 | 4.8788 |
| 837 | 14.2 | 14.866 | 3.2 | 1489.249 | 746.180 | 91753.820 | 10.178 | |
| 1543 | 7.6 | 10.63 | 1.6 | 1166.386 | 675.608 | 84324.392 | 8.654 | |
| 1876 | 4.6 | 8.632 | 1.3 | 1036.762 | 663.054 | 80936.946 | 8.004 | |
| 2128 | 3.4 | 7.12 | 3.4 | 947.276 | 755.444 | 78344.556 | 7.539 | |
| 2314 | 5 | 6.004 | 5 | 885.664 | 833.283 | 76466.717 | 7.209 | |
| 3126 | 2.8 | 1.132 | 2.8 | 656.113 | 727.953 | 69272.047 | 5.885 | |
| 3395 | 2 | -0.482 | 2 | 592.639 | 692.674 | 67007.326 | 5.493 | |
| 5780 | -12.3 | -14.792 | -12.6 | 227.442 | 265.181 | 49734.819 | 2.842 | |
| 6121 | -15.1 | -16.838 | -15.7 | 196.613 | 213.266 | 47586.734 | 2.569 | |
| 7105 | -19.7 | -22.742 | -20.9 | 127.431 | 146.211 | 41753.789 | 1.897 | |
| 7460 | -22.1 | -24.872 | -23.3 | 108.426 | 122.185 | 39877.815 | 1.691 | |
| 8631 | -30.7 | -31.898 | -32.5 | 62.371 | 59.396 | 33940.604 | 1.143 | |
| 9510 | -38.1 | -37.172 | -41.5 | 40.302 | 27.749 | 29972.251 | 0.837 | |
| 10730 | -49.1 | -44.492 | -53.5 | 21.262 | 9.130 | 24990.870 | 0.529 | |
| 12160 | -61.1 | -53.072 | -64.7 | 9.519 | 2.882 | 19997.118 | 0.296 | |

**Table 5.8. Observed rainfall in Botetourt County**

| Time (local) | Observed Rainfall (cm) |
|---|---|
| 15:45 | 0.7112 |
| 16:15 | 1.6002 |
| 16:45 | 0.6096 |

**Table 5.9. Calculation of Average down draft velocity (w)**

| Time (local) | Rain (cm) | Rain rate ($kg/m^2/s$) | w (m/s) |
|---|---|---|---|
| 15:45 | 0.7 | 0.003888889 | -0.0642 |
| 16:15 | 1.6 | 0.008888889 | -0.20741 |
| 16:45 | 0.61 | 0.003388889 | -0.03951 |
| | | **Average w** | -0.103703 |

**Table 5.10 Calculation of rain amount using average w**

| Time (local) | Term 1 d/dt (IPW)($kg/m^2/s$) | Term 2 d/dt (VIL) ($kg/m^2/s$) | Terms 3 and 4 (Avg.w(-0.045)) $kg/m^2/s$) | Rain rate Calculated ($kg/m^2/s$) | Rain Calculated (cm) | Oberved Rainfall (cm) |
|---|---|---|---|---|---|---|
| 15:45 | 0.001 | -0.00334 | 0.004667 | 0.002327 | 0.4188 | 0.7112 |
| 16:15 | -0.00044 | 0.00334 | 0.004667 | 0.007562 | 1.3612 | 1.6002 |
| 16:45 | 0.001611 | -0.00334 | 0.004667 | 0.002938 | 0.5288 | 0.6096 |

# Chapter 6 – Summary

## 6.1 Contributions of this thesis

Chapter 1 presents the objective of the thesis. In Chapter 2 general working principle of GPS is described. In chapter 3, the theoretical equations behind GPS-IPW estimation are summarized from the literature. This chapter contains the methodology to get IPW values using the delays of the GPS signals when they travel through the atmosphere. In Chapter 4 two types of analyses are conducted. Significant rain days were identified solely based on the GPS-IPW peaks and these days clearly captured the observed significant rain days. Also, the GPS-IPW peaks and radar VIL and reflectivity and rainfall peaks displayed a decipherable pattern. The correlations were significant and to rule out false alarms an acceptable threshold was necessary. The accuracy of the GPS-IPW data was evaluated by comparing it with the GOES satellite and the radiosonde observations. The match was quite close.

Chapter 4 also focuses on realtime forecasting aspect. By analyzing the historical radiosonde PW data for Blacksburg, the monthly $75^{th}$ percentile was chosen as the threshold for an impending significant rain event defined as 0.25 inches of observed rainfall in one half hour; and 0.5 inch of observed rainfall in one half hour is defined as the heavy rain event. It is found that for frontal events there is a long lead time; summer time convective events have short lead times. The winter time GPS-IPW behavior is very similar between stations under suitable transformation of data. Standardized variate is employed as the transformation with a phase shift. This similarity in behavior is attributed to lack of moisture in the atmosphere and as pointed out by Wolfe and Gutman (2000) the variability in GPS-IPW is mostly attributable to the wet delay. To minimize false alarms two additional criteria are added: an exceedance duration of at least 4 hours above the threshold and the behavior if GPS-IPW at the surrounding stations. The analyses show that the criteria lead to minimum number of false alarms and identify heavy rain events with an improved lead-time in comparison to the radar. The criteria can be improved based on a large number of events and the methodology shows potential in gaining lead time for significant rain events.

Chapter 5 describes the mathematical equation in predicting the actual amount of rainfall using meteorological variables. An example using the data from Botetourt County on April 28, 2002 is also presented and the actual amount of rainfall values from the rain gauges are compared with the calculated values. Results for this event are very close.

### 6.2 Future Improvements

One of the factors influencing the calculation of rain amount using the mathematical equation is the VIL data. This data is collected manually from the PUP server at the NWS in Blacksburg. Availability of digital version of the data would enable the process at a much faster rate. For many events the VIL data are archived during the time of the event. If the VIL data is archived at a much larger interval then comparison of rain can be done at more number of points. Also, real time meteorologic variable values are not available. The radiosonde data obtained at 12-hr intervals do not lend themselves for use in the proposed predictive scheme.

## Chapter 7 – Bibliography

Alber, C., R. Ware, C. Rocken and F. Solheim, GPS surveying with 1 mm precision using corrections for atmospheric slant path delay, Geophysical Research Letters, Vol. 24, No. 15, pp 1859-1862, August 1997.

Anthes, R., M. Exner, C. Rocken, and R. Ware, Results from the GPS/MET Experiment and Potential Applications to GEWEX, GEWEX News, 7, 3-6, Feb., 1997.

Bevis, M., S. Businger, S. Chiswell, T.A. Herring, R.A. Anthes, C. Rocken and R.H. Ware, GPS Meteorology: Mapping zenith wet dealys onto precipitable water, Journal of Applied Meteorology, 379-386, 1994.

Bevis M., S. Businger, T.A. Herring, C. Rocken, R.A. Anthes and R.H. Ware, GPS Meteorology: Remote Sensing of Atmospheric Water Vapor Using the Global Positioning System, Journal of Geophys. Research, Vol. 97, No. D14, pp 15,787-15,801, October, 1992.

Businger, S., S.R. Chiswell, M. Bevis, J. Duan, R. A. Anthes, C. Rocken, R. H. Ware, T. VanHove, and F. S. Solheim, The Promise of GPS in Atmospheric Monitoring, Bulletin. American Meteorological Society., 77, pp 5-18, 1996.

Chiswell, S., S. Businger, M. Bevis, F. Solheim, C. Rocken, and Randolph Ware, Improved Retrieval of Integrated Water Vapor from Water Vapor Radiometer Measurements Using Numerical Weather Prediction Models, Journal of Atmospheric. and Oceanographic Tech, Vol. 11, No.5 , October 1994.

Chiswell, S., S. Businger, M. Bevis, J. Duan, C. Rocken, Randolph Ware, F. Solheim, and T. Van Hove, Application of GPS Water Vapor Data in the Analysis of Severe Weather, submitted to Monthly Weather Review, January, 1995.

Duan, J., M. Bevis, P. Fang, Y.Bock, S. Chiswell, S. Businger, C. Rocken, F. Solheim, T. VanHove, R. Ware, S. Mc Clusky, T. A. Herring, and R. W. King, GPS Meteorology: Direct Estimation of the Absolute Value of Precipitable Water, J. of Applied Metorology., Vol. 35, No. 6, pp 830-838, June 1996.

Gutman, S., R. Chadwick, D. Wolfe, A. Simon, T. VanHove, and C. Rocken, Toward an Operational Water Vapor Remote Sensing System Using GPS, FSL Forum, September 1994.

Rocken C., The Global Positioning System: A New Tool for Tectonic Studies, Ph.D. Thesis, University of Colorado at Boulder, 298 pp., 1988.

Rocken, C., J. Johnson, R.E. Neilan, M. Cerezo, J. Jordan, M. Falls, L. Nelson, R. Ware, M. Hayes, The Measurement of Atmospheric Water Vapor: Radiometer Comparison and Spatial Variations, IEEE Trans. on Geosciences and Remote Sensing., Vol., 29., No.1, pp. 3 - 8, Jan., 1991.

Rocken, C. R. H. Ware, T. Van Hove, F. Solheim, C. Alber, J. Johnson, M. Bevis, S. Businger, Sensing Atmospheric Water Vapor with the Global Positioning System, Geophysical Research Letters, Vol. 20, No. 23, pp 2631-2634, Dec., 1993.

Rocken, C. T. Van Hove, J. Johnson, F. Solheim, R. H. Ware, M. Bevis, S. Businger, S. Chiswell, GPS/STORM - GPS Sensing of Atmospheric Water Vapor for Meteorology, Journal of Atmospheric Science and Oceanography. Tech., Vol. 12, No. 3, pp 468-478, June 1995.

Rocken, C, F S Solheim, R H Ware, M Exner, D Martin, M Rothacher, Application of IGS Data to GPS Sensing of the Atmopsphere for Weather and Climate Research, Proceeding for the 1995 IGS Meeting, Potsdam, Germany, May 15-17, 1995.

Rocken, C., R. Anthes, M. Exner, D. Hunt, S. Sokolovsky, R. Ware, M. Gurbunov, W. Schreiner, D. Feng, B. Herman, Y.-H. Kuo, X. Zou, Verification of GPS/MET Data in the Neutral Atmosphere, J. of Geophysical Research, accepted for pub., Nov., 1997.

Rocken, C., T. VanHove. R. Ware, Near real-time GPS sensing of atmospheric water vapor, Geophysical Research Letters., Vol. 24, No. 24, pp 3221-3224, 1997.

Ware, R.H., M. Exner, D. Feng, M. Gorbunov, K. Hardy, B. Herman, Y. Kuo, T. Meehan, W. Melbourne, C. Rocken, W. Schreiner, S. Sokolovskiy, F. Solheim, X. Zou, R. Anthes, S. Businger and K. Trenberth, GPS Sounding of the Atmosphere from Low Earth Orbit: Preliminary Results, Bulletin American Meteorological. Society., 77, pp 19-40, 1996.

Ware, R.H., C. Alber, C. Rocken, F. Solheim, Sensing integrated water vapor along GPS ray paths, Geophysical. Research. Letters., Vol. 24, No. 4, pp 417-420, Feb. 15, 1997.

Yuan L., R. A. Anthes, R.H. Ware, C. Rocken, W. Bonner, M. Bevis and S. Businger, Sensing Climate Change Using the Global Positioning System, Journal of Geophysical. Research., Vol. 98, No. D8, pp 14,925-14,937, 1993.

Srivastava, R.C., “A Study of the Effect of Precipitation on Cumulus Dynamics”, Journal of Atmospheric Sciences., 24, 36-45, 1966.

Georgakakos, K.P., and R.L.Bras, “A Hydrologically Useful Station Precipitation Model”, Water Resources Research., 1585-1596, 1984.

Rogers, R.R., Yau, M.K., “A Short Course in Cloud Physics”, 1989.

Kessler, E., “On the distribution and continuity of water substance in atmosphere circulation”, Meteorological Monographs.,10, 86 pp., 1969.

Adler, R., and A. Negri, “A Satellite Infrared Technique to Estimate Tropical Convective and Stratiform Rainfall,” J. Applied. Meteorology., vol 27, pp. 30-51, 1998.

Arkin, P., and P.Ardanuy, “Estimating Climate-Scale Precipitation from Space: A Review,” J. Clim., vol. 2, no. 11, pp. 1229-1238, 1989.

Atlas, D., D. Rosenfield, and D. Short, “The Estimation of Convective Rainfall by Area Integrals, 1, The Theoretical and Emperical Basis,” J. Geophysical Research., vol. 95(D3), pp. 2153- 2160, 1990.

Austin, G., and A. Bellon, “The Use of Digital Weather Radar Records for Short-Term Precipitation Forecasting,” J. Applied Meteorol0gy., vol. 100, p.658, 1974.

Barret, E. C., and D.W. Martin, “The Use of Satellite Data in Rainfall Monitoring, Academic Press,” San Diego, 1981.

Collier, C., “Accuracy of Rainfall Estimates by Radar; Calibration by Telemetring Raingauges,” J. Hydrology., vol. 83, pp.207-223, 1986.

Fritsch, J. M., R.J.Kane, and C.R.Chelius, “The Contribution of Mesoscale Convective Weather Systems to the Warm Season Precipitation in the United States,” J. Clim.Appll.Meteorol., vol 25, pp. 1333-1345, 1986.

Georgakakos, K.P., “A Generalized Stochastic Hydrometeorological Model for Flood and Flash-Flood Forecasting 1. Formulation,” Water Resour.Res., vol 22, no. 13, pp.2083-2095, 1986.

Johnson, E.R., and R.L. Bras, “Multivariate Short-Term Rainfall Prediction,” Water Resour. Res., vol 16, no 1, pp.173-185, 1980.

Richards, F., and P.Arkin, “On the Relationship between Satellite-Observed Cloud Cover and precipitation,” Mon.Weather Rev. vol 109, pp. 1081-1093, 1981.

Smith, J.A., and A.F.Karr, “A Statistical Model of Extreme Storm Rainfall,” J.Geophys.Res., vol 95(D3), pp.2083-2092, 1990.

French, M.N., and W.F., Krajewski, “A model for real-time quantitative forecasting”, Water Resour.Res., 30, 1075-1083, April 1994.

Seo, D.J., and Smith, J.A., “ Radar-based short-term rainfall prediction”, Journal of Hydrology, 341-367, 131(1992).

Wolfe,D.E.,S.Gutman, “Developing an Operational, Surfaced-Based, GPS, Water Vapor Observing System for NOAA: Network Design and Results”, Journal of Atmospheric and Oceanography., 17, 426-440, June 1999.

## Appendix A - RAIN Program

RAIN program requires inputting the rain gauge numbers or the lid numbers of the gauges into the program. First all the counties in Virginia, which come within 40 nautical mile region, are selected. Gauges and their numbers in that region given by the NWS are then given as input to the rain program. Once after creating the database of rain gauges it is saved and given a name in the rain program. This database can be accessed with that name at any later time.

**Software Installation:**

Create an IFLOWS subdirectory on your hard drive. (C:\MD IFLOWS)

Edit your autoexec.bat file path statement to include the IFLOWS subdirectory.

(C:\>PATH=%PATH; C:\IFLOWS)

Copy the FILOWS software from the software subdirectory of the archive disk into the IFLOWS subdirectory of the hard drive.

(C:\IFLOWS>COPY drive:\path*.*)

To Use the Archived Database Files:

Archived database files are named using the convention MMMYY.DAT and MMMYY.NDX

Where MMM = Three letter month of the year

YY = Last 2 digits of the calendar year

.DAT = Database File

.NDX = Index Pointer File

From the Archived Data Subdirectory:

Copy and Rename the Archive Files to the IFLOWS subdirectory.

COPY MMMYY.DAT C:\IFLOWS\IFLDAT.DAT (Y to Overwrite)

COPY MMMYY.NDX C:\IFLOWS\IFLNDX.DAT (Y to Overwrite)

Execute or run Rain.exe

**Rain Main Menu Options**

| Option | Activities Supported by Options. |
|---|---|
| File | Controls learn and playback modes, and supports eXit option. |
| Select List | Defines save, qualifies, and sorts select list. |
| Report Format | Defines time span of data columns in RAIN data table. |
| Output | Establishes printer characteristics and printer current report. |
| Base Time | Defines base time of data table. |
| About… | Displays program name and version number, number of entries in select list, and settings of key parameters. |
| Xfer | Transfers control directory to DOS or to another application. |

**IFLOWS COMMANDS**

FILE: Gives the file name of the program

eXit: Terminates program execution, returning control to the DOS prompt.

**SELECT LIST:**

Add: Adds items to the current list.

Delete: Deletes items from the current list.

New: Enables us to enter LID's and create new list.

Save: Saves the qualified select list under the name entered.

Qualify: This defines the criterion that determines whether gauges in the current select list appear in the qualified list and in RAIN reports. This has the following three options in it.

Age: Qualifies gauges based on the time elapsed since the last report, called age, expressed as a time interval. After choosing this options, select Exceeds Limit to see gauges not reporting for some time, or Within Limit to see those within the interval. Enter the desired time interval in the dialogue box when requested.

Rainfall: Qualifies a gauge based on the amount of rain accumulated over a specified period. After choosing this option, select Exceeds Limit to see gauges with rainfall exceeding a specified limit, or Within Limit to see gauges with specified amount or less.

Next, enter the accumulation time interval in the dialogue box when requested. Finally, enter the rainfall limit in inches and hundredths.

Cancel Qualify: This makes the qualified select list equivalent to the current select list and inhibits further qualification.

sOrt: This defines the order in which gauges appear in the qualified list and in RAIN reports. This is not actually recorded until the Home key is next pressed after choosing the sort order. The following options are available in sOrt option.

Age: Sort by length of time since the gauge last reported

LID: Sort by LID number.

Jurisdiction: Sort by installation location, state and count with in the state

Name: Sort by gauge name.

Rainfall: Sort by rainfall accumulated over a specified time interval.

Cancel Sort: Select list order remains as it is.

After choosing any of these options other than Cancel Sort, select Ascending or Descending, which display the list either in the ascending or in descending order respectively. For example Name Ascending shows the names in alphabetical order and Name Descending shoes in reverse alphabetical order.

**REPORT FORMAT OPTION**: This defines the format of the rain window and printed reports. It has eight options.

Qtr-Hour: Represents 15-minuits interval

Hour: Represents 1 hour interval

3-Hour: Represents 3 hour interval

6-Hour: Represents 6 hour interval

12-Hour: Represents 12 hour interval

Day: Represents 24 hours

Week: Represents a week interval for the data

Other: Permits non-standard formats.

**OUTPUT OPTION**: Output writes reports to destinations other than the display, chiefly the system printer. It has four options.

Print: Prints 6 data columns when the print width is 80 columns, but

Prints 15 data columns when the width is 6 data columns.

Export: Export writes specially formatted rainfall report to a DOS file generally used as input to another program. When this option is chosen, RAIN displays a dialog box requesting the export file name.

If only a file name is (with or without extension) is entered, the file is written in the IFLOWS directory.

To write the file elsewhere, enter a complete path name.

If no extension is given .ROF is assumed.

RAIN next displays a dialogue box, requesting heading. A heading is a line of Text appearing before the rainfall report in the export file. After entering the heading press enter and one more dialogue box appears in which another heading can be entered. This process is repeated until a blank heading is entered and this blank line does not appear in the file.

(c) 80 columns and 132 columns: These options are there to adjust the type of print format. A reported printed contains 15 data columns after selecting 132 column option and 6 data columns after selecting 80 columns option.

**BASE TIME OPTIONS**: This is the end time of the leftmost columns of a rainfall report. This has two options in it.

Anchor: Looks base time to a specific date and time. Whenever base time is recalculated, it is set to the anchor date and time. This time is shown in a dialogue box and one can edit this for a new anchor time.

Float: When Float is selected RAIN displays the current report using the new base time.

## Appendix B - Radiosonde output format

(http://raob.fsl.noaa.gov)

**Input Format**

Input dates: Enter the dates at which the data is required and the time in UTC.

Sounding Specification Information: One can have the access to the data at all times or at specific times (like 0z, 12z…etc). Wind units can be obtained in knots or tenths of meters per second.

Select Stations/Data: Select the option saying WMO Station Identifier.

Select Stations: In this for Option 1 user can say No if he is interested only the data at one site else Yes if he is interested in having the data at various sites. For Option 2 user has to enter 72318 (Blacksburg station identification number) to get the data for Blacksburg station.

Select Output Option: In this text format is selected so that it is easy to convert it to a Microsoft Excel file.

**Output file format**

The first 4 lines of the sounding are identification and information lines. All additional lines are data lines. An entry of 32767 (original format) or 99999 (new format) indicates that the information is missing, not reported, or not applicable.

Column Number

| 1 | 2 | 3 | 4 | 5 | 6 | 7 |
|---|---|---|---|---|---|---|
| LINTYP | | | | | | |
| Header Lines | | | | | | |
| 254 | HOUR | DAY | MONTH | YEAR | (blank) | (blank) |
| 1 | WBAN# | WMO# | LAT **D** | LON **D** | ELEV | RTIME |
| 2 | HYDRO | MXWD | TROPL | LINES | TINDEX | SOURCE |
| 3 | (blank) | STAID | (blank) | (blank) | SONDE | WSUNITS |

Data lines

9 PRESSURE HEIGHT TEMP DEWPT WIND DIR WIND SPD

4

5

6

7

8

**LEGEND**

LINTYP: type of identification line

254 = indicates a new sounding in the output file

1 = station identification line

2 = sounding checks line

3 = station identifier and other indicators line

4 = mandatory level

5 = significant level

6 = wind level (PPBB) (GTS or merged data)

7 = tropopause level (GTS or merged data)

8 = maximum wind level (GTS or merged data)

9 = surface level

HOUR: time of report in UTC

LAT: latitude in degrees and hundredths

LON: longitude in degrees and hundredths

D: direction latitude ('N' or 'S') or longitude ('E' or 'W') -note this only appears in the online archive containing international observations.

ELEV: elevation from station history in meters

RTIME: is the actual release time of radiosonde from TTBB. Appears in GTS data only.

HYDRO: the pressure of the level to where the sounding passes the hydrostatic check

MXWD: the pressure of the level having the maximum wind in the sounding.

TROPL: the pressure of the level containing the tropopause.

LINES: number of levels in the sounding, including the 4 identification lines.

TINDEX: indicator for estimated tropopause. A "7" indicates that sufficient data was available to attempt the estimation; 11 indicates that data terminated and that tropopause is a "suspected" tropopause.

SOURCE: 0 = National Climatic Data Center (NCDC)

1 = Atmospheric Environment Service (AES), Canada

2 = National Severe Storms Forecast Center (NSSFC)

3 = GTS or FSL GTS data only

4 = merge of NCDC and GTS data (sources 2,3 merged into sources 0,1)

SONDE: type of radiosonde code from TTBB. Only reported with GTS data

10 = VIZ "A" type radiosonde

11 = VIZ "B" type radiosonde

12 = Space data corp.(SDC) radiosonde.

WSUNITS: wind speed units (selected upon output)

ms = tenths of meters per second

kt = knots

PRESSURE: in whole millibars (original format)

in tenths of millibars (new format)

HEIGHT: height in meters (m)

TEMP: temperature in tenths of degrees Celsius

DEWPT: dew point temperature in tenths of a degree Celsius

WIND DIR: wind direction in degrees

WIND SPD: wind speed in either knots or tenths of a meter per second

(selected by user upon output)

## Appendix C - GPS-IPW data

In real time GPS-IPW data is available at half an hour intervals. The following link gives the site at which the data is available.
http://gpsmet.fsl.noaa.gov/realtimeview/jsp/rti.jsp

**Input Data Format**

In the web page enter the start and end dates for which data is required. Data is obtained at UTC time.
Data Type: From this option list of the data products for which the data is required can be selected
Quality Control option and select type can be left at the default values
FSL Demo Network: This option is available on the right side in the home page. This contains the list of all the GPS networking stations. Choosing one of the sites form in this box gives the GPS data at that site
Below the option FSL Demo Network user can see Balloon Data, UNB3 Delay Model, Experimental or Removed. Clicking on one of those options gives the list of sites, which have that data in the entire country in the same box. Then selecting one of the sites form that list gives the data for that site. For example to get the PW data from Balloon at Blacksburg user can check the box saying IPW form the Data Type option and click on the Balloon data to get the location names at which the Balloon data is available. Then user can choose VA-Blacksburg (RAOBS)-RNK to get the data at the Blacksburg location.

**Balloon Data**

Rawinsonde (balloon) precipitable water is calculated from pressure and dew point temperature measurements made as a balloon travels from the surface to the top of its trajectory, typically about 100 mb.
UNB3 Delay Model Predictions

The UNB3 model was developed by the University of New Brunswick. This provides predictions of both the hydrostatic and wet components of the zenith signal delay. The model input parameters are day-of-year, elevation angle, height and latitude.

Experimental or Removed

These sites have either been decommissioned or they were used as part of a scientific data collection campaign. Hence, current data from these sites are most likely not available.

Output Format

The data appears in several columns. The labels appear below in the correct order of how they appear, when we download the data from the web.

SITE -- This is the four digit alphanumeric designation for the site this data corresponds to.

YEAR – Year on which data is obtained.

JJJ.dd -- This is the decimal representation of the time for this data where JJJ is Julian day of the year and dd is the decimal portion of the day. All times are in UTC.

HH:MM:SS -- This is the time this sample is attributed to
where HH is hours
MM is minutes
SS is seconds
all times are in UTC

IPW -- This is the measurement of total column water vapor for this site at the time indicated measured in cm's of water vapor.

PRESS -- This is the pressure in millibars.

TEMP -- This is the temperature in degrees C

RH -- This is the station-measured humidity in %.

TD -- This is the total delay of the GPS signal as it passes through the atmosphere

WD -- This is the portion of the delay due to water vapor

HD -- This is the portion of the delay due to factors other than water vapor.

TM -- The mean temperature of the atmosphere. Used in the calculation of water vapor.

PI -- This is the value of the function that maps signal delay to water vapor

FERR -- This is the calculation error attributed to the Time Delay Estimate

QCFLAGS -- These are internal quality control checks they (government) do on the data.

## Appendix D - Glossary

**Absolute Humidity:** This is defined as the mass of water vapor in a given volume of air.

$$AbsoluteHumidity = \frac{massofwatervapor}{volumeofair}$$

**Dew Point:** It represents the temperature to which the air would have to be cooled for saturation to occur.

**Evaporation:** The process of change of phase from the liquid state to vapor state is called evaporation.

**Humidity:** The measure of the air's water vapor content is called humidity.

**IPW or IPWV:** Integrated Precipitable Water Vapor

**Isentropic Surface**: A two-dimensional surface containing points of equal potential temperature.

**Lapse Rate**: The rate of change of an atmospheric variable, usually temperature, with height.

**Mixing Ratio:** This is the ratio of mass of water vapor in the air parcel to the mass of the remaining dry air.

**Mixing Ratio= mass of water vapor / mass of dry air**

**Potential Temperature**: The temperature a parcel of dry air would have if brought adiabatically to a standard pressure level of 1000 mb.

**Precipitable Water:** Then total mass of water vapor in a column of unit area extending to the top of the atmosphere is called the precipitable water. The amount of precipitable water can be computed using the upper air observations of temperature, pressure and relative humidity.

**Relative Humidity:** This is the ratio of the amount of water vapor actually in the air compared to the maximum amount of water vapor in the air can hold at that particular temperature and pressure. It is the ratio of the air's water vapor content to its capacity.

Relative Humidity = amount of water vapor in the air / (amount of water vapor the air can hold)

**Saturation vapor pressure:** This is the maximum pressure water vapor molecules cold exert if the air were saturated with vapor at a given temperature.

**Specific Humidity:** This is the ratio of mass of water vapor in a parcel of air to the total mass of air parcel.

**Specific Humidity = mass of water vapor / total mass of air**

$= 0.622\frac{e}{p}$ where e is the vapor pressure and p is the absolute pressure of the gas.

**Sublimation:** When the molecule changes from an ice molecule directly into a vapor molecule without passing through the liquid state that is ice-to-vapor phase change is called sublimation.

**Updraft**: A small-scale current of rising air.

**VIL**: Vertically Integrated Liquid water

**WSR-88D**: Weather Surveillance Radar - 1988 Doppler